

# ornl

**OAK RIDGE  
NATIONAL  
LABORATORY**

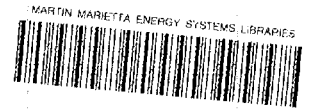
**MARTIN MARIETTA**

**Age-Specific Models for  
Evaluating Dose and Risk from  
Internal Exposures to Radionuclides**

**Report of Current Work of the  
Metabolism and Dosimetry Research Group,  
July 1, 1985–June 30, 1987**

OAK RIDGE NATIONAL LABORATORY  
CENTRAL RESEARCH LIBRARY  
CIRCULATION SECTION  
ADJORN ROOM 173  
**LIBRARY LOAN COPY**  
DO NOT TRANSFER TO ANOTHER PERSON  
If you wish someone else to see this  
report, send in name with report and  
the library will arrange a loan.

OPERATED BY  
MARTIN MARIETTA ENERGY SYSTEMS, INC.  
FOR THE UNITED STATES  
DEPARTMENT OF ENERGY



3 4456 0278655 4

ORNL/TM-10080



Printed in the United States of America. Available from  
National Technical Information Service  
U.S. Department of Commerce  
5285 Port Royal Road, Springfield, Virginia 22161  
NTIS price codes—Printed Copy: A09 Microfiche A01

This report was prepared as an account of work sponsored by an agency of the United States Government. Neither the United States Government nor any agency thereof, nor any of their employees, makes any warranty, express or implied, or assumes any legal liability or responsibility for the accuracy, completeness, or usefulness of any information, apparatus, product, or process disclosed, or represents that its use would not infringe privately owned rights. Reference herein to any specific commercial product, process, or service by trade name, trademark, manufacturer, or otherwise, does not necessarily constitute or imply its endorsement, recommendation, or favoring by the United States Government or any agency thereof. The views and opinions of authors expressed herein do not necessarily state or reflect those of the United States Government or any agency thereof.

Health and Safety Research Division  
Metabolism and Dosimetry Research Group

AGE-SPECIFIC MODELS FOR EVALUATING DOSE AND RISK  
FROM INTERNAL EXPOSURES TO RADIONUCLIDES

Report of Current Work of the Metabolism  
and Dosimetry Research Group,  
July 1, 1985 - June 30, 1987

R. W. Leggett and B. P. Warren, Editors

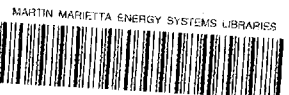
K. F. Eckerman, Group Leader  
M. Gristy  
G. D. Kerr  
G. G. Killough  
D. C. Kocher  
R. W. Leggett  
J. C. Ryman (C&TD)  
J. L. Davis (Visiting Scientist)  
G. M. Luccioni (Visiting Scientist)  
L. R. Williams (Visiting Scientist)

**NOTICE** This document contains information of a preliminary nature.  
It is subject to revision or correction and therefore does not represent a  
final report.

Date Published - September 1987

Prepared for the  
Office of Health and Energy Research

Prepared by the  
OAK RIDGE NATIONAL LABORATORY  
Oak Ridge, Tennessee 37831  
operated by  
MARTIN MARIETTA ENERGY SYSTEMS, INC.  
for the  
U.S. DEPARTMENT OF ENERGY  
under contract DE-AC05-84OR21400



3 4456 0278655 4



## CONTENTS

|  | <u>Page</u> |
|--|-------------|
| PREFACE . . . . .  | v           |
| ABSTRACT . . . . .   | vii         |
| INTRODUCTION . . . . .   | 1           |
| PART 1. ILLUSTRATIONS OF OUR APPROACH TO CONSTRUCTION<br>OF AGE-SPECIFIC BIOKINETIC MODELS . . . . .   | 5           |
| Problems with the Current Approach to Modeling<br>the Biological Behavior of Radionuclides . . . . .   | 6           |
| Biokinetics of Potassium: An Example of the Detail that<br>Can be Achieved with a Physiological Systems Model . . . . .                                    | 8           |
| Biokinetics of Cesium: An Example of a Simple Model with<br>a Physiological Basis . . . . .  | 16          |
| Biokinetics of Rubidium: Another Example of a Simple<br>Age-Specific Biokinetic Model with Physiological Underpinnings . . . . .                           | 24          |
| Biokinetics of Plutonium, Americium, and Curium: Illustrations<br>of Modeling Age-Specific Translocation of Activity within the<br>Skeleton . . . . .      | 29          |
| A Generic Scheme to Aid in the Construction of Age-Specific<br>Biokinetic Models for Bone-Seeking Radionuclides . . . . .                                  | 42          |
| Application of the Generic Scheme to Thorium . . . . .   | 46          |
| Biokinetics of Uranium: An Example of the Value of the<br>Physiologically Based Approach in Revealing Some Uncertainties<br>in Estimates of Dose . . . . . | 51          |
| Models for the Alkaline Earth Elements . . . . .   | 56          |
| Age Dependence in Intake of Radioactivity and in Functions<br>of the Gastrointestinal and Respiratory Tracts . . . . .                                     | 59          |
| PART 2. DOSIMETRIC MODELS . . . . .  | 67          |
| Specific Effective Energies (SEE Values) . . . . .   | 68          |
| Specific Absorbed Fractions of Energy at Various Ages from<br>Internal Photon Sources . . . . .  | 76          |
| Specific Absorbed Fractions for the Pregnant Female . . . . .  | 81          |
| Absorbed Fraction in Active Marrow for Electrons Within<br>Trabecular Bone . . . . .   | 82          |
| Estimating Dose in Active Marrow and Osteogenic Tissue from<br>Photons from Internal or External Sources . . . . .   | 93          |

|   |     |
|---|-----|
| Estimating Dose in Active Marrow and Osteogenic Tissue from<br>Photons. Fluence-Conversion Functions . . . . .                                | 99  |
| Electron Dose-Rate Conversion Factors for External Exposure<br>of the Skin from Uniformly Deposited Activity on the<br>Body Surface . . . . . | 111 |
| PART 3. APPLICATIONS OF THE BIOKINETIC AND DOSIMETRIC MODELS . . . . .  | 119 |
| How Computations are Performed . . . . .  | 120 |
| Comparison of Our Age-Specific Dose Commitment Factors with<br>Values Produced by Other Approaches . . . . .                                  | 124 |
| A Closer Look at Age-Specific Estimates of Dose to Bone<br>Surfaces Following Inhalation of Thorium-230 . . . . .                             | 130 |
| A Closer Look at Age-Specific Estimates of Dose to Bone<br>Surfaces Following Acute Inhalation or Ingestion of<br>Uranium-238 . . . . .       | 137 |
| PART 4. THE NEXT STEP: CALCULATION OF RADIOGENIC RISK . . . . .   | 145 |
| Factors Considered in Calculations of Risk . . . . .  | 146 |
| Potential Variation with Age at Intake in Radiogenic Risk:<br>Some Examples . . . . .   | 148 |
| DISTRIBUTION LIST . . . . .   | 157 |

## PREFACE

The Metabolism and Dosimetry Research Group has been funded continuously for over two decades by the Office of Health and Environmental Research (OHER) of the Department of Energy (DOE). In recent years our funding from OHER has been supplemented through short-term contracts with other agencies, including the Environmental Protection Agency (EPA), the Nuclear Regulatory Commission (NRC), the Food and Drug Administration (FDA), and the Department of Transportation (DOT). This additional support has been critical to the development of our research program and has provided the opportunity to help standardize the dosimetric methods used by the various federal agencies.

In general, our efforts for all of the funding agencies contribute to and benefit from a common pool of experience, information, and analytical capability. With few exceptions, each summary of work given in this report represents a combination and distillation of work from several projects supported by several agencies, and no attempt is made here to assign percentages of support to specific summaries.



## ABSTRACT

A projection of the health risk to a population internally exposed to a radionuclide requires explicit or implicit use of demographic, biokinetic, dosimetric, and dose-response models. The level of detail applied in these four types of models has varied considerably among different radiation protection bodies. Some efforts have been made to address representative members of subgroups, particularly certain age groups, that might experience distinctive doses or risks and to include considerations of competing non-radiogenic risks. For the most part, however, exposure guidelines have been based on models for a reference adult with a fixed life span. In this report we describe recent efforts of the Metabolism and Dosimetry Research Group of the Oak Ridge National Laboratory to develop a comprehensive methodology for estimation of radiogenic risk to individuals and to heterogeneous populations. Emphasis is on age-dependent biokinetics and dosimetry for internal emitters, but consideration also is given to conversion of age-specific doses to estimates of risk using realistic, site-specific demographic models and best available age-specific dose-response functions. We discuss how the methods described here may also improve estimates for the reference adult usually considered in radiation protection.



## INTRODUCTION

A projection of the health risk to a population internally exposed to a radionuclide requires explicit or implicit use of demographic, biokinetic, dosimetric, and dose-response models. A demographic model is used to define the composition of the population and perhaps competing risks that may remove some members who would otherwise eventually die from the radiation exposure. Biokinetic models are needed to describe the time-dependent distribution and elimination of internal activity. Exposure-dose models combine theoretical considerations of radiation transport and energy deposition to predict the fraction of internally emitted energy absorbed by radiosensitive organs and tissues. Dose-response models are applied to estimate the probability of a health effect based on the dosimetric and demographic considerations.

The level of detail applied in these four types of models has varied considerably among different radiation protection bodies. Some efforts have been made to address representative members of subgroups, particularly certain age groups, that might experience distinctive doses or risks and to include considerations of competing non-radiogenic risks. It is much more common, however, to use biokinetic, dose-response, and in some cases activity-dose models developed for a "reference" member of the whole population. Moreover, demographic considerations are usually reduced to the implicit assumption that the reference individual has a life expectancy of 50 or 70 years with no competing risks; this is the case, for example, when 50-year dose commitments or committed effective dose equivalents are used as surrogates for risk.

In a methodology implemented recently by the U. S. Environmental Protection Agency (EPA) (Sullivan et al. 1981) to estimate health risk to the public from exposure to any of about 150 radionuclides, metabolic and dosimetric models for the adult as given in ICRP Publication 30 (1979) were applied to all age groups, and radiation risk factors were assumed to be independent of age. Yet detailed consideration of age-specific mortality rates from competing causes was a central feature of the methodology.

In some tabulations of age-specific dose conversion factors, the metabolic properties of the adult have been assigned to all age groups but account has been taken of the generally greater dose per unit activity that would result from the smaller organ masses in children. This approach was taken for most radionuclides in a recent report issued by the National Radiological Protection Board (NRPB) of the United Kingdom, although age-specific metabolic models were used for hydrogen, carbon, sulfur, and iodine (Greenhalgh, Fell, and Adams 1985). A similar approach was taken in an earlier document issued by the U. S. Nuclear Regulatory Commission (Hoenes and Soldat 1977), except that metabolic models and general dosimetric methods were based on ICRP Publication 2 (1959).

The purpose of this report is to describe current efforts of the Metabolism and Dosimetry Research Group of the Oak Ridge National Laboratory to develop a comprehensive methodology for estimation of radiogenic risk to individuals and to heterogeneous populations. While emphasis in the present report is on age-dependent biokinetics and dosimetry for internal emitters, consideration also is given to the importance of converting age-specific doses to estimates of risk using realistic, site-specific demographic models and best available age-specific dose-response functions. We also discuss how the methods described here may in some cases improve estimates even for the reference adult usually considered in radiation protection.

#### REFERENCES

- Greenhalgh, J. R., Fell, T. P., and Adams, N., 1985, *Doses from Intakes of Radionuclides by Adults and Young People*, Report of the National Radiological Protection Board, NRPB-R162, Chilton, Didcot, Oxon OX11 0RQ.
- Hoenes, G. R. and Soldat, J. K., 1977, *Age-Specific Radiation Dose Commitment Factors for a One-Year Chronic Intake*, U.S. Nuclear Regulatory Commission Report NUREG-0172.
- International Commission on Radiological Protection, 1959, *Publication 2, Report of Committee 2 on Permissible Dose for Internal Radiation*, Pergamon Press, Oxford.

International Commission on Radiological Protection, 1979, *Publication 30, Limits for Intakes by Workers*, Pergamon Press, Oxford.

Sullivan, R. E., Nelson, N. S., Ellett, W. H., Dunning, D. E., Leggett, R. W., Yalcintas, M. G., and Eckerman, K. F., 1981, *Estimates of Health Risk from Exposure to Radioactive Pollutants*, Oak Ridge National Laboratory Report ORNL/TM-7745.



PART 1. ILLUSTRATIONS OF OUR APPROACH TO CONSTRUCTION  
OF AGE-SPECIFIC BIOKINETIC MODELS

PROBLEMS WITH THE CURRENT APPROACH TO MODELING  
THE BIOLOGICAL BEHAVIOR OF RADIONUCLIDES

The metabolic models recommended in ICRP Publication 30 (1979) are generally considered to be the best supported comprehensive set of models describing the biokinetics of radioelements. These models were designed and intended for interpreting occupational exposures of a typical adult; however, for lack of commonly accepted approaches applicable to special subgroups of the population, they are frequently viewed as the proper point of departure for evaluation of internal exposures to the general population.

Each of the metabolic models of ICRP 30 is a concise mathematical summary of observations and assumptions concerning the net retention of a radioelement in organs or the whole body of adult humans. For the most part, these models are based on direct observations of the early distribution and the net retention of radioelements in organs or whole bodies of experimental animals and humans, the equilibrium distribution of elements in Reference Man as described in ICRP Publication 23 (1975), analogies among chemical families of elements, and broad assumptions where information is lacking. Physiological considerations occasionally enter model construction or choice of parameter values, but not in any uniform or consistent manner.

The format for the type of metabolic models eventually used in ICRP Publication 30 evolved at a time when computations were done largely by hand and simplicity of model structure was an overriding concern. Unfortunately, in many cases the requirement of a simple mathematical format and the lack of a firm physiological foundation lead to a rather inflexible retention model with some major disadvantages. For example, the underlying curve-fitting approach precludes the incorporation of a great deal of valuable physiological information and physiologically reasonable assumptions that could be used in characterizing the sometimes complex behavior of radioelements in humans. We believe that lack of requirement of internal physiological consistency often leads to uncritical use of empirical data in selection of parameter values (e.g., see the example given later for rubidium). Another disadvantage with the ICRP approach is that, although the models have been constructed

largely from animal data, they are not constructed in such a way that extrapolation to humans has strong logical support. Other problems also become apparent: doses from short-lived nuclides or doses to heterogeneously distributed radiosensitive tissues of an organ (e.g., skeleton) cannot be estimated accurately, since the actual movement of radionuclides in the body is usually not accurately tracked, even in cases where the whole-body retention is estimated fairly well; the models often do not yield accurate estimates of excretion even for the average adult, so that better models are needed for bioassay programs; and the format of the models often does not permit extension to non-standard man (person with anatomical or metabolic characteristics different from Reference Man, such as a child), because there is usually insufficient data with which to develop new parameter values for special subgroups by the fitting techniques that characterize most of the reference man models.

We have found that these problems can be overcome to a large extent by building biokinetic models upon a strong physiological foundation. The complexity of the structure needed for such a model may vary markedly from one situation to another. For example, to estimate doses accurately for a very short-lived isotope, it may be necessary to have a highly detailed and realistic representation of the movement of the isotope during the time shortly after entry into the body. For many longer-lived radionuclides one may be able to simplify and/or combine many tissues and fluids that are important only for descriptions of very short-term kinetics. In a few cases it may suffice to have an ICRP-type representation of retention, provided parameters in the model can be tied to a suitable physiological index. These concepts are illustrated in the following sections.

#### REFERENCES

International Commission on Radiological Protection, 1975, *Publication 23, Report of the Task Group on Reference Man*, Pergamon Press, Oxford.

International Commission on Radiological Protection, 1979, *Publication 30, Limits for Intakes by Workers*, Pergamon Press, Oxford.

BIOKINETICS OF POTASSIUM: AN EXAMPLE OF THE DETAIL THAT  
CAN BE ACHIEVED WITH A PHYSIOLOGICAL SYSTEMS MODEL

DIFFERENT APPROACHES TO MODELING THE BIOKINETICS OF K

The scheme currently recommended by the International Commission on Radiological Protection (ICRP 1979) for evaluation of occupational exposures to radiopotassium depicts the body as a single well-mixed pool from which K is lost with a biological half-time of 30 days. More detailed models of the behavior of K in the body have appeared in the physiological and medical literature, but these models generally consist of hypothetical, mathematically derived compartments that may not correspond to identifiable anatomical compartments.

In this section we outline a recent model of Leggett and Williams (1986) that describes the normal movement of K through the human body in much greater qualitative and quantitative detail than has been offered previously. Although potassium is of limited interest in the field of radiation protection, the model serves as a good illustration of the detail and accuracy that can arise from a physiologically oriented approach. Moreover, the same model structure can be applied to some more important radioelements (e.g., cesium and rubidium) that mimic the behavior of potassium in a qualitative if not a quantitative sense.

DESCRIPTION OF THE DETAILED MODEL

The compartments and directions of flow of material in this model are indicated in Fig. 1. Inflow and outflow rates are summarized in Table 1. Plasma (solid arrows) serves as a primary feeding compartment, although it cannot be regarded as a central compartment since transport of K among compartments by other materials (dashed arrows) is also considered. The rate of flow of K from plasma into a compartment is viewed as being related to blood flow but not totally controlled by this factor. Other factors, such as the tissue-specific fraction of K extracted by a compartment during a single passage from arterial to venous plasma, are also considered. At points in the construction of the model where data for humans are sparse or nonexistent, extrapolation from data for other species is made by appealing as much as possible to

the apparent similarity among species in the behavior of K at the tissue level.

Movement of K among the compartments is viewed as a system of first-order processes. Based on a review of experimental data for non-humans and comparisons of model predictions with data for humans it was concluded that this approach is adequate provided attention is restricted to the net movement of K over periods of at least 2-3 minutes. Thus, no attempt was made to incorporate into the model any delays or other peculiarities associated with the extracellular-membrane-intracellular exchange of K that may occur on the order of seconds. For consideration of net movement of K over periods of 2-3 minutes or longer, it was not necessary to consider cellular and extracellular fluids within an organ or tissue as separate pools of K except in the case of skeletal muscle. Skeletal muscle appears to be an exception due to a combination of two factors. First, the cells of this compartment equilibrate more slowly with ECF than do cells of most other tissues, so that the assumption of uniform mixing over a short period is less reasonable for skeletal muscle than for most other compartments. Second, the assumption of uniform mixing in skeletal muscle would yield an unrealistically rapid increase of K in skeletal muscle, which would lead to substantial errors for all compartments in the model because of the large fraction of total-body K in muscle, particularly in teenagers and adults.

The parameter values described in Table 1 are for a typical, healthy, resting male about 35 years old. To apply the model to other situations we require the equilibrium distribution of K and the regional blood flow rates appropriate for those conditions. Additionally, there may be information available on the condition-specific change in the extraction fraction during passage of K from arterial to venous plasma, although we expect this change to be small in most cases. For example, to apply the model to a non-resting adult male, we would alter blood flow rates (increasing the rate to muscle) and decrease the K extraction fraction for muscle slightly to correspond to the greater blood flow. To apply the model to an adult female or to a child, we would reduce the fraction of total-body K in muscle and increase the fractions in other organs, with the greatest increase in the concentration of K in children

being in the skeleton. Also we would modify the cardiac output appropriately, decrease the fraction of cardiac output going to muscle, and, in children, increase the fraction of cardiac output going to skeleton. Many of these changes can be based on actual experimental values, while others can be based on consistency with other physiological phenomena. (For example, the blood flow to the skeleton as a function of age is not a measurable quantity, but there is considerable physiological information on vascularity and cellularity of the skeleton and in skeletal deposition of many substances at different ages.) In either case, no blind assumptions need be made.

Comparisons of model predictions with observations of adult human subjects receiving oral or intravenous doses of radiopotassium (Burch, Threefoot, and Ray 1955; Corsa et al. 1950; Hamilton 1938) are made in Figs. 2 and 3. In Fig. 3 the model predictions are given in terms of a "disequilibrium factor". For a given tissue, the disequilibrium factor is defined as the fraction of the unexcreted tracer K in the substance at a given time after ingestion or injection of a unit activity of tracer K, divided by the fraction of whole-body K in that compartment at equilibrium. For urine, the disequilibrium factor at any given time is the urinary excretion rate of the administered unit activity of tracer K, divided by the urinary excretion rate of tracer K after equilibration with body K has been attained.

#### REFERENCES

- Burch, G. E., Threefoot, S. A., and Ray, C. T., 1955, "The Rate of Disappearance of Rb-86 from the Plasma, the Biologic Decay Rates of Rb-86, and the Applicability of Rb-86 as a Tracer of Potassium in Man with and without Chronic Congestive Heart Failure," *J. Lab. Clin. Med.* 45, 371-394.
- Corsa, L., Olney, J. M., Steenburg, R. W., Ball, M. R., and Moore, F. D., 1950, "The Measurement of Exchangeable Potassium in Man by Isotope Dilution," *J. Clin. Inv.* 29, 1280-1295.
- Hamilton, J. G., 1938, "The Rates of Absorption of the Radioactive Isotopes of Sodium, Potassium, Chlorine, Bromine, and Iodine in Normal Human Subjects," *Am. J. Physiol.* 124, 667-678.

International Commission on Radiological Protection (ICRP), 1979, *Limits for Intakes of Radionuclides by Workers*, Publication 30, Pergamon Press: Oxford.

Leggett, R. W. and Williams, L. R., 1986, A Model for the Kinetics of Potassium in Healthy Humans, *Phys. Med. Biol.* 31, 23-42.

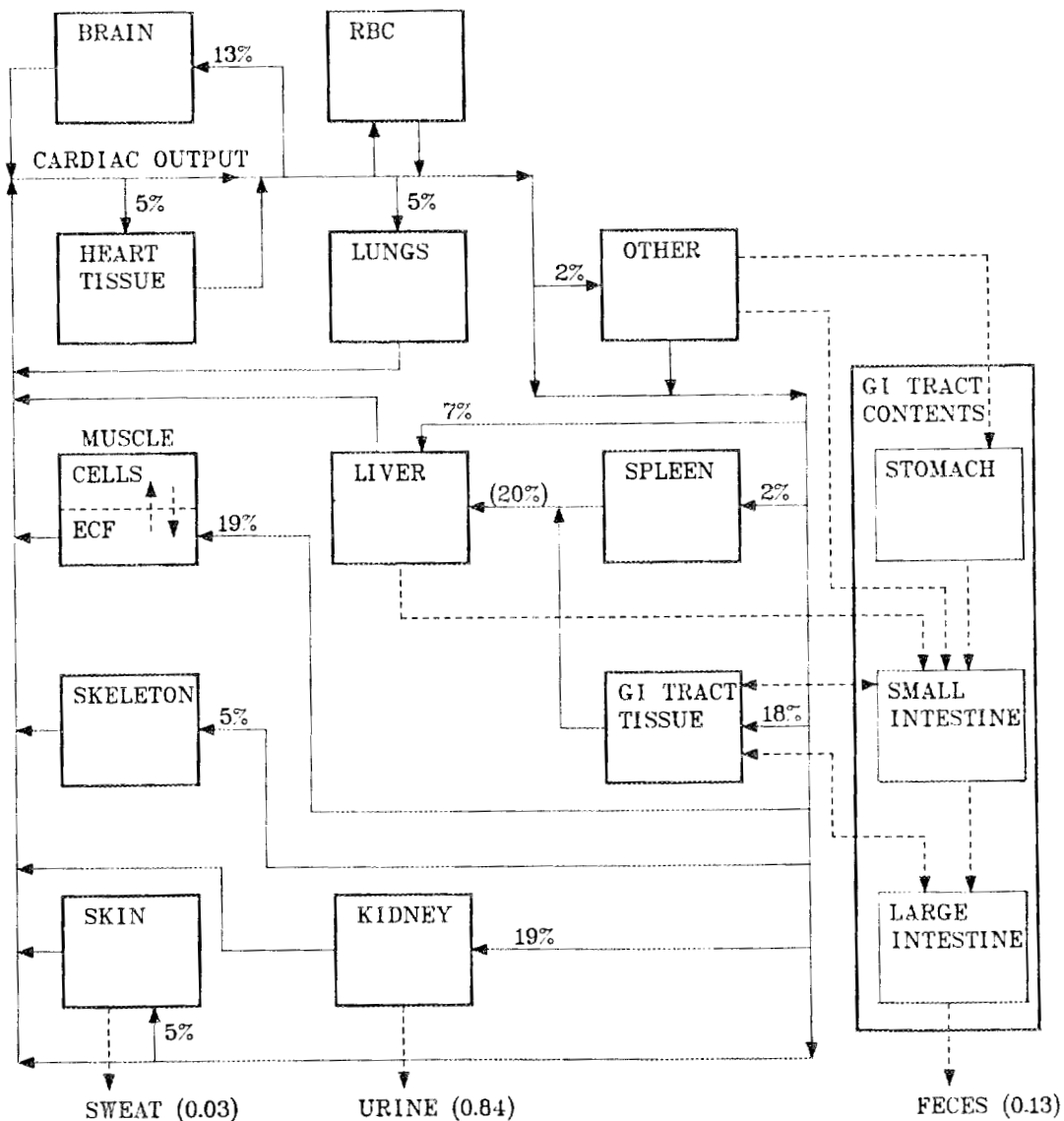


Figure 1. Direction of flow of potassium among compartments of model. Solid arrows indicate plasma flow and dashed arrows indicate flow not involving plasma. Numbers next to compartments refer to percentages of cardiac output passing through the compartments. Numbers to the right of sweat, urine, and feces are typical relative fractions of potassium excreted along these routes.

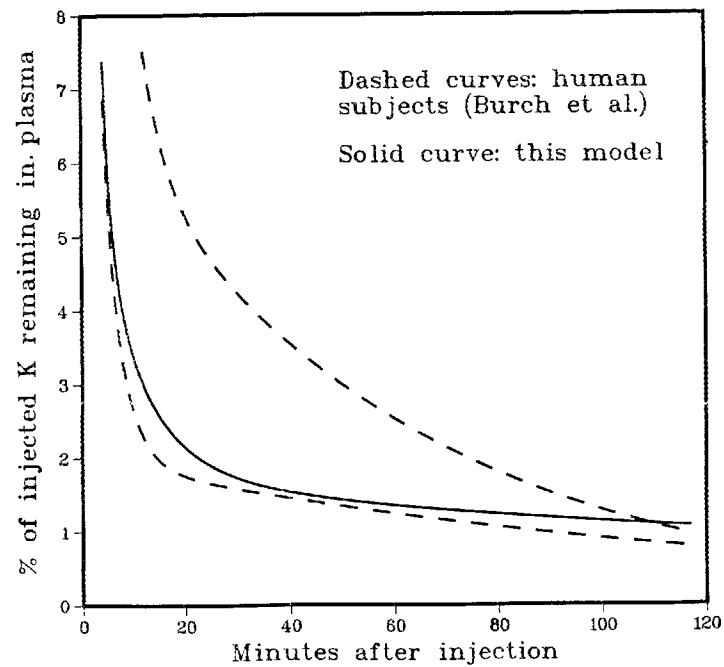
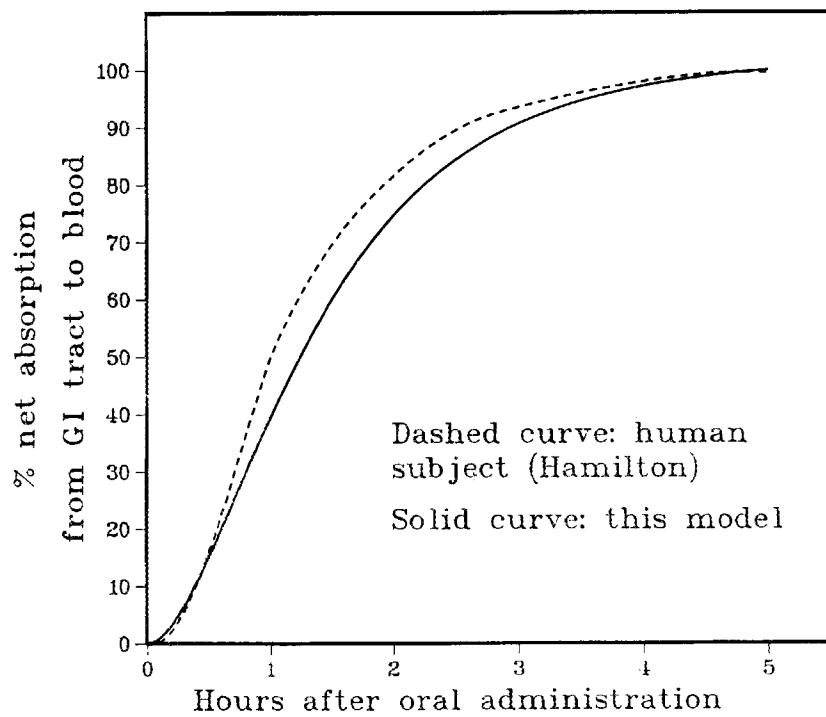


Figure 2. Net absorption of potassium from GI tract to blood and percent of injected potassium remaining in plasma, as measured in human subjects and predicted by this model.

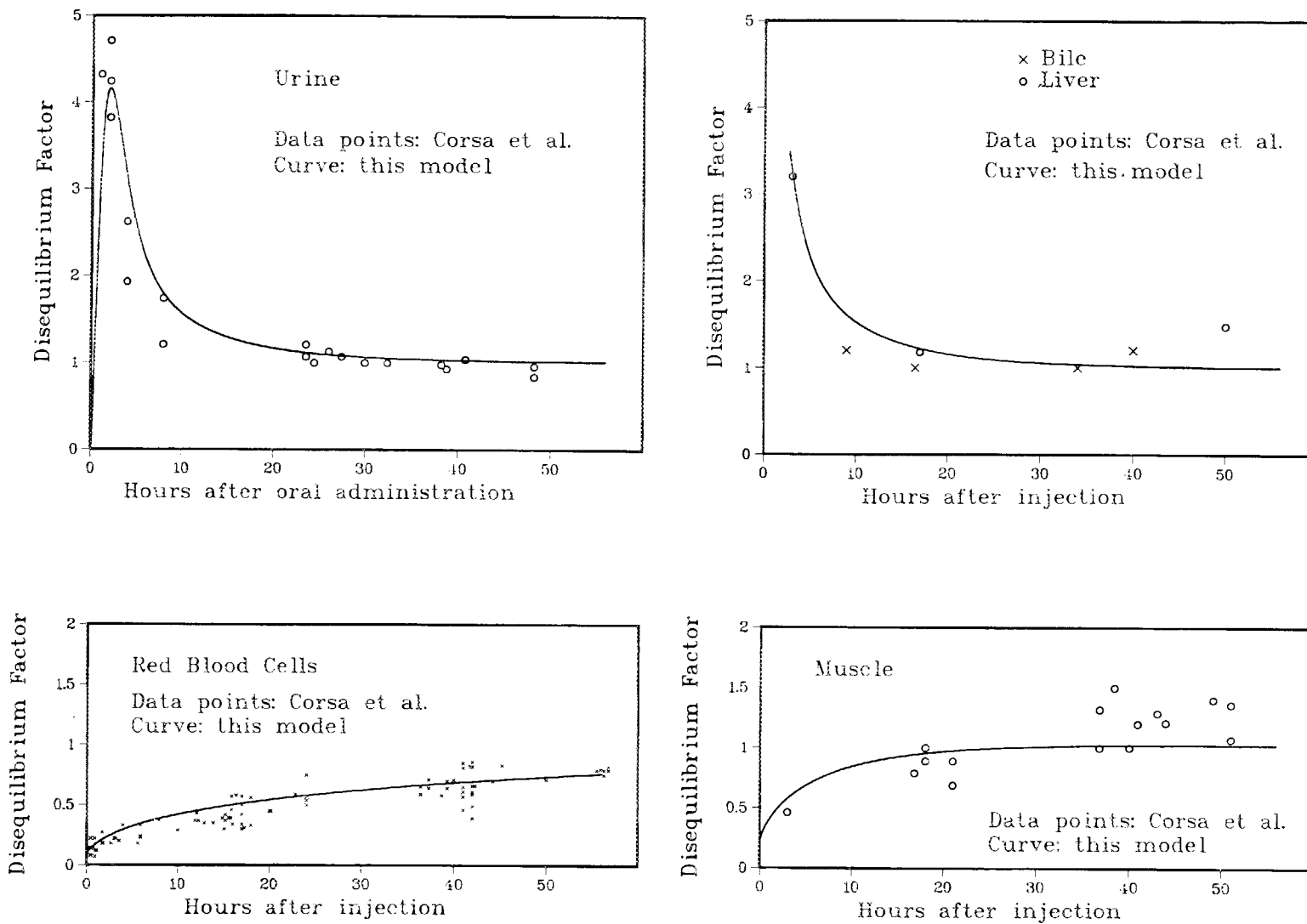


Figure 3. Relative concentration of ingested potassium in urine and injected potassium in liver, bile, red blood cells, and muscle, as measured in human subjects and predicted by this model.

Table 1. Inflow and outflow rates for compartments and subcompartments.

| Compartment      | Inflow <sup>a</sup> | Source                      | Outflow <sup>b</sup> | Destination                               |
|------------------|---------------------|-----------------------------|----------------------|---|
| RBC              | 6                   | Plasma                      | 0.38                 | Plasma                                    |
| Kidneys          | 257                 | Plasma                      | 209.4<br>4.6         | Plasma<br>Urine                           |
| Muscle ECF       | 242                 | Plasma                      | 242                  | Plasma                                    |
|                  | 2.65                | Muscle cells                | 500                  | Muscle cells                              |
| Muscle cells     | 500                 | Muscle ECF                  | 2.65                 | Muscle ECF                                |
| Skeleton         | 56                  | Plasma                      | 2.9                  | Plasma                                    |
| Heart            | 67.5                | Plasma                      | 42.2                 | Plasma                                    |
| Lungs            | 67.5                | Plasma                      | 33.8                 | Plasma                                    |
| Stomach contents | 3.3                 | Food                        | 40                   | SI contents                               |
|                  | 0.11                | Other                       |                      |   |
|                  | 0.48                | GI tract walls              |                      |   |
| SI contents      | 40                  | Stomach contents            | 11.35                | Plasma                                    |
|                  | 0.36                | GI tract walls              | 17                   | Liver                                     |
|                  | 0.03                | Other                       | 1.65                 | LI contents                               |
|                  | 0.05                | Liver                       |                      |   |
| LI contents      | 1.65                | SI contents                 | 0.43                 | Feces                                     |
|                  | 0.13                | GI tract walls              | 0.06                 | Plasma                                    |
|                  |                     |                             | 0.09                 | Liver                                     |
| GI tract walls   | 216                 | Plasma                      | 0.48                 | Stomach contents                          |
|                  |                     |                             | 0.36                 | SI contents                               |
|                  |                     |                             | 0.13                 | LI contents                               |
|                  |                     |                             | 23.6                 | Plasma                                    |
|                  |                     |                             | 35.4                 | Liver                                     |
| Spleen           | 21                  | Plasma                      | 7                    | Plasma                                    |
|                  |                     |                             | 10.5                 | Liver                                     |
| Liver            | 100.8               | Plasma (direct)             | 0.05                 | SI contents                               |
|                  | 10.5                | Spleen <sup>c</sup>         | 26.35                | Plasma                                    |
|                  | 0.09                | LI contents <sup>c</sup>    |                      |   |
|                  | 17                  | SI contents <sup>c</sup>    |                      |   |
|                  | 35.4                | GI tract walls <sup>c</sup> |                      |   |
| Skin             | 67.5                | Plasma                      | 8.206<br>0.024       | Plasma<br>Sweat                           |
| Brain            | 2.9                 | Plasma                      | 0.38                 | Plasma                                    |
| Other            | 120                 | Plasma                      | 7.06<br>0.11<br>0.03 | Plasma<br>Stomach contents<br>SI contents |

<sup>a</sup>Source compartment volumes of potassium per day, except food, which is in g/day.

<sup>b</sup>Compartment or subcompartment volumes of potassium per day.

<sup>c</sup>A brief intermediate residence in plasma is ignored.

BIOKINETICS OF CESIUM: AN EXAMPLE OF A  
SIMPLE MODEL WITH A PHYSIOLOGICAL BASIS

DEVELOPMENT OF A DETAILED MODEL FOR SHORT-LIVED Cs

The general modeling scheme described for potassium can also be used to develop a detailed model of the biokinetics of cesium, since cesium tends to follow the movement of K in the body in a qualitative manner (Leggett 1983). Because Cs has a slower transport rate than K across cell membranes (Leggett 1983), somewhat different parameter values are needed for the cesium model. The development of such parameter values for cesium is now under way. In this section we describe a simpler age-specific retention model that can be applied to long-lived isotopes of Cs (Cs-134, Cs-135, and Cs-137). The reader is referred to an article by Leggett (1986) for a more detailed description.

THE ICRP MODEL FOR Cs

The model for retention of cesium given in ICRP Publication 30 (1979) represents whole-body retention as a two-exponential expression

$$R(t) = a \exp(-0.693t/T_1) + (1 - a) \exp(-0.693t/T_2). \quad (1)$$

Here  $R(t)$  is the fraction of activity at reference time zero still retained in the body  $t$  days later,  $a$  and  $1-a$  are fractions of the initial activity associated with two hypothetical compartments that together make up the total body, and  $T_1$  and  $T_2$  are the biological half-times of cesium in those compartments. These parameter values are defined only for a reference adult.

EXTENSION OF THE ICRP MODEL TO OTHER AGE GROUPS (FOR LONG-LIVED Cs ISOTOPES)

An analysis of the physiological and radiobiological literature on cesium and biologically similar elements led to the conclusion that the parameters  $a$ ,  $T_1$ , and  $T_2$  of Eq. (1) could be expressed in terms of  $K_t$ , the amount of K in the total body. Each of these parameters appears to depend on the fraction  $F$  of  $K_t$  that is in skeletal muscle, where most of the body's K resides; in turn,  $F$  appears to increase with  $K_t$ . It has

been found that in comparison with most other tissues, particularly the viscera, the skeletal muscles exchange Cs with plasma at a slow rate. In relative terms, a smaller value of F should correspond to a smaller slow-exchange pool for Cs and a larger amount of Cs entering plasma and available for excretion over the first few days after exposure. Thus, decreasing values of F should correspond to increasing values of the short-term fraction  $a$  in Eq. (1). Also, a smaller value of F means a smaller muscle pool, which should correspond to a smaller value of  $T_2$  in Eq. (1), not only because of a potentially shorter time for a single turnover of that pool but also because of a smaller fraction of material being recycled to that pool. A similar argument applies to the correspondence between decreasing values of F and increasing values of  $T_1$ , although the argument may be weaker in this case because of the more heterogeneous nature of the fast-exchange "pool". A positive correlation between F and  $K_t$  is suggested by some results. Differences with sex in the relations between  $K_t$  and the parameters of Eq. (1) might be expected since there could be differences with sex in the relation between the fraction F defined above and  $K_t$ .

The relation between  $K_t$  and the parameters of Eq. (1) was investigated using data from a study by Lloyd and coworkers (1973), who measured the retention of Cs-137 and Rb-83 in 38 persons of various ages, some healthy and some with muscle disease. It was found that  $T_2$  increases with  $K_t$  in a nearly linear fashion (Fig. 1), and  $1-a$  also increases with  $K_t$  but in a nonlinear fashion (Fig. 2). A relation between  $K_t$  and  $T_1$  is revealed indirectly by first relating  $K_t$  and  $1-a$  (Fig. 2) and then relating  $a$  and  $T_1$  (Fig. 3). The pairs  $(K_t, T_2)$  for healthy males are approximated by the line

$$T_2 = -1.22 + 0.72K_t \quad (R=0.91). \quad (2)$$

The pairs  $(K_t, T_1)$  for healthy males may be better approximated by an exponentially declining curve:

$$T_1 = 18 \exp(-0.016K_t) \quad (R=0.87). \quad (3)$$

Curves (2) and (3) intersect at about  $K_t = 20$  g, which is the value of  $K_t$  at approximately one year of age. At  $K_t = 20$  g,  $T_1 = T_2 = 13$ . For smaller values of  $K_t$  it will be assumed that  $T_1 = T_2$ ; based on empirical

data, this common value is assumed to decrease linearly with  $K_t$  from 22 days at  $K_t = 5$  g (birth) to 13 days at  $K_t = 15$  g (approximately 6 months of age), and then remain at 13 days through  $K_t = 20$  g. For healthy males, the pairs  $(K_t, a)$  also may decline more in an exponential pattern than a linear one, with the best-fitting exponential function being

$$a = 0.81 \exp(-0.014K_t) \quad (R=0.92). \quad (4)$$

Because of the small number of data points for females, especially for small values of  $K_t$ , the information for males was used as a point of departure for constructing a model for females, by appealing to the apparent lack of difference with sex in young children in  $K_t$  and in retention of cesium. The model for females was taken to be the same as that for males through age 6-7 years ( $K_t=43$  g), and functions agreeing with the model for males at  $K_t=43$  g and representing the data for females for higher ages were found. These are given in Eqs. (5-7).

$$T_2 = -17.1 + 1.09K_t \quad (K_t > 43 \text{ g}); \quad (5)$$

$$T_1 = 14 \exp(-0.01K_t) \quad (K_t > 43 \text{ g}); \quad (6)$$

$$a = 0.89 \exp(-0.016K_t) \quad (K_t > 43 \text{ g}). \quad (7)$$

The equations given above can be used to estimate the parameter values in Eq. (1) as a function of age. We require only an estimate of the mass of K in the whole body at each age. For example, age-specific values for typical males of various ages are given in Table 1.

In dosimetric applications of this simplified retention function (recall that it should be applied only to long-lived isotopes of Cs), it is assumed that activity is uniformly distributed in the body except for the skeleton. Activity in the skeleton is assumed to be deposited uniformly on bone surfaces; this oversimplification may be modified soon since it may yield slight overestimates of dose to bone surfaces and underestimates to active marrow, which is expected to contain part of the skeletal Cs (cf. Williams and Leggett 1986). The uptake fraction for the skeleton of an adult is assumed to be 0.07 (Williams and Leggett 1986); until better data are available the fraction assigned to the skeleton in children is derived by scaling to the cellularity of the bone marrow as estimated by Cristy (1981). Estimated age-specific

uptake fractions for the skeleton are listed in Table 1. The given two-exponential removal function is applied both to the skeleton and to the rest of the body.

## REFERENCES

- Cristy, M., 1981, Active Bone Marrow Distribution as a Function of Age in Humans, *Phys. Med. Biol.* 26, 389-400.
- International Commission on Radiological Protection, 1975, *Publication 23, Report of the Task Group on Reference Man*, Pergamon Press, Oxford.
- International Commission on Radiological Protection (ICRP), 1979, *Limits for Intakes of Radionuclides by Workers*, Publication 30, Pergamon Press: Oxford.
- Leggett, R. W., 1983, *Metabolic Data and Retention Functions for the Intracellular Alkali Metals*, NUREG/CR-3245, ORNL/TM-8630.
- Leggett, R. W., 1986, Predicting the Retention of Cs in Individuals, *Health Phys.* 50, 747-759.
- Lloyd, R. D., Mays, C. W., McFarland, S. S., Zundel, W. S., and Tyler, F. H., 1973, Metabolism of Rb-83 and Cs-137 in Persons with Muscle Disease, *Radiat. Res.* 54, 463-478.
- Wagner, W. W., Mays, C. W., Lloyd, R. D., Pendleton, R. C., and Zundel, W. S., 1966, Potassium Studies in Humans, in *Research in Radiobiology*, University of Utah Report COO-119-235, 107-136.
- Williams, L. R. and Leggett, R. W., 1986, The Distribution of Intracellular Alkali Metals in Reference Man, *Phys. Med. Biol.* 31, in press.

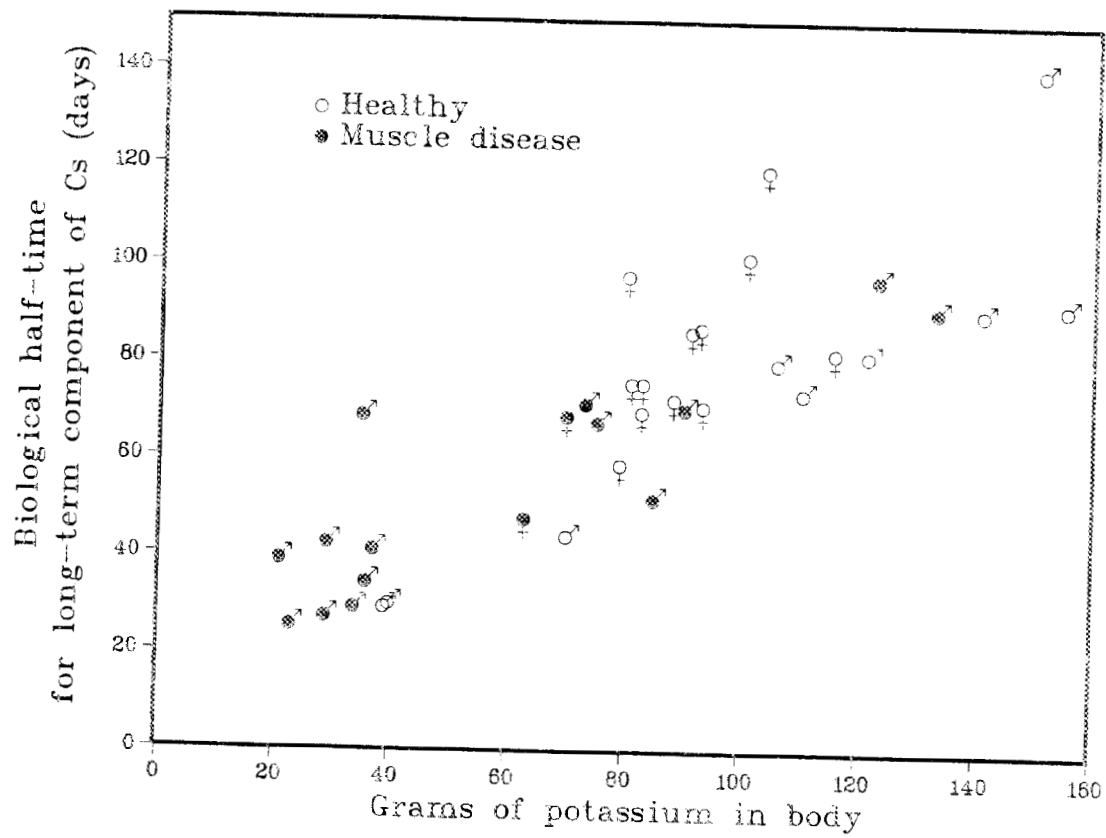


Figure 1. Total-body potassium vs. the biological half-time for the long-term component of cesium retention in the Utah subjects.

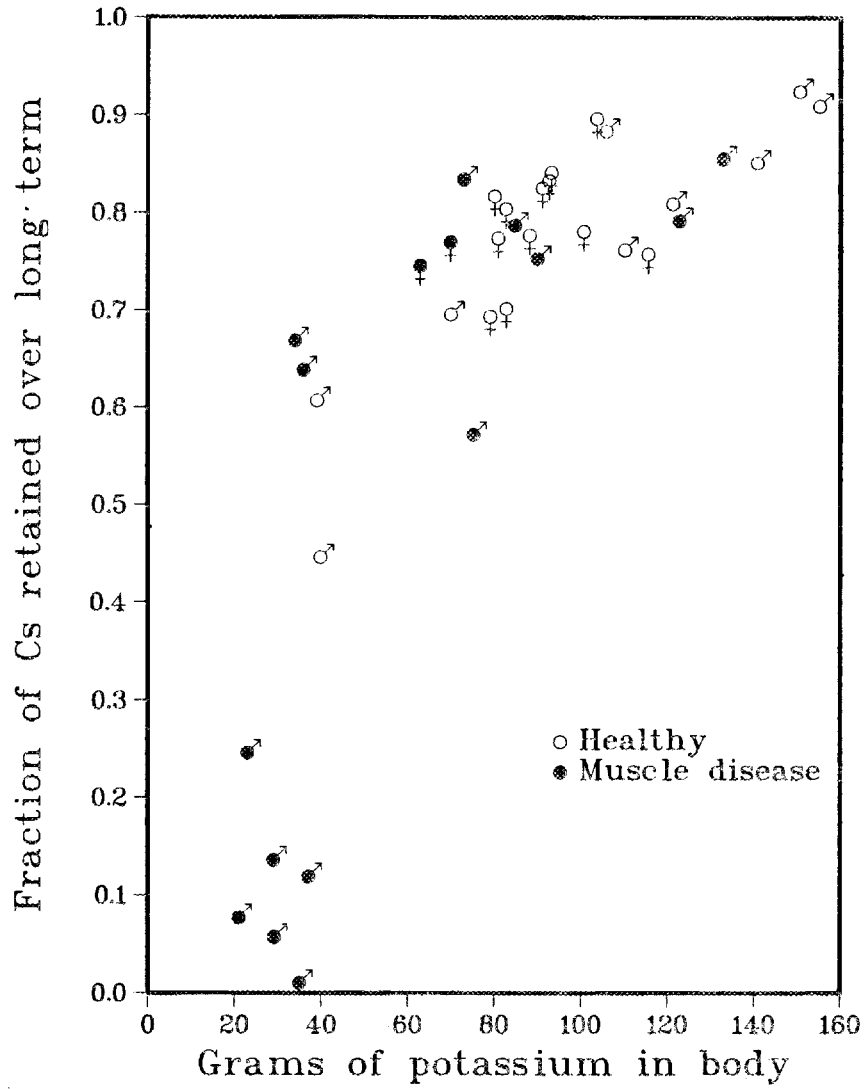


Figure 2. Total-body potassium vs. the fraction of cesium retained over a long term by the Utah subjects.

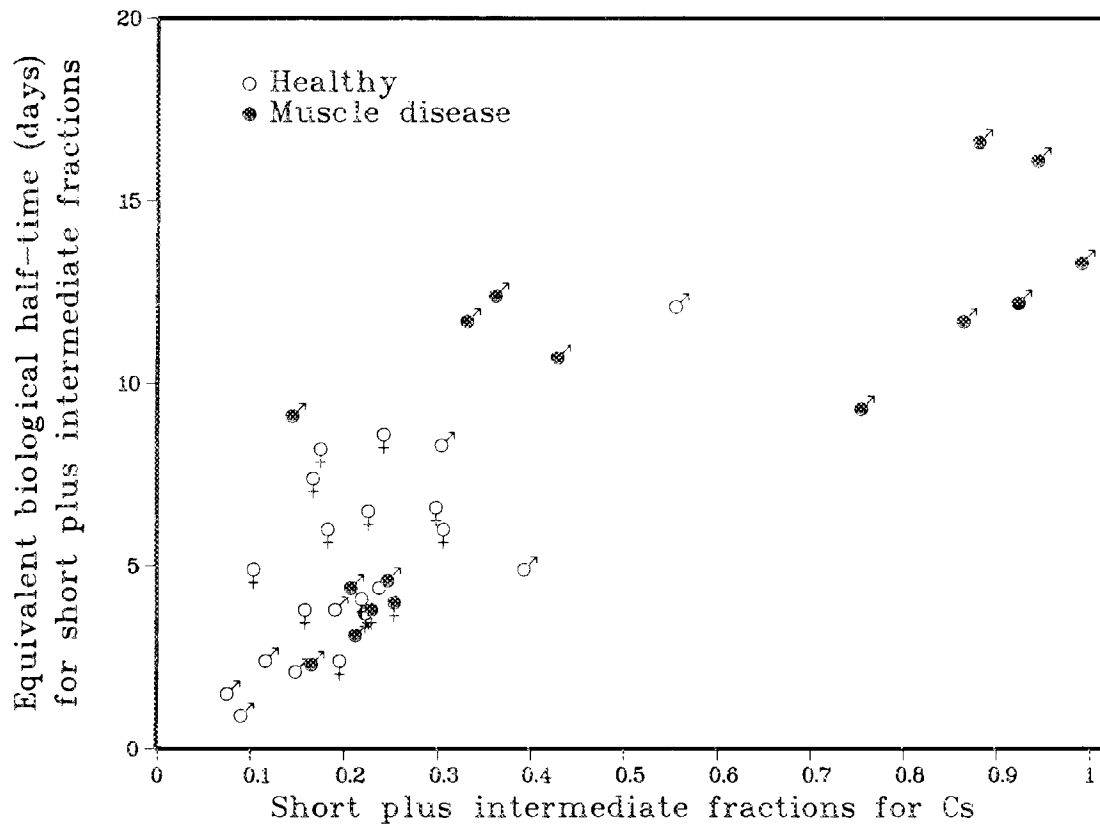


Figure 3. Total-body potassium vs. the equivalent biological half-time for the fraction of cesium in the Utah subjects associated with early excretion.

Table 1. Age-specific biological half-times and compartmental fractions in the simplified retention model for long-lived cesium isotopes in males.

| Age      | Total-body K <sup>a</sup><br>(g) | Short plus<br>intermediate term<br>fraction | Short plus<br>intermediate term<br>half-time T <sub>1</sub> (d) | Long-term<br>fraction | Long-term half-<br>time T <sub>2</sub> (d) | Fractional<br>uptake by<br>skeleton |
|----------|----------------------------------|---|---|-----------------------|--|-------------------------------------|
| Newborn  | 5.2                              | 0.60  | 22  | 0.40                  | 22   | 0.22                                |
| 100 days | 11.4                             | 0.60  | 16  | 0.40                  | 16   | 0.20                                |
| 1 year   | 20.8                             | 0.60  | 13  | 0.40                  | 13   | 0.19                                |
| 5 years  | 42.7                             | 0.45  | 9.1   | 0.55                  | 30   | 0.15                                |
| 10 years | 71.0                             | 0.30  | 5.8   | 0.70                  | 50   | 0.11                                |
| 15 years | 131.4                            | 0.13  | 2.2   | 0.87                  | 93   | 0.09                                |
| Adult    | 150                              | 0.10  | 1.6   | 0.90                  | 107  | 0.07                                |

<sup>a</sup>From combined data of Wagner et al. (1966) and ICRP Publication 23 (1975).

BIOKINETICS OF RUBIDIUM: ANOTHER EXAMPLE OF A SIMPLE  
AGE-SPECIFIC BIOKINETIC MODEL WITH PHYSIOLOGICAL UNDERPINNINGS

DEVELOPMENT OF A DETAILED MODEL FOR SHORT-LIVED Rb

The physiological behavior of rubidium is very similar to that of potassium, although the two elements have slightly different distributions and retention times apparently arising primarily from slower passive transport of Rb across cell membranes (Leggett 1983). The modeling scheme indicated earlier for K applies well to Rb with some minor adjustments in parameter values. Rate constants for Rb can be estimated using direct measurements in humans and animals, modification of rate constants for K based on relative rates of membrane transport that have been established for Rb versus K, and a careful determination of equilibrium values of Rb in human organs and tissues.

With regard to determination of proper equilibrium values, we have found that the Rb content assigned to the organs of ICRP Reference Man (ICRP 1975) involves substantial errors. For example, the assignment of a high content of Rb to the skeleton (~30% of whole-body Rb) can be traced to a single reported value on which the decimal point was apparently misplaced by the compilers of ICRP Reference Man. We believe that a more reasonable estimate, based on reanalysis of older data together with more recent information, is 5% of whole-body Rb in the adult male (Williams and Leggett 1986), but the percentage may be greater in children. Rubidium in the skeleton appears to reside primarily near bone surfaces and in red marrow (Williams and Leggett 1986). We believe that the cellularity of the bone marrow is a good index for the age-specific fraction of Rb taken up by the skeleton.

PROBLEMS WITH THE ICRP MODEL FOR Rb

In the metabolic model for rubidium given in ICRP Publication 30 (1979), 25% of activity reaching the bloodstream is assumed to be uniformly distributed in the skeleton. The remainder is assumed to be uniformly distributed throughout the rest of the body. Activity in all parts of the body, including the skeleton, is assumed to be removed with a biological half-time of 44 days.

The large amount assumed to go to the skeleton in the ICRP model is based on the high percentage erroneously assigned to the skeleton in the earlier ICRP Publication 23 on Reference Man; this assumption is also defended on the basis that Rb and K are chemically similar and "bone tissue fluid has a much higher concentration of potassium than does plasma". Yet, in the ICRP model for potassium, the skeleton was not assigned an elevated deposition fraction. This is an illustration of the use and misuse of physiological considerations in the ICRP retention models. These considerations are scattered and inconsistent and generally are not used in such a way as to contribute much to selection of parameter values.

CORRECTION OF THE ICRP MODEL AND EXTENSION TO OTHER AGE GROUPS (FOR LONG-LIVED ISOTOPES OF Rb)

The methods illustrated earlier for long-lived Cs isotopes can also be used to derive a simple age-dependent model for long-lived isotopes of Rb. That is, measurements of Rb and K in humans (Lloyd and coworkers 1973) can be used to develop an age-specific, exponentially declining retention function whose parameters vary with an "observable" or predictable quantity, namely, total-body K. While two exponential terms were needed for Cs, a single exponential term may suffice for description of retention of whole-body Rb, since the component of rapid clearance is always small and is even absent in many cases. It may be prudent to give separate consideration to the skeleton, not only to emphasize the change in assumptions from those in ICRP Publication 30 but also because the fraction going to skeleton may vary substantially with age. Because there appears to be no particularly long residence time in the skeleton and because there is considerable remixing of Rb among body tissues and fluids, we will assign a common biological half-time to the skeleton and to the rest of the body.

Comparison of the equivalent biological half-time (T) of Rb in the body with total-body K ( $K_t$ ) is made in Fig. 1. The following best-fitting line is obtained from the data for healthy males:

$$T = 13 + 0.23K_t \quad (R=0.89). \quad (1)$$

An estimate of T as a function of  $K_t$  for females is obtained by assuming that there is no difference between males and females until age 6-7 years (as with Cs); this is, we obtain the best-fitting line for data for healthy females, with the restriction that the line must go through the point (43,22.9), where 43 g is the estimated value for  $K_t$  for age 6.5 years and 22.9 days is the value of T for males when  $K_t=43$  g. For females we obtain the relation:

$$T = 6.6 + 0.38K_t, K_t > 43 \text{ g} \quad (2)$$

Age-specific estimates for the biological half-time T can be obtained by substituting age-specific values for  $K_t$  into Eqs. (1) and (2). Age-dependent parameter values for the simplified retention function for males are given in Table 1. The age-specific estimates for the fraction of whole-body Rb residing in the skeleton are based on cellularity data for marrow. For dosimetric purposes skeletal Rb may be assumed to be equally divided between skeletal surfaces and red marrow.

#### REFERENCES

- Cristy, M., 1981, Active Bone Marrow Distribution as a Function of Age in Humans, *Phys. Med. Biol.* 26, 389-400.
- International Commission on Radiological Protection, 1975, *Publication 23, Report of the Task Group on Reference Man*, Pergamon Press, Oxford.
- International Commission on Radiological Protection (ICRP), 1979, *Limits for Intakes of Radionuclides by Workers*, Publication 30, Pergamon Press: Oxford.
- Leggett, R. W., 1983, *Metabolic Data and Retention Functions for the Intracellular Alkali Metals*, NUREG/CR-3245, ORNL/TM-8630.
- Lloyd, R. D., Mays, C. W., McFarland, S. S., Zundel, W. S., and Tyler, F. H., 1973, Metabolism of Rb-83 and Cs-137 in Persons with Muscle Disease, *Radiat. Res.* 54, 463-478.
- Wagner, W. W., Mays, C. W., Lloyd, R. D., Pendleton, R. C., and Zundel, W. S., 1966, Potassium Studies in Humans, in *Research in Radiobiology*, University of Utah Report COO-119-235, 107-136.
- Williams, L. R. and Leggett, R. W., 1986, The Distribution of Intracellular Alkali Metals in Reference Man, *Phys. Med. Biol.* 31, in press.

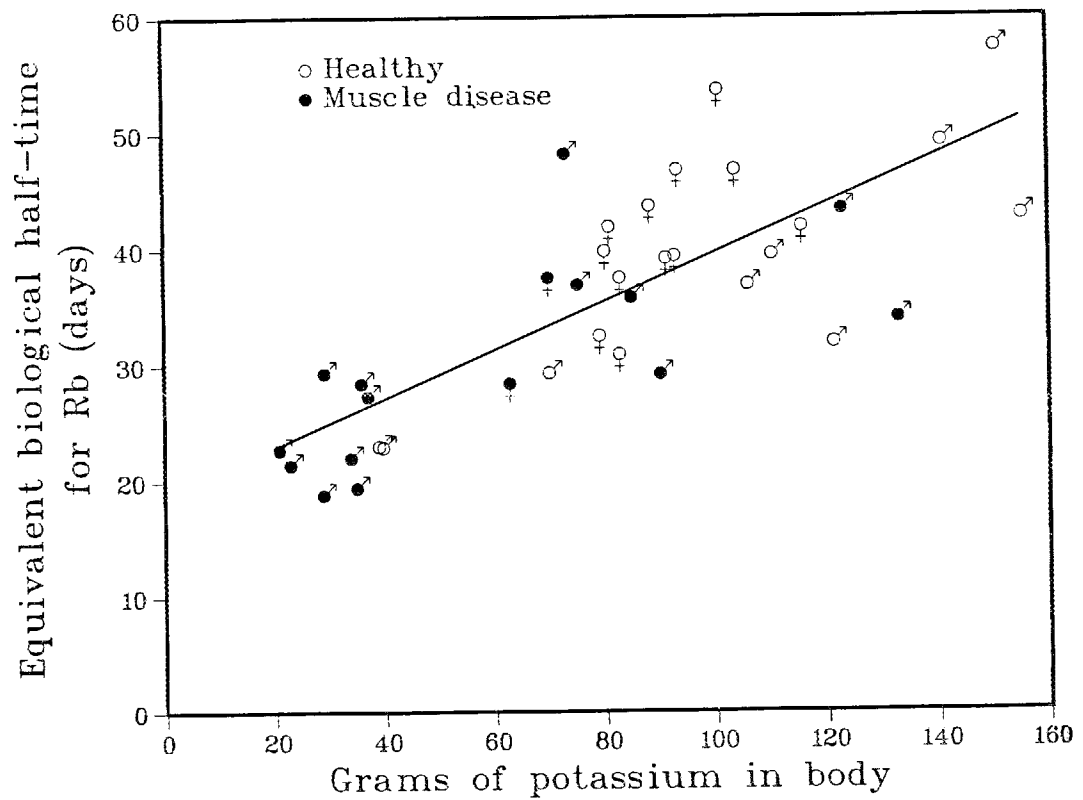


Figure 1. Relation between total-body K and biological half-time for Rb.

Table 1. Age-specific biological half-time and uptake fraction for skeleton in the simplified retention model for Rb in males.

---

| Age      | Total-body K<br>(g) | Biological<br>half-time (d) | Fraction assigned<br>to skeleton |
|----------|---------------------|-----------------------------|----------------------------------|
| Newborn  | 5.2                 | 14                          | 0.16                             |
| 100 days | 11.4                | 16                          | 0.15                             |
| 1 year   | 20.8                | 18                          | 0.14                             |
| 5 years  | 42.7                | 23                          | 0.11                             |
| 10 years | 71.0                | 29                          | 0.08                             |
| 15 years | 131.4               | 43                          | 0.06                             |
| Adult    | 150                 | 48                          | 0.05                             |

---

BIOKINETICS OF PLUTONIUM, AMERICIUM, AND CURIUM: ILLUSTRATIONS OF  
MODELING AGE-SPECIFIC TRANSLOCATION OF ACTIVITY WITHIN THE SKELETON

Although there is a large amount of information on biokinetics of plutonium and related elements in various species, there is a paucity of direct information on age-specific behavior of these elements in humans. Some information can be gained from observations of differences with age in biokinetics in experimental animals and from a few studies of humans of different ages exposed accidentally or from radioactive fallout. However, construction of meaningful age-specific biokinetic models for these elements in humans must rely to a large extent on information concerning the processes controlling their movement in the body, particularly their movement within the skeleton and liver and recycling of activity between these organs.

In the following we describe a model for plutonium and then discuss known or suspected differences in the biobehaviors of the related elements americium and curium. It should be pointed out that there are no really sound observations with which to check the accuracy of predictions produced by these models for children. Until such observations are available (if ever), the degree of confidence in the predictions must depend primarily on the quality of the model foundation, the bases for selection of parameter values, and the credibility of assumptions made when no direct evidence is available. As will be illustrated in later sections, however, the physiological systems approach to biokinetic model has a major advantage even when parameter values and assumptions cannot be firmly based, namely, it provides a more meaningful basis for analysis of uncertainties and/or sensitivities than can usually be made for purely empirical models.

A more detailed discussion of the model for plutonium in adult humans of different ages can be found in an article by Leggett (1985). (Also see Report ORNL/TM-8795 (Leggett 1984), which includes a sensitivity/uncertainty analysis.) In this report we do not consider differences among adults. Also, attention is restricted to plutonium that reaches the bloodstream in monomeric or highly soluble form; some of the parameter values would be much different for polymeric, colloidal, or insoluble forms.

## THE INITIAL DISTRIBUTION OF Pu IN THE BODY

Retention and translocation of Pu that has reached the bloodstream can be modeled using three principal compartments: skeleton, liver, and remaining tissue. As indicated in Fig. 1, a detailed examination of the biokinetics in the skeleton and liver requires consideration of further subdivision of these compartments as described in the following (also see Leggett 1985).

It appears from data for man and other species that, at all ages, approximately 80% of Pu in the bloodstream is divided between the skeleton and liver, and approximately 20% goes to remaining tissue and excretion. In experiments with beagles, the division of Pu between skeleton and liver varied with age, with skeletal uptake being near 70% in juveniles and between 40 and 60% in adults (Lloyd et al. 1976, 1978a, 1978b). Langham et al. (1950) estimated that in persons injected with Pu, approximately 66% was deposited in the skeleton and 23% in the liver. Durbin (1972) reanalyzed the human data to account for the non-uniformity of Pu in samples of bone; she estimated that about 49% was in the skeleton and 31% in the liver at 4 to 457 days after injection. A few years ago, a major portion of the skeleton of one of the injected persons, a young woman injected at age 18 years and dying 17 months later (case HP-4), was analyzed and found to contain about 55% of the injected amount (Larsen, Oldham, and Toohey 1979). Since there was ample time for a small portion of the Pu to be translocated from the skeleton before this woman's death, the fraction originally deposited in her skeleton may have been higher than 55%.

Our model relies on both the human and beagle data. We assume that skeletal uptake is 70% for newborns and 50% for adults. For persons 1-15 years of age, the average of the adult and newborn values is applied. At all ages, the sum of the skeletal and hepatic fractions is assumed to be 80%, with 20% going to remaining tissue and excretion.

## UPTAKE AND TRANSLOCATION OF Pu BY THE SKELETON

To describe retention of Pu in the skeleton, it is convenient to view the skeleton as being divided into two primary compartments, one associated with cortical bone and the other with trabecular bone. Each

of these primary compartments is further divided into three subcompartments: bone surface, bone volume, and a compartment containing the associated bone marrow. The latter compartment may receive Pu that is removed from bone surface or volume; Pu may reside in this compartment temporarily before being returned either to the bloodstream or to bone surfaces (Fig. 1). Because of the large amount of recycling of Pu among the skeletal compartments, blood, and other organs, recycling is considered explicitly in the model. In the following discussion, the indicated pathways correspond to the arrows in Fig. 1.

*Pathways K and L.* Plutonium is deposited initially on bone surfaces, with highest deposition being at sites with red (hematopoietic) marrow and lowest deposition at sites of yellow (fatty) marrow (Wronski, Smith, and Jee 1980). (Pathways K\* and L\* from plasma to bone marrow are also included in the model for consideration of insoluble, colloidal, or polymeric material that has reached the blood; parameter values for these forms are not discussed here.) Since red marrow is more highly vascularized than yellow marrow, the degree of vascularity at a given skeletal site may be a determining factor in the initial distribution of Pu (Wronski, Smith, and Jee 1980; Humphreys, Fisher, and Thorne 1977). In the adult, nearly all of the red marrow is in trabecular bone (Cristy 1981), and deposition on trabecular bone may be greater than on cortical bone. In children, some or all of the marrow in cortical bone is active (Cristy 1981), and a more uniform distribution on cortical and trabecular bones is expected. There is at least as much trabecular surface in the skeleton as cortical surface, and possibly more (Beddoe, Darley, and Spiers 1976; Beddoe 1977). If Pu deposited uniformly on all surfaces, then at least 50% of the initial deposit in the skeleton should be assigned to trabecular surfaces. Since it is known that Pu deposits more heavily in areas of active marrow and almost all active marrow in adults is in trabecular bone, it seems reasonable to assign more than 50% of the initial deposit to trabecular surfaces of the adult skeleton. On the other hand, data of Larsen, Oldham, and Toohy (1979) for an adult human subject injected with Pu suggest that trabecular bone may not have received much more Pu than cortical bone. Thus a 60%-40% division between cortical and

trabecular bone was arbitrarily assigned for adults, and a 50%-50% division was assigned for nonadults because the distribution of Pu is probably more uniform in the skeleton of nonadults.

*Pathways A, B, C, and D*

Bone surfaces labeled with Pu may remain unchanged, or they may be buried by formation of new bone (A and C) or resorbed by osteoclasts (B and D) (Jee 1972a, 1972b). The rate of removal from surfaces by burial or resorption depends on the age of the individual and on the bone surface type (trabecular or cortical). To estimate rate constants for pathways A, B, C, and D, it is necessary to understand the relationship between bone formation and bone resorption. There are two somewhat different pictures of this relationship presented in the literature. Some authors describe bone addition and resorption as occurring on opposite sides of a bone (or bone trabecula), so that the bone is pictured as continually "drifting" in a given direction (Priest and Hunt 1979, Enlow 1963). Other authors describe resorption and addition as occurring in the same location; first an area of bone is excavated by osteoclasts, and then the same area is refilled with osteoid which is later mineralized (Frost 1976). The actual events appear to involve some combination of these models. Bone "drift" may be the predominant process during growth and perhaps into young adulthood but may diminish considerably after the skeleton has matured fully, although drift apparently occurs to some extent at all ages.

If bone formation and resorption always occurred on opposite surfaces of a bone segment, then the removal rate for Pu on bone surface would be approximately the sum of the resorption rate  $\lambda_1$  and the formation rate  $\lambda_2$ . This situation is assumed for children. On the other hand, if formation represented only the immediate replacement of resorbed bone, then the removal rate would be approximately  $\lambda_1$  and Pu would be buried in volume only by depositing in unmineralized osteoid and moving to the mineralized surface underneath the osteoid. In this model, an intermediate scenario is assumed for adults, with the burial rate in bone volume being  $0.5 \lambda_2$ , and the removal rate from bone surface being  $\lambda_1 + 0.5 \lambda_2$ .

Characterization of the age-dependent resorption rate  $\lambda_1$  is discussed in an article by Leggett, Eckerman, and Williams (1982). The simplifying assumption is made in this model that  $\lambda_1 = \lambda_2$ . In older adults  $\lambda_1$  may be larger than  $\lambda_2$ , resulting in a net bone loss, but we believe the difference  $\lambda_1 - \lambda_2$  is small at most adult ages. In children,  $\lambda_1$  may be smaller than  $\lambda_2$ , but the assumption that  $\lambda_1 = \lambda_2$  adds an element of conservatism to estimates of dose to radiosensitive tissues (assuming our estimate of  $\lambda_1$  is reasonably accurate). Since more detailed modeling of  $\lambda_2$  would involve large uncertainties, it would be difficult to justify adjusting the model to account for growth processes not already implicitly considered in the present estimate of  $\lambda_2$ .

Plutonium resorbed by osteoclasts may be released and concentrated by macrophages in bone cavities, particularly in marrow (Jee 1972a). The length of time that Pu remains in these macrophages is not known. In beagles receiving low doses of Pu, peak labeling of macrophages in bone marrow was at two years post injection, and all labeled macrophages had disappeared at four years post injection (Jee 1972b). This suggests a half-time in bone marrow of beagles that is short compared with two years. We have assigned a half-time of 90 days for all ages. This could be somewhat conservative with regard to estimates of dose to bone surfaces and marrow, since some Pu in resorbed bone may be dissolved and recycled systemically without being taken up by macrophages, and with little or no sojourn time in the marrow.

#### *Pathways E and F*

Pu buried in bone volume may eventually become volume distributed as the bone section "drifts" due to remodeling. The time required for Pu to become volume distributed is assumed to depend on the bone turnover time. If the resorption rate for trabecular bone is  $k$  per year, then buried Pu may begin to be resorbed in about  $1/k$  years after exposure. (Account must be taken of the fact that  $k$  varies with age.) Because of the slow turnover time for cortical bone at most ages, much of the Pu buried in cortical bone of adolescents and adults may never be recycled.

*Pathways G, H, I, and J*

Autoradiographs suggest that both local (G and H) and systemic (I and J) redeposition onto bone surfaces occurs (Wronski, Smith, and Jee 1980; Priest and Giannola 1980). If Pu is released in a highly vascularized area and more remote from bone surfaces, then systemic deposition is likely. If Pu is released in a less vascularized area, it is likely that most Pu will be deposited locally. For lack of precise values, it seems reasonable to assume that 50% of the Pu in the transfer compartments is redeposited locally and 50% is carried back to the bloodstream, from where it may still be deposited on bone surfaces. Because of the recycling of Pu from the bloodstream, any error in the assumption of an even split between locally and systemically recycled Pu is automatically adjusted to some extent.

## THE MODEL FOR Pu IN THE LIVER

It is known from animal studies (Boocock et al. 1970, Taylor et al. 1966, Stevens et al. 1971) that some Pu may leave the liver via blood while some may leave in bile, that Pu is taken up by hepatocytes but later transferred to RE cells, and that Pu may reside for years in the RE system. It is also suggested by autopsies of persons exposed to Pu several years previously that this nuclide may reside for many years in the human liver and that the ratio of Pu in skeleton to Pu in liver is larger in pre-adults than in adults. This supposedly smaller activity in liver in children could result from a smaller deposition in liver at younger ages, as we have assumed, or a more rapid removal from liver at younger ages, or both. It might be suspected that Pu is removed more rapidly from the liver at younger ages because of similarities between Pu and Fe, but we believe the Fe-Pu analogy is too weak in this case to justify such a non-conservative assumption at this time. In fact, other than the fraction of activity initially deposited in liver, we cannot find reason to impose any assumptions regarding age dependence with regard to the liver.

The movement of Pu within the liver, as described in the preceding paragraph, is depicted explicitly in our model (Fig. 1). Selection of rate constants for liver is discussed in detail in the article by

Leggett (1985). Almost all of the loss of Pu from the liver is assumed to be due to movement of activity from RE cells to blood, which is assumed to occur with a half-time of 10 years at all ages. This half-time, together with our assumptions concerning Pu in the skeleton, yields estimates of the ratio of Pu in liver to Pu in skeleton that agree with autopsy data for different age groups (Leggett 1985).

#### THE MODEL FOR Pu IN SOFT TISSUE AND EXCRETION

Although only one soft tissue compartment is indicated in Fig. 1, soft tissue is, in effect, assumed to consist of two compartments which together receive 20% of the Pu in blood minus an amount excreted fairly rapidly after reaching blood (4%) (Leggett 1985). One soft tissue compartment is associated with excretion pathways such as kidney, bladder, intestines, and bile. This compartment is assumed to receive 6% of the activity in blood, and activity leaves only via excretion. Although liver is considered separately, for computational convenience we consider activity that may actually leave liver via bile as being channeled through this soft tissue excretion compartment. The second soft tissue compartment is associated with the remaining tissue, that is, all soft tissue not including liver and not lying in a direct excretion pathway. This would include most muscle tissue, lung tissue, and portions of the viscera, for example. This compartment is assumed to receive 10% of the activity in blood, and activity leaving this compartment is recycled to blood. Pu is assumed to leave both soft tissue compartments with a half-time of 500 days, which is based loosely on conclusions reached by Durbin (1972).

In addition to activity reaching excretion after a delay in soft tissue, some activity will be rapidly excreted from blood. In this model we assume that 4% of Pu reaching blood is rapidly excreted. Our estimates for the amount excreted are from data for adult humans (Durbin 1972, Langham et al. 1950, Rundo 1979, Voelz et al. 1979, Leggett 1985).

#### THE MODELING FOR RECYCLING OF SYSTEMIC Pu

Plutonium reaching the bloodstream after removal from skeleton, liver, or soft tissue is assumed to trace the same pathways as the initial deposit in blood. It is assumed that activity leaves blood with

an effective half-time of 0.85 days. A more detailed blood model is available for situations in which short-term kinetics are of interest (Leggett 1985).

#### ADJUSTMENTS IN THE MODELS FOR AMERICIUM AND CURIUM

Plutonium, americium, and curium appear to have fairly similar metabolic properties, with one important exception being that plutonium has a much higher affinity for  $\beta$  globulins in blood (Turner and Taylor 1968). Differences in affinity for proteins may result in a much more rapid clearance of americium and curium from blood, a higher filtration fraction by the kidney, and less propensity to follow iron pathways over the short term as compared with plutonium. Since there is little information on comparative behavior of these elements in humans, the following quantifications of differences were based primarily on results of animal studies.

1. It is suggested by results of Turner and Taylor (1968) that the effective half-time of Am or Cm in blood may be 2 or 3 orders of magnitude lower than that of Pu. We have assumed a half-time of 0.01 days for Am and Cm in blood.
2. Studies of Lloyd and coworkers (1972, 1974, 1976, 1978a, 1978b) indicate that about 80% of Pu, Am, or Cm goes to skeleton and liver, but Pu may have a relatively higher affinity for skeleton and/or Am and Cm a relatively higher affinity for liver. Basing our estimates on these results for dogs, we assume that 80% of Pu, Am, or Cm goes to skeleton plus liver but that the relative percentages going to skeleton in adults are Pu:Am:Cm = 50%:30%:45%. For newborns, 70% of Pu, Am, or Cm is assumed to go to skeleton, and for persons of 1-15 years of age, the average of the adult and newborn values is applied.
3. The distribution of Am in the skeleton may be more uniform than the distribution of Pu (Lloyd et al. 1972). Also, the distributions of Am and Cm in the skeleton appear to be very similar (Nenot et al. 1972). We assume that 50% of Am or Cm that goes to skeleton is deposited on trabecular surfaces and 50% is deposited on cortical

surfaces at all ages; this compares with a ratio for Pu of 60%:40% for adults and 50%:50% for non-adults.

4. Experimental evidence for dogs indicates that early urinary excretion of Am or Cm is greater than for Pu (Lloyd et al. 1972, 1974, 1976, 1978a, 1978b), probably because of the weaker attachment to proteins exhibited by Am and Cm. We assume that the comparative fractions of rapid excretion of Pu, Am, and Cm in blood are 0.04:0.07:0.06, based on studies with dogs. Since fecal excretion data for actinides in animals cannot be readily extrapolated to humans, we cannot improve on the simple assumption that fecal excretion of Pu, Am, and Cm are identical in humans. Also, we shall assume that the model for Pu concerning excretion via soft tissue applies to Am and Cm.
5. Data for humans indicate that Am may have a net biological half-time in the liver as short as 2-8 years (see the article by Griffith et al. 1983, including remarks by M. E. Wrenn on p. 554). Durbin and Schmidt (1985) estimated a net half-time of about 3 years for Am in liver but a removal rate from liver to plasma of slightly less than 1.0 per year. We adopt a rate of 1.0 per year for removal of Am or Cm from liver to plasma.

All other features of the Pu model are assumed to apply to Am and Cm.

#### REFERENCES

- Beddoe, A. H., 1977, Measurements of the Microscopic Structure of Cortical Bone, *Phys. Med. Biol.* 22, 298-308.
- Beddoe, A. H., Darley, P. J., and Spiers, F. W., 1976, Measurements of Trabecular Bone Structure in Man, *Phys. Med. Biol.* 21, 589-607.
- Boocock, G., Danpure, C. J., Popplewell, D. S., and Taylor, D. M., 1970, The Subcellular Distribution of Plutonium in Rat Liver, *Radiat. Res.* 42, 381-396.
- Bruenger, F. W., Stover, B. J., Stevens, W., and Atherton, D. R., 1969, Exchange of Pu(IV) Between Transferrin and Ferritin *In Vitro*,

- Health Phys.* 16, 339-340.
- Cristy, M., 1981, Active Marrow Distribution as a Function of Age in Humans, *Phys. Med. Biol.* 26, 389-400.
- Durbin, P. W., 1975, Plutonium in Mammals: Influence of Plutonium Chemistry, Route of Administration, and Physiological Status of the Animal on Initial Distribution and Long-Term Metabolism, *Health Phys.* 29, 495-510.
- Durbin, P. W., 1972, Plutonium in Man: a New Look at the Old Data, in *Radiobiology of Plutonium*, ed. B. J. Stover and W. S. S. Jee, J. W. Press, Salt Lake City, 469-530.
- Durbin, P. W., Horovitz, M. W., and Close, E. R., 1972, Plutonium Deposition Kinetics in the Rat, *Health Phys.* 22, 731-741.
- Durbin, P. W. and Schmidt, C. T., 1985, Part V. Implications for Metabolic Modeling, *Health Phys.* 49, Special Issue on The U. S. Transuranium Registry Report on the Am-241 Content of a Whole Body, pp. 623-661.
- Enlow, D. H., 1963, *Principles of Bone Remodelling*, Charles C. Thomas, Publishers, Springfield, Ill.
- Frost, H. M., 1976, A Method of Analysis of Trabecular Bone Dynamics, in *Bone Histomorphometry*, ed. P. J. Meunier, Armour Montagu, Paris, 445-473.
- Griffith, W. C., Mewhinney, J. A., Muggenburg, B. A., Boecker, B. B., and Cuddihy, R. G., 1983, Bioassay Model for Estimating Body Burdens of Am-241 from Excretion Analyses, *Health Phys.* 44, Supplement No. 1, 545-554.
- Humphreys, E. R., Fisher, G., and Thorne, M. C., 1977, The Measurement of Blood Flow in Mouse Femur and Its Correlation with Pu-239 Deposition, *Calcif. Tiss. Res.* 23, 141-145.
- International Commission on Radiological Protection, 1972, *Publication 19, The Metabolism of Compounds of Plutonium and Other Actinides*, Pergamon Press, Oxford.
- International Commission on Radiological Protection, 1979, *Publication 30, Limits for Intakes by Workers*, Pergamon Press, Oxford.
- Jee, W. S. S., 1972a, Distribution and Toxicity of Pu-239 in Bone, *Health Phys.* 22, 583-595.
- Jee, W. S. S., 1972b, Pu-239 in Bones as Visualized by Photographic and

- Neutron-Induced Autoradiography, in *Radiobiology of Plutonium*, J. W. Press, Salt Lake City, 171-193.
- Langham, W. H., Bassett, S. H., Harris, P. S., and Carter, R. E., 1950, *Distribution and Excretion of Plutonium Administered to Man*, Los Alamos Scientific Laboratory, LA-1151.
- Larsen, R. P., Oldham, R. D., and Toohy, R. E., 1979, Macrodistribution of Plutonium in the Human Skeleton, in *Actinides in Man and Animals, Proceedings of the Snowbird Actinide Workshop*, ed. M. E. Wrenn, 191-196.
- Leggett, R. W., 1985, A Model of the Retention, Translocation, and Excretion of Systemic Plutonium, *Health Phys.* 49, 1115-1137.
- Leggett, R. W., 1984, *Bioassay Data and a Retention-Excretion Model for Systemic Plutonium*, NUREG/CR-3346, ORNL/TM-8795.
- Leggett, R. W., Eckerman, K. F., and Williams, L. R., 1982, Strontium-90 in Bone: a Case Study in Age-Dependent Dosimetric Modeling, *Health Phys.* 43, 307-322.
- Lindenbaum, A., and Rosenthal, M. W., 1972, Deposition Patterns and Toxicity of Plutonium and Americium in the Liver, *Health Phys.* 22, 597-605.
- Lloyd, R. D., Atherton, D. R., Mays, C. W., McFarland, S. S., and Williams, J. L., 1974, The Early Excretion, Retention, and Distribution of Injected Curium Citrate in Beagles, *Health Phys.* 27, 61-67.
- Lloyd, R. D., Atherton, D. R., McFarland, S. S., Mays, C. W., Stevens, W., Williams, J. L., and Taylor, G. N., 1976, Studies of Pu(IV) Citrate in Beagles, *Health Phys.* 30, 47-52.
- Lloyd, R. D., Jee, W. S. S., Atherton, D. R., Taylor, G. N., and Mays, C. W., 1972, Americium-241 in Beagles: Biological Effects and Skeletal Distribution, in *Radiobiology of Plutonium*, ed. B. J. Stover and W. S. S. Jee, J. W. Press, Salt Lake City, 141-148.
- Lloyd, R. D., McFarland, S. S., Atherton, D. R., and Mays, C. W., 1978a, Plutonium Retention, Excretion, and Distribution in Juvenile Beagles Soon after Injection, *Radiat. Res.* 75, 633-641.
- Lloyd, R. D., McFarland, S. S., Atherton, D. R., Bruenger, F. W., Taylor, G. N., and Mays, C. W., 1978b, Early Retention of Pu-237 +

- Pu-239 in Mature Beagles," *Health Phys.* 35, 211-215.
- Nenot, J. C., Masee, R., Morin, M., and Lafuma, J., 1972, An Experimental Comparative Study of the Behavior of Np-237, Pu-238, Pu-239, Am-241, and Cm-242 in Bone, *Health Phys.* 22, 657-665.
- Priest, N. D., and Hunt, B. W., 1979, The Calculation of Annual Limits of Intake for Plutonium-239 in Man Using a Bone Model which Allows for Plutonium Burial and Recycling, *Phys. Med. Biol.* 24, 525-546.
- Priest, N. D., and Giannola, S. J., 1980, Plutonium-241 Deposition and Redistribution in the Rat Rib, *Int. J. Radiat. Biol.* 37, 281-298.
- Rundo, J., 1979, The Late Excretion of Plutonium Following Acquisition of Known Amounts, in *Actinides in Man and Animals, Proceedings of the Snowbird Actinide Workshop*, ed. M. E. Wrenn, 253-260.
- Stevens, W., Bruenger, F. W., Atherton, D. R., and Stover, B. J., 1971, *Subcellular Distribution of Am(III) and Pu(IV) in Livers Studied Serially*, Univ. of Utah Report COO-119-244, 159-174.
- Stevens, W., Bruenger, F. W., and Stover, B. J., 1968, *In vivo* Studies on the Interaction of Pu(IV) with Blood Constituents, *Radiat. Res.* 33, 490-500.
- Stover, B. J., Bruenger, F. W., and Stevens, W., 1968, The Reaction of Pu(IV) with the Iron Transport System in Human Blood Serum, *Radiat. Res.* 33, 381-394.
- Stover, B. J., Atherton, D. R., and Keller, N., 1959, Metabolism of Pu-239 in Adult Beagle Dogs, *Radiat. Res.* 10, 130-147.
- Taylor, G. N., Jee, W. S. S., Dockum, N. L., Hromyk, E., and Brewster, L., 1966, *Translocation of Pu-239 in Beagle Livers*, Univ. of Utah Report COO-119-234, 70-84.
- Turner, G. A., and Taylor, D. M., 1968, The Transport of Plutonium, Americium, and Curium in the Blood of Rats, *Phys. Med. Biol.* 13, 535-546.
- Voelz, G. L., Hempelmann, L. H., Lawrence, J. N. P., and Moss, W. D., 1979, A 32-Year Medical Follow-Up of Manhattan Project Plutonium Workers, *Health Phys.* 37, 445-485.
- Wronski, T. J., Smith, J. M., and Jee, W. S. S., 1980, The Microdistribution and Retention of Injected Pu-239 on Trabecular Bone Surfaces of the Beagle: Implications for the Induction of Osteosarcoma, *Radiat. Res.* 83, 74-89.

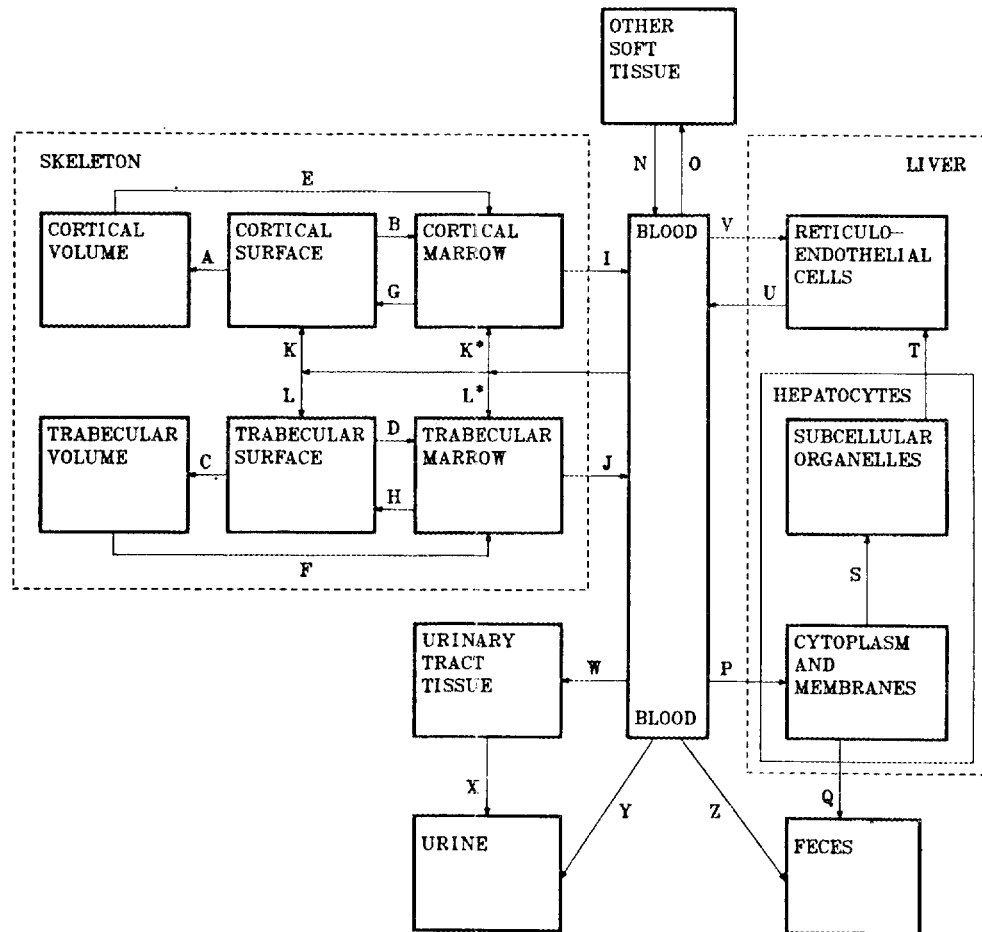


Figure 1. Diagram of the compartments used in the model and the direction of movement of activity among these compartments.

A GENERIC SCHEME TO AID IN THE CONSTRUCTION OF AGE-SPECIFIC  
BIOKINETIC MODELS FOR BONE-SEEKING RADIONUCLIDES

The model described for Pu and related elements in the preceding section has been expanded to a generic scheme that is useful in the study of the behavior of many bone-seeking radionuclides, particularly those with daughter products that may tend to migrate from the parent nuclide. This generic model is indicated in Fig. 1.

In this scheme, some potential paths of movement within the skeleton have been added to those already considered for Pu. For example, direct removal of activity from bone surfaces or volume to plasma has been included for consideration of radium, uranium, and other radioelements. An option to consider movement from bone volume to bone surface may also be added soon. Spleen has been included for treatment of certain important decay products with a propensity for this organ (such as isotopes of polonium). The boxes labeled "Respiratory Tract" and "GI Tract" in Fig. 1 refer not to single compartments but to multi-compartmental sub-models of the system; these sub-models are described in a later section. Also, the user may supply detailed models for liver, kidneys, spleen, or other tissues, but a single compartment in each case often suffices, particularly in situations where most decays occur in the skeleton.

In applying this or any other scheme to develop an age-specific biokinetic model, one must often select parameter values in the absence of element-specific quantitative data. As indicated in the section on Pu and related elements, element-independent data on bone growth and turnover may be useful in this regard. For example, radiobiological studies on species other than man yield the qualitative information that Pu remains fixed to bone surfaces until removed by bone modeling or remodeling. This can be used to estimate removal rates of Pu from bone surfaces in humans by appealing to Pu-independent quantitative data on bone remodeling. As another example, it appears that long-term removal of some radioelements from bone volume is due mainly to bone turnover, particularly in the growing animal. Element-independent data on bone turnover therefore is useful in estimating age-specific removal rates of these elements from bone volume.

Of course, this approach is not a panacea. For example, qualitative information indicates to us that many important radioelements, including radium and uranium, may remain on or near bone surfaces for several days before being removed to plasma and, to a lesser extent, bone volume. However, physiological considerations alone will not yield supportable age-specific removal rates for these elements from bone surfaces, since removal processes may be strongly element-specific. In fact, it is often easier to determine age-specific parameter values associated with bone mineral than those associated with soft tissues, including the non-mineral skeleton, because retention in soft tissues tends to depend much more on special properties of the element than does retention in bone mineral.

There is evidence that net biological half-times of some radioelements (e.g., K, Rb, Cs, I) in soft tissues are much shorter in children than adults. Other elements, including some toxic heavy metals, may have net biological half-times in some soft tissues that are as great (or greater) in growing animals as in adults (Jugo 1977). This could result from any of a variety of factors, including a higher rate of intestinal recycling of the biliary excreted fraction, a lower excretion rate, and greater binding with body ligands at younger ages (Jugo 1977). Whenever direct information or reasonable physiologically based assumptions concerning age-specific rate constants for soft tissues are lacking, we prefer to apply rate constants for adult soft tissues to all age groups. This may result in overestimates of dose to soft tissues of children in some cases, but we do not believe that substantial underestimates will often result. At least, we have not found evidence of any element with a radically greater biological half-time in soft tissues of growing animals than in soft tissues of adults.

In a recent article (Leggett, Dunning, and Eckerman 1985) we discussed the importance of a physiologically based modeling approach with regard to proper treatment of radioactive decay products born in the body. Examples were given in which the different types of assumptions concerning decay products made in ICRP Publication 2 (1959) and ICRP Publication 30 (1979) lead to differences of an order of magnitude in 50-year dose commitments to organs. In ICRP 2, daughter products born in an organ are assumed to be removed according to the

retention function of the daughter rather than that of the parent; in ICRP 30, daughters are assumed to remain with the parent, with a few exceptions. Our study revealed many cases in which neither of these blanket assumptions is appropriate and in which the structure of the ICRP models is too inflexible to allow a more realistic treatment. In addition to the benefit of allowing more realistic assumptions concerning decay products, the exercise of selecting age-specific parameter values for decay products born in an organ, using a physiologically based scheme such as that indicated in Fig. 1, reveals many important sources of uncertainties that may go unnoticed when employing more conventional retention models. For example, there is sometimes a "synergistic" effect on potential errors resulting from uncertainties associated with variation with age and those associated with treatment of decay products.

In the following two sections we describe parameter values for the generic scheme in Fig. 1 appropriate for thorium and uranium. We will not address the problem of modeling behavior of daughter products of specific isotopes of these elements; in fact, for lack of space we do not go into detail anywhere in this report on the problem of treating chains of nuclides. The reader is referred to the article by Leggett, Dunning, and Eckerman (1985) for an example of considerations that may go into selection of parameter values for decay products using a model framework similar to the generic scheme shown in Fig. 1.

#### REFERENCES

- International Commission on Radiological Protection, 1959, *Publication 2, Report of Committee 2 on Permissible Dose for Internal Radiation*, Pergamon Press, Oxford.
- International Commission on Radiological Protection, 1979, *Publication 30, Limits for Intakes by Workers*, Pergamon Press, Oxford.
- R. W. Leggett, D. E. Dunning, Jr., and K. F. Eckerman, 1985, Modelling the Behaviour of Chains of Radionuclides inside the Body, *Radiat. Prot. Dosim.* 9, 77-91.
- Yugo, S., 1977, Metabolism of Toxic Heavy Metals in Growing Organisms: A Review, *Environmental Res.* 13, 36-46.

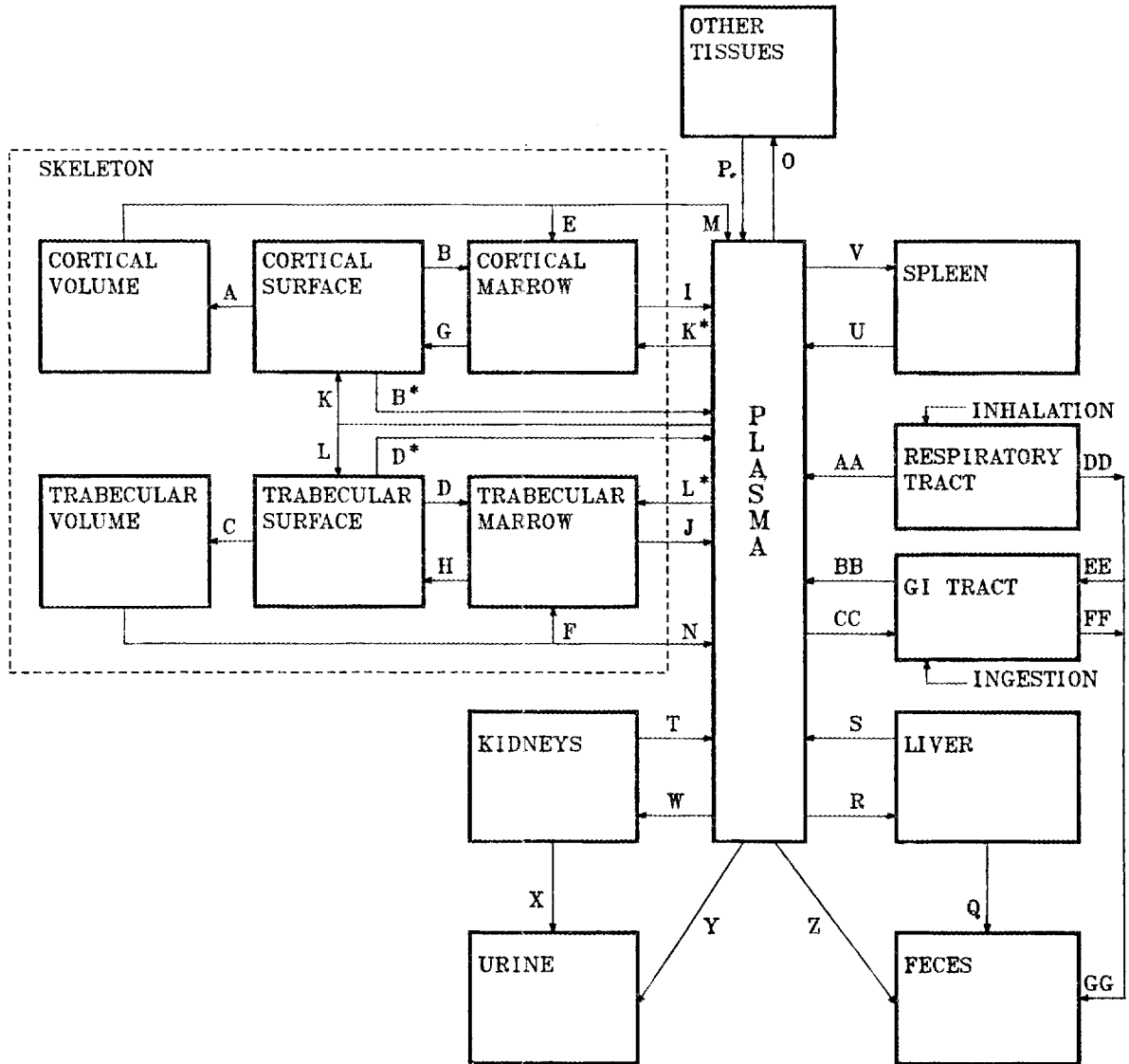


Figure 1. A generic scheme for bone-seeking radionuclides.

## APPLICATION OF THE GENERIC SCHEME TO THORIUM

In this section we outline our choices of parameter values for biokinetics of thorium. These are related to the generic modeling scheme described in the preceding section. It will become evident that many of the parameter values are somewhat arbitrary. As discussed in a later section, however, sensitivity analyses reveal that resulting estimates of long-term dose commitment to bone surfaces from Th-230, for example, may not be as uncertain as we at first might think. We later discuss another nuclide (U-238) for which substantial uncertainties associated with certain parameter values are not mitigated in resulting estimates of dose commitment to bone surfaces.

As is the case for Pu, Am, and Cm, there is a paucity of direct information on variation with age in the biobehavior of Th, so appeal must be made to information on age dependence in the processes known or thought to be involved in uptake, translocation, and excretion of this element. In this case parameter values are based on consideration of information on the behavior of Th in young adult animals and adult humans (Stover et al. 1960, 1965; Maletskos et al. 1969), the distribution of environmental Th found in humans (Wrenn et al. 1980; Singh, Wrenn, and Ibrahim 1983), comparison of the behavior of Th and Pu in the body (Singh, Wrenn, and Ibrahim 1983; Leggett 1985; Jee et al. 1962), and basic physiological information on modeling and remodeling processes in the human skeleton at various ages (Leggett, Eckerman, and Williams 1982; Leggett 1985).

The age-dependent parameter values for our thorium retention model are given in Table 1. These values can be related to paths indicated in the generic scheme described in the previous section.

Thorium deposits primarily in the skeleton, and its behavior there appears to be governed by the same processes that control the behavior of plutonium, namely, bone growth and remodeling processes (Leggett 1985; Jee et al. 1962). Bone-seeking elements generally have a higher affinity for the younger skeleton than for the mature skeleton (Leggett and Crawford-Brown 1983), but in the case of thorium the fraction of systemic activity going to the skeleton cannot be substantially higher in children than adults because this fraction is large (perhaps 0.7)

even in the mature adult (ICRP 1979). Thus, in the case of an age-specific skeletal deposition fraction, there simply does not appear much room for a large error to enter.

We assume that, in the adult, 70% of the unexcreted activity in plasma is deposited in the skeleton, with equal amounts going to trabecular and cortical surfaces; 4% in the liver; 0.7% in the kidneys; 0.4% in the spleen; and the remainder (24.9%) in other tissues. Based on limited data for adult humans (Maletskos et al. 1969) approximately 6% of an initial unit activity of thorium in plasma will be promptly excreted. ('Prompt excretion' refers to the fraction of activity in plasma which goes to excretion along paths Y, Z, and CC-FF but not X or Q in the generic scheme.) This description is fairly consistent with that given in ICRP Publication 30 (1979), but is more detailed; it is based to some extent on measurements of environmental thorium in human tissues but also relies on results from animal studies.

For nonadults we assume that 80% of the unexcreted activity is deposited uniformly in the skeleton. This value is somewhat arbitrary but is based on two factors: (1) skeletal deposition in nonadults is expected to be somewhat higher and more uniform than in adults on the basis of results for other elements; and (2) we should not assign a percentage closer to 100% because there is the danger of substantially underestimating deposition in liver and other soft tissues in children (cf. data for 1.5-year-old human in the report by Wrenn et al. 1980). The other deposition fractions are assumed to be the same as in the adult, except that only 14.9% remains to go to other tissues because of the higher percentage assigned to skeleton. The percentage of activity that is promptly excreted might be slightly less in children than in adults because of the slightly greater skeletal deposition expected in children. There is little effect, however, on estimates of dose rate or committed dose caused by reducing this value for children. We assume that it is independent of age.

As with plutonium, thorium going to the skeleton appears to deposit initially on skeletal surfaces but gradually may become buried in bone volume during bone remodeling processes; thorium may also gradually be uncovered and returned to systemic circulation by these processes (Jee et al. 1962). The rate constants for these processes are greater in

children than adults; hence it is expected that thorium will be removed from the radiosensitive cells near the bone surfaces faster in children than in adults (Leggett and Eckerman 1984). The rate constants for movement of Th among the skeletal compartments and plasma are based on the same principles as our age-dependent skeletal model for Pu discussed earlier.

## REFERENCES

- Cristy, M., Leggett, R. W., Dunning, D. E., and Eckerman, K. F., 1986, *Relative Age-Specific Radiation Dose Commitment Factors for Major Radionuclides Released from Nuclear Fuel Facilities*, NUREG/CR-4628, ORNL/TM-9890.
- International Commission on Radiological Protection, 1979, *Publication 30, Limits for Intakes by Workers*, Pergamon Press, Oxford.
- Jee, W. S. S., Arnold, J. S., Cochran, T. H., Twente, J. A., and Mical, R. S., 1962, Relationship of Microdistribution of Alpha Particles to Damage, in *Some Aspects of Internal Irradiation*, ed. by T. F. Dougherty, W. S. S. Jee, C. W. Mays, and B. J. Stover, Pergamon Press, Oxford, 27-45.
- Leggett, R. W., 1985, A Model of the Retention, Translocation, and Excretion of Systemic Plutonium, *Health Phys.* 49, 1115-1137.
- Leggett, R. W. and Crawford-Brown, D. J., 1983, The Role of Age in Human Susceptibility to Radiation, *Sci. Prog., Oxford* 68, 227-258.
- Leggett, R. W., Eckerman, K. F., and Williams, L. R., 1982, Strontium-90 in Bone: a Case Study in Age-Dependent Dosimetric Modeling, *Health Phys.* 43, 307-322.
- Maletskos, C. J., Keane, A. T., Telles, N. C., and Evans, R. D., 1969, Retention and Absorption of Ra-224 and Th-234 and Some Dosimetric Consequences of Ra-224 in Human Beings, in *Delayed Effects of Bone Seeking Radionuclides*, ed. by C. W. Mays, University of Utah Press, Salt Lake City, 29-49.
- Singh, N. P., Wrenn, M. E., and Ibrahim, S. A., 1983, Plutonium Concentration in Human Tissues: Comparison to Thorium, *Health Phys.* 44, Supplement No. 1, 469-476.
- Stover, B. J., Atherton, D. R., Keller, N., and Buster, D. S., 1960,

Metabolism of the Th-228 Decay Series in Adult Beagle Dogs. 1. Th-228 (RdTh), *Radiat. Res.* 12, 657-671.

Stover, B. J., Atherton, D. R., Buster, D. S., and Bruenger, F. W., 1965, The Th-228 Decay Series in Adult Beagles: Ra-224, Pb-212, and Bi-212 in Selected Bones and Soft Tissues, *Radiat. Res.* 26, 132-145.

Wrenn, M. E., Singh, N. P., Cohen, N., Ibrahim, S. A., and Saccomanno, G., 1980, *Thorium in Human Tissues*, New York University Medical Center, NUREG/CR-1227.

Table 1. Age-specific parameter values for thorium model

|   | Age (days) |           |           |           |           |           |           |
|---|------------|-----------|-----------|-----------|-----------|-----------|-----------|
|   | 0          | 100       | 365       | 1825      | 3650      | 5475      | >7300     |
| Fraction of ingested activity absorbed from small intestine to plasma   | 0.100E-01  | 0.500E-02 | 0.500E-03 | 0.500E-03 | 0.500E-03 | 0.500E-03 | 0.200E-03 |
| Removal rate from plasma to organs or to excretion (day <sup>-1</sup> ) | 0.139E+01  | 0.139E+01 | 0.139E+01 | 0.139E+01 | 0.139E+01 | 0.139E+01 | 0.139E+01 |
| Fraction of activity going from plasma directly to excretion            | 0.600E-01  | 0.600E-01 | 0.600E-01 | 0.600E-01 | 0.600E-01 | 0.600E-01 | 0.600E-01 |
| Fraction of non-excreted activity in plasma going to compartment:       |            |           |           |           |           |           |           |
| trabecular bone surface   | 0.400E+00  | 0.400E+00 | 0.400E+00 | 0.400E+00 | 0.400E+00 | 0.400E+00 | 0.350E+00 |
| cortical bone surface   | 0.400E+00  | 0.400E+00 | 0.400E+00 | 0.400E+00 | 0.400E+00 | 0.400E+00 | 0.350E+00 |
| kidneys   | 0.700E-02  | 0.700E-02 | 0.700E-02 | 0.700E-02 | 0.700E-02 | 0.700E-02 | 0.700E-02 |
| liver   | 0.400E-01  | 0.400E-01 | 0.400E-01 | 0.400E-01 | 0.400E-01 | 0.400E-01 | 0.400E-01 |
| spleen  | 0.400E-02  | 0.400E-02 | 0.400E-02 | 0.400E-02 | 0.400E-02 | 0.400E-02 | 0.400E-02 |
| other1  | 0.745E-01  | 0.745E-01 | 0.745E-01 | 0.745E-01 | 0.745E-01 | 0.745E-01 | 0.124E+00 |
| other2  | 0.745E-01  | 0.745E-01 | 0.745E-01 | 0.745E-01 | 0.745E-01 | 0.745E-01 | 0.124E+00 |
| Non-zero removal rates from compartments (day <sup>-1</sup> ):          |            |           |           |           |           |           |           |
| trabecular bone surface to bone volume                                  | 0.102E-01  | 0.822E-02 | 0.288E-02 | 0.181E-02 | 0.132E-02 | 0.959E-03 | 0.246E-03 |
| cortical bone surface to bone volume                                    | 0.102E-01  | 0.822E-02 | 0.288E-02 | 0.153E-02 | 0.904E-03 | 0.521E-03 | 0.410E-04 |
| trabecular bone volume to bone marrow                                   | 0.102E-01  | 0.822E-02 | 0.288E-02 | 0.181E-02 | 0.132E-02 | 0.959E-03 | 0.493E-03 |
| cortical bone volume to bone marrow                                     | 0.102E-01  | 0.822E-02 | 0.288E-02 | 0.153E-02 | 0.904E-03 | 0.521E-03 | 0.821E-04 |
| trabecular bone surface to bone marrow                                  | 0.102E-01  | 0.822E-02 | 0.288E-02 | 0.181E-02 | 0.132E-02 | 0.959E-03 | 0.493E-03 |
| cortical bone surface to bone marrow                                    | 0.102E-01  | 0.822E-02 | 0.288E-02 | 0.153E-02 | 0.904E-03 | 0.521E-03 | 0.821E-04 |
| trabecular bone marrow to plasma  | 0.770E-02  | 0.770E-02 | 0.770E-02 | 0.770E-02 | 0.770E-02 | 0.770E-02 | 0.770E-02 |
| cortical bone marrow to plasma  | 0.770E-02  | 0.770E-02 | 0.770E-02 | 0.770E-02 | 0.770E-02 | 0.770E-02 | 0.770E-02 |
| kidneys to plasma   | 0.139E-02  | 0.139E-02 | 0.139E-02 | 0.139E-02 | 0.139E-02 | 0.139E-02 | 0.139E-02 |
| liver to plasma   | 0.125E-02  | 0.125E-02 | 0.125E-02 | 0.125E-02 | 0.125E-02 | 0.125E-02 | 0.125E-02 |
| liver to excretion  | 0.139E-03  | 0.139E-03 | 0.139E-03 | 0.139E-03 | 0.139E-03 | 0.139E-03 | 0.139E-03 |
| spleen to plasma  | 0.139E-02  | 0.139E-02 | 0.139E-02 | 0.139E-02 | 0.139E-02 | 0.139E-02 | 0.139E-02 |
| other1 to plasma  | 0.139E-02  | 0.139E-02 | 0.139E-02 | 0.139E-02 | 0.139E-02 | 0.139E-02 | 0.139E-02 |
| other2 to plasma  | 0.139E-02  | 0.139E-02 | 0.139E-02 | 0.139E-02 | 0.139E-02 | 0.139E-02 | 0.139E-02 |

BIOKINETICS OF URANIUM: AN EXAMPLE OF THE VALUE OF THE PHYSIOLOGICALLY  
BASED APPROACH IN REVEALING SOME UNCERTAINTIES IN ESTIMATES OF DOSE

Despite the large number of studies on uranium in man and other species, the biobehavior of this element remains poorly understood in many respects. For example, little is known about the residence time of uranium on bone surfaces even in the adult. As discussed in this section and in more detail later in this report, however, the development of a realistic model framework for uranium has been valuable in revealing that there may be subtle reasons why simplifications suitable for models for adults may not be suitable for other age groups.

We have appealed again to the generic model framework described earlier and have attempted to select best age-specific parameter values for the applicable uptake fractions and rate constants. These parameter values, given in Table 1, are based on data for uranium in humans (see discussions and reviews by Bernard, Muir, and Royster 1957; Wrenn et al. 1985); Hursh and Spoor 1975), data for experimental animals (Durbin and Wrenn 1976, Stevens et al. 1979, Rowland and Farnham 1969), comparison of the behavior of the uranyl ion with alkaline earth metals (Rowland and Farnham 1969, Neuman and Neuman 1958), and general physiological information concerning growth and remodeling of the skeleton (Leggett, Eckerman, and Williams 1982; Leggett 1985).

The initial deposition of the uranyl ion in the skeleton may be closely related to that of calcium and strontium (Durbin and Wrenn 1976; Stevens et al. 1979; Neuman and Neuman 1958). Experimental studies indicate that, in the adult, roughly 25% of the activity in plasma not destined for prompt excretion is deposited on bone surfaces, although this may be highly variable. This corresponds to about 10% of the total initial activity in plasma since the excretion rate is high for uranium. Age-specific skeletal deposition fractions are assumed to be proportional to those for strontium (see Leggett, Eckerman, and Williams 1982; Cristy et al. 1984), and the relative age-specific fractions deposited on cortical and trabecular bone are assumed to be the same as for strontium (Leggett, Eckerman, and Williams 1982).

Uranium leaves bone surfaces by returning to blood, by being buried in bone volume during bone remodeling processes, or by penetrating canalicular pathways to form a diffuse deposition in bone volume (Durbin and Wrenn 1976; Stevens et al. 1979; Neuman and Neuman 1958). The rates of removal of uranium from bone surfaces to plasma and bone surfaces to bone volume in adults were chosen to be consistent with best estimates of the short-term removal of uranium from total bone (assumed to be from bone surfaces) and the fraction of the initial bone deposit retained over a long period (assumed to be due to retention in bone volume).

The estimated residence time for uranium on bone surfaces involves considerable uncertainties. In a later section we show that our assumption of a temporary residence on bone surfaces can lead to very different conclusions regarding variation with age of dose to bone surface than would an assumption similar to that made for adults in Publication 30 of the ICRP (1979). In that document long-lived isotopes such as U-238 are assumed, in effect, to by-pass bone surfaces and to be uniformly distributed throughout mineral bone at all times following their deposition in the skeleton. If our estimated residence time is not badly in error for adults, then the ICRP-type assumption may not seriously underestimate integrated dose to bone surface from U-238, for example. On the other hand, if our parameter values for non-adults are not badly in error, then an ICRP-type assumption of lack of residence on bone surfaces would lead to very large underestimates of dose from U-238 to bone surfaces of infants and young children.

Deposition fractions and removal rates for two compartments within other soft tissue are estimated from data for adult humans. Long-term retention in soft tissues may be associated to a large extent with mitochondria (cf. Stevens et al. 1979). The deposition fractions and removal rates for uranium in all soft tissue, including the kidneys, are assumed to be independent of age.

Results of a study on normal humans and humans with various skeletal abnormalities suggest that the fraction of uranium excreted in the first two or three days after injection into blood is decreased under conditions that favor the increased deposition of uranium in the skeleton (see data of Terepka in the article by Hursh and Spoor 1975). This observation is useful in estimating an age-specific fraction of

uranium promptly excreted from plasma. It is assumed that the sum of the total fraction going to skeleton (as contrasted with the "unexcreted fraction" listed in Table 1) and the fraction promptly excreted is constant throughout life, which leads to a lower estimated prompt excretion fraction for younger ages because of a higher estimated skeletal deposition.

## REFERENCES

- M. Cristy, R. W. Leggett, D. E. Dunning, Jr., and K. F. Eckerman, 1984, *Age-Dependent Dose-Conversion Factors for Selected Bone-Seeking Radionuclides*, U.S. Nuclear Regulatory Commission Report NUREG/CR-3535 (Oak Ridge National Laboratory Report ORNL/TM-8929).
- International Commission on Radiological Protection, 1979, *Publication 30, Limits for Intakes by Workers*, Pergamon Press, Oxford.
- Leggett, R. W., 1985, A Model of the Retention, Translocation, and Excretion of Systemic Plutonium, *Health Phys.* 49, 1115-1137.
- Leggett, R. W., Eckerman, K. F., and Williams, L. R., 1982, Strontium-90 in Bone: a Case Study in Age-Dependent Dosimetric Modeling, *Health Phys.* 43, 307-322.
- Bernard, S. R., Muir, J. R., and Royster, G. W., 1957, The Distribution and Excretion of Uranium in Man, Proceedings of the Health Physics Society, First Annual Meeting, June 25-27, 33-48.
- Wrenn, M. E., Durbin, P. W., Howard, B., Lipsztein, J., Rundo, J., Still, E. T., and Willis, D. L., 1985, Metabolism of Ingested U and Ra, *Health Phys.* 48, 601-633.
- Hursh, J. B. and Spoor, N. L., 1975, Data on Man, in *Handbook Exptl. Pharmacol.* 36 (*Uranium, Plutonium, Transplutonic Elements*), ed. by H. C. Hodge, J. N. Stannard and J. B. Hursh, Springer-Verlag, New York, 197-240.
- Durbin, P. W. and Wrenn, M. E., 1976, Metabolism and Effects of Uranium in Animals, in *Conference on Occupational Health; Experience with Uranium*, Arlington, Va. (April 28-30, 1975), ERDA 93, 67-129.
- Stevens, W., Bruenger, F. W., Atherton, D. R., Smith, J. M., and Taylor, G. N., 1979, The Distribution and Retention of Hexavalent U-233 in the Beagle, in *Actinides in Man and Animals, Proceedings*

*of the Snowbird Workshop*, ed. M. E. Wrenn, 457-472.

Rowland, R. E. and Farnham, J. E., 1969, The Deposition of Uranium in Bone, *Health Phys.* 17, 139-144.

Neuman, W. F. and Neuman, M. W., 1958, *The Chemical Dynamics of Bone Mineral*, Univ. of Chicago Press.

Table 1. Age-specific parameter values for uranium model

|   | Age (days) |           |           |           |           |           |           |
|---|------------|-----------|-----------|-----------|-----------|-----------|-----------|
|   | 0          | 100       | 365       | 1825      | 3650      | 5475      | >7300     |
| Fraction of ingested activity absorbed from small intestine to plasma   | 0.160E+00  | 0.150E+00 | 0.100E+00 | 0.700E-01 | 0.800E-01 | 0.900E-01 | 0.500E-01 |
| Removal rate from plasma to organs or to excretion (day <sup>-1</sup> ) | 0.693E+01  | 0.693E+01 | 0.693E+01 | 0.693E+01 | 0.693E+01 | 0.693E+01 | 0.693E+01 |
| Fraction of activity going from plasma directly to excretion            | 0.386E+00  | 0.406E+00 | 0.506E+00 | 0.576E+00 | 0.556E+00 | 0.526E+00 | 0.606E+00 |
| Fraction of non-excreted activity in plasma going to compartment:       |            |           |           |           |           |           |           |
| trabecular bone surface   | 0.980E-01  | 0.101E+00 | 0.810E-01 | 0.710E-01 | 0.900E-01 | 0.105E+00 | 0.157E+00 |
| cortical bone surface   | 0.423E+00  | 0.404E+00 | 0.324E+00 | 0.236E+00 | 0.248E+00 | 0.274E+00 | 0.960E-01 |
| kidneys   | 0.244E+00  | 0.253E+00 | 0.304E+00 | 0.354E+00 | 0.338E+00 | 0.316E+00 | 0.381E+00 |
| liver   | 0.293E-01  | 0.303E-01 | 0.364E-01 | 0.425E-01 | 0.405E-01 | 0.380E-01 | 0.457E-01 |
| spleen  | 0.107E-01  | 0.970E-02 | 0.116E-01 | 0.135E-01 | 0.135E-01 | 0.140E-01 | 0.153E-01 |
| other1  | 0.162E+00  | 0.168E+00 | 0.202E+00 | 0.236E+00 | 0.225E+00 | 0.211E+00 | 0.254E+00 |
| other2  | 0.326E-01  | 0.337E-01 | 0.406E-01 | 0.473E-01 | 0.451E-01 | 0.423E-01 | 0.509E-01 |
| Non-zero removal rates from compartments (day <sup>-1</sup> ):          |            |           |           |           |           |           |           |
| trabecular bone surface to plasma                                       | 0.274E-01  | 0.274E-01 | 0.274E-01 | 0.274E-01 | 0.274E-01 | 0.274E-01 | 0.274E-01 |
| cortical bone surface to plasma   | 0.274E-01  | 0.274E-01 | 0.274E-01 | 0.274E-01 | 0.274E-01 | 0.274E-01 | 0.274E-01 |
| trabecular bone surface to bone volume                                  | 0.411E-02  | 0.411E-02 | 0.405E-02 | 0.384E-02 | 0.370E-02 | 0.356E-02 | 0.274E-02 |
| cortical bone surface to bone volume                                    | 0.411E-02  | 0.411E-02 | 0.405E-02 | 0.384E-02 | 0.370E-02 | 0.356E-02 | 0.274E-02 |
| trabecular bone volume to plasma  | 0.102E-01  | 0.822E-02 | 0.288E-02 | 0.181E-02 | 0.132E-02 | 0.959E-03 | 0.493E-03 |
| cortical bone volume to plasma  | 0.102E-01  | 0.822E-02 | 0.288E-02 | 0.153E-02 | 0.904E-03 | 0.521E-03 | 0.821E-04 |
| kidneys to plasma   | 0.0        | 0.0       | 0.0       | 0.0       | 0.0       | 0.0       | 0.0       |
| kidneys to excretion  | 0.139E+00  | 0.139E+00 | 0.139E+00 | 0.139E+00 | 0.139E+00 | 0.139E+00 | 0.139E+00 |
| liver to plasma   | 0.126E-01  | 0.126E-01 | 0.126E-01 | 0.126E-01 | 0.126E-01 | 0.126E-01 | 0.126E-01 |
| spleen to plasma  | 0.126E-01  | 0.126E-01 | 0.126E-01 | 0.126E-01 | 0.126E-01 | 0.126E-01 | 0.126E-01 |
| other1 to plasma  | 0.347E-01  | 0.347E-01 | 0.347E-01 | 0.347E-01 | 0.347E-01 | 0.347E-01 | 0.347E-01 |
| other2 to plasma  | 0.301E-02  | 0.301E-02 | 0.301E-02 | 0.301E-02 | 0.301E-02 | 0.301E-02 | 0.301E-02 |

## MODELS FOR THE ALKALINE EARTH ELEMENTS

The importance of Sr-90 as an environmental contaminant has led to the development over the past three decades of several models describing the age-specific skeletal uptake and retention of strontium. One recent model (Leggett, Eckerman, and Williams 1982) demonstrates how the body's accumulation of environmental strontium can be closely predicted for humans of all ages through consideration of physiological similarities and discrimination of strontium and calcium, bone modeling and remodeling kinetics as estimated from various sources, and the assumption that the fraction of ingested Ca that is absorbed to blood and eventually retained in the skeleton for an extended period depends largely on the skeletal needs for Ca at the age at intake. This approach obviated the need for the customary procedure of estimating separate values for the absorption of Sr from the gastrointestinal tract to blood and the uptake of Sr by the skeleton.

This model for strontium is somewhat less detailed than the newer models described earlier in this report, including those for potassium, plutonium, and thorium. For example, it does not involve explicit consideration of recycling of Sr or accumulation in soft tissues. Also, the model applies only to fairly long-term kinetics and would not be suitable for application to relatively short-lived isotopes of Sr. Still, the Sr model served to demonstrate the plausibility of viewing age-specific behavior of radioelements in the context of a physiological system, and the age-specific rate constants for bone modeling and remodeling derived in the construction of that model have been important in the development of more detailed models for several radioelements. Moreover, these rate constants have held up well in tests of these more detailed models (for example, see Leggett 1985, Leggett and Eckerman 1986).

We are currently developing more detailed models for the alkaline earth elements that are intended to provide fairly accurate descriptions of the short-term behavior of these metals. These models will take into account the fact that calcium and its physiological analogues undergo considerable recycling among fluids and tissues, particularly between plasma and bone surfaces. According to current information, movement of

calcium between plasma and bone is controlled largely by bone-lining cells. In our newer models use is made of the strong association among bone-lining cells, bone marrow cellularity, vascularity, and bone apposition rate. Two primary routes of transfer between bone fluids and extracellular fluids are pictured: ions may enter one side of the flattened bone-lining cells and exit on the opposite side, or they may traverse the spaces between adjacent cells. Calcium and its analogues are viewed as entering bone fluid by passing with tissue water between the bone-lining cells; these cells continuously extrude the alkaline earth metals into the interstitial fluid on their vascular sides. There is mitochondrial uptake of these metals, and heavier metals are released only slowly from the mitochondria. Osteocytes within lacunae communicate with the lining cells by cell processes that are extended into the canaliculi. Potassium, which is moving in opposite directions to Ca in this system, would be taken up by the bone-lining cells directly from the extracellular fluid, and K in bone fluid would reach the extracellular fluids by passing through the spaces between bone-lining cells. There also may be an exchange of K and Ca in uptake of Ca by mitochondria within bone-lining cells.

Experimental evidence indicates that bone discriminates against calcium in favor of the heavy alkaline earths, barium and radium, in the sense that the short-term skeletal accumulation of the heavy elements is greater than that of calcium when related to an integrated concentration in plasma. This discrimination has been attributed to a greater adsorption of heavy alkaline earths to the bone mineral based on an *in vitro* experiment. While this possibility should not be ignored, it also would appear that there is little or no discrimination between these metals in passage through the spaces between bone-lining cells but that there may be discrimination against the heavier metals in passage through the bone lining cells from bone fluid to plasma and in extrusion from mitochondria. Thus, the apparent discrimination against calcium by the skeleton may actually result in large part from discrimination in favor of calcium by the bone cells.

These concepts cannot be used independently in the selection of parameter values for a biokinetic model for alkaline earth metals. However, they serve as useful indicators for changes with age in bone

function and hence appear to be helpful in avoiding blind assumptions in the development of age-specific models.

Our newer alkaline earth models are still under development. Until they are complete we are using the generic model framework described earlier and parameter values based on the modeling approach described in the earlier paper of Leggett, Eckerman, and Williams (1982).

#### REFERENCES

- Leggett, R. W., 1985, A Model of the Retention, Translocation, and Excretion of Systemic Plutonium, *Health Phys.* 49, 1115-1137.
- Leggett, R. W. and Eckerman, K. F., 1986, A Method for Estimating the Systemic Burden of Plutonium from Urinalyses, *Health Phys.*, in press.
- Leggett, R. W., Eckerman, K. F., and Williams, L. R., 1982, Strontium-90 in Bone: a Case Study in Age-Dependent Dosimetric Modeling, *Health Phys.* 43, 307-322.

AGE DEPENDENCE IN INTAKE OF RADIOACTIVITY AND IN FUNCTIONS  
OF THE GASTROINTESTINAL AND RESPIRATORY TRACTS

INGESTION

In exposures to environmental radioactivity through the ingestion pathway there are two factors that could lead to substantial variation with age in accumulation of radionuclides in humans. First, the amount of activity ingested may vary with age because of different diets and quantities consumed at different ages; this has been given considerable attention in the literature and will not be discussed here. Second, the fraction of activity in the tract that is absorbed to blood, called  $f_1$ , may vary age.

Studies on laboratory animals indicate that fractional absorption of metals from the small intestine to blood is higher in neonates than in adults and may be considerably higher for poorly absorbed metals (see reviews by Harrison 1982, Cristy and Leggett 1986). The absorption fraction appears to decrease substantially in the first few days, weeks, or months of life, but no clear picture has been developed concerning relative absorption fractions in juvenile and adult animals.

Recent work indicates to us that the wall of the small intestine is a more selective tissue than was previously thought and that absorption of elements may be related to the body's needs to a greater extent than had been believed. In particular, there is evidence of an enhanced absorption of certain essential elements during the period of growth, and chemically related elements or elements transported by the same mechanisms may also experience enhanced absorption during this period.

Best information is for iron, lead, calcium, strontium, and zinc. Fractional absorption of each of these elements appears to be higher in juveniles than in adults. Moreover, data for each of these elements are consistent with the hypothesis that fractional absorption changes with the rate of growth until adulthood. For example, studies with human children from infancy through 4 years indicate that the absorption fraction for iron falls steadily as does the rate of growth (Garby and Sjolín 1959; Schulz and Smith 1958; Gorten, Hepner, and Workman 1963), and another study with children of ages 7-10 years indicates that the

absorption fraction rises during that period as does the rate of growth and the demand for iron (Darby et al. 1947).

Lead appears to share an absorption pathway with iron (Barton et al. 1978; Barton, Conrad, and Holland 1981) and may also be absorbed to some extent along the transport system for calcium (Task Group on Metal Accumulation 1973). Results of a balance study of human children from 2 weeks to 8 years of age indicate that the absorption of lead is much greater than the adult level during that period (Ziegler et al. 1978; Alexander, Clayton, and Delves 1974). Absorption of lead in the juvenile has been studied most extensively in the rat with isolated duodenal loops (Conrad and Barton 1978, Barton 1984). The animals in one study (Conrad and Barton 1978) weighed from 79 to 660 g and varied from recently weaned rats to rats more than one year old. The fraction of lead absorbed decreased substantially (and highly significantly) with increases in age and body weight.

The fractions of the alkaline earth metals calcium, strontium, and radium absorbed by juvenile rats were 2-3 times higher at age 6-8 weeks than at 60-70 weeks (Taylor, Bligh, and Duggan 1962). Another study with rats showed absorption of calcium declining from 98% in weanling rats 4 weeks old to 57, 46, 41, and 24% at ages 12-24, 48-72, and 106 weeks, respectively (Hansard and Crowder 1957). Data for calcium in humans are piecemeal and less definitive but appear to follow the same general pattern (Harrison 1959, Kahn et al. 1969, ICRP 1975). The strong age dependence in the numerous measurements of environmental Sr-90 in the skeletons of humans over three decades can be explained uniformly by a model in which the fraction of ingested Sr-90 absorbed depends on the body's growth requirements for calcium (Leggett, Eckerman, and Williams 1982). The concentration of environmental radium in human bone as a function of age (Muth and Gloebel 1983) appears to follow a pattern very similar to that for Sr-90.

The fraction of zinc absorbed by rats is also greater at younger ages (Weigand and Kirchgessner 1979; Kirchgessner, Weigand, and Schwarz 1981). In these studies it was shown that "the physiological ability to absorb zinc did not decrease with age, but rather adapted to the particular supply status" (Kirchgessner, Weigand, and Schwarz 1981) and that the "marked differences between age groups in utilizing dietary

zinc reflected the efficient homeostatic adjustments in absorption and endogenous excretion of zinc to the respective supply status" (Weigand and Kirchgessner 1979).

For radiation protection it has generally been assumed that the fraction of a radionuclide absorbed by children after weaning from a milk diet is similar to that absorbed by adults (e.g., NRPB 1984). This assumption does not appear to be based on strong evidence for the entire period of growth. Rather, it is apparently based on observations that the fractional absorption of many metals by laboratory animals decreases sharply toward the adult level after weaning, the conclusion that the enhanced absorption during infancy is related at least in part to the milk diet, and the fact that the structure and function of the small intestine are similar in juveniles (after weaning) and adults (Koldovsky 1969). However, even though the small intestine does appear to be mature in juveniles, the enhanced need during growth for essential metals such as calcium, iron, and zinc result, we believe, in enhanced absorption of these metals and perhaps also some non-essential metals such as lead or plutonium that may share absorption pathways with essential metals. There may be other mechanisms involved in conserving essential metals when the demand is high, but available data suggest to us that enhanced absorption is at least one of the homeostatic processes brought into play in the growing animal.

In view of the data discussed above, we believe that estimates of age-specific organ doses should include consideration of (1) the elevated absorption fractions during the neonatal period indicated by the data for animals and to a lesser extent by that for humans; and (2) the changes with growth in absorption fractions indicated by studies with animals and by the few available studies on humans. For those radioelements with no direct information on changes with age in absorption, relative values for different ages might be assigned by analogy with better understood elements.

Another factor that conceivably could affect dosimetry of ingested radionuclides to some extent is the potential variation with age in transit times through segments of the GI tract. The small amount of available information, primarily on species other than man, would indicate that variation with age in transit times may not be large

(Crawford-Brown 1983). Also, sensitivity analyses indicate that incorporation of variations with age in GI-transit times within reasonable limits of uncertainty usually will not have much influence on estimates of dose to organs or tissues of primary concern. Still, it would be desirable to have an accurate age-dependent model for movement of activity through the GI tract, particularly for evaluation of situations concerning non-penetrating radiations or short-lived nuclides. Until a well supported age-specific model becomes available, we will apply the transit model recommended by the ICRP (Eve 1966) to all age groups.

#### INHALATION

In exposures to environmental radioactivity through the inhalation pathway, an important source of variation with age in accumulation of radioactivity by humans is the air-intake rate. The amount of activity inhaled from a contaminated atmosphere typically would increase sharply with age; for example, the inhalation rate for the newborn infant may be only 4-5% of the adult level, and that of the one-year-old may be only about 15% of the adult level (e.g., ICRP 1975). Another potentially important source of variation is the fraction of inhaled material that is deposited in the respiratory tract rather than exhaled. A third factor of conceivable importance in the dosimetry of inhaled radionuclides is the potential age dependence in transit times of activity from the respiratory tract to blood or the gastrointestinal tract.

Models have been developed to predict age dependence in the fractional deposition and rate of transport of material in the respiratory tract (Hofmann, Steinhausler, and Pohl 1979; Crawford 1982); these are based primarily on physical considerations, such as diameters of airways in relation to particle sizes. Also, some experimental information on animals is available (e.g., Mewhinney and Muggenburg 1985). These models and experimental results suggest that there may be some dependence on age in deposition and transport in the respiratory tract, although evidence certainly is not conclusive.

Until better information on behavior of material in the respiratory tract is available, we will use the Task Group Lung Model (TGLM) of the ICRP (1979), which was designed to apply to a reference adult and does not include age-dependent parameters. Our opinion is that present information on variation with age in fractional deposition and rate of transport of material in the respiratory tract is still too uncertain to be of benefit in reducing uncertainties involved in applying the TGLM to all age groups, particularly for the small particle sizes expected in most environmental exposures.

#### REFERENCES

- Alexander, F. W., Clayton, B. E., and Delves, H. T., 1974, Mineral and Trace-Metal Balances in Children Receiving Normal and Synthetic Diets, *Q. J. Med.* 43, 89-111.
- Barton, J. C., 1984, Active Transport of Lead-210 by Everted Segments of Rat Duodenum, *Am. J. Physiol.* 247, G193-G198.
- Barton, J. C., Conrad, M. E., Nuby, S., and Harrison, L., 1978, Effects of Iron on the Absorption and Retention of Lead, *J. Lab. Clin. Med.*, 92, 536-547.
- Barton, J. C., Conrad, M. E., and Holland, R., 1981, Iron, Lead, and Cobalt Absorption: Similarities and Dissimilarities, *Proc. Soc. Exp. Biol. Med.*, 166, 64-69.
- Conrad, M. E. and Barton, J. C., 1978, Factors Affecting the Absorption and Excretion of Lead in the Rat, *Gastroenterology* 74, 731-740.
- Crawford, D. J., 1982, Identifying Critical Human Subpopulations by Age Groups: Radioactivity and Lung, *Phys. Med. Biol.* 27, 539-552.
- Crawford-Brown, D. J., 1983, An Age-Dependent Model for the Kinetics of Uptake and Removal of Radionuclides from the GI Tract, *Health Phys.* 44, 609-622.
- Cristy, M. and Leggett, R. W., 1986, *Determination of Metabolic Data Appropriate for HLW Dosimetry. II. Gastrointestinal Absorption*, U.S. Nuclear Regulatory Commission Report NUREG/CR-3572 Vol. II (Oak Ridge National Laboratory Report ORNL/TM-8939/V2), February 1986.
- Darby, W. J., Hahn, P. F., Kaser, M. M., Steinkamp, R. C., Densen,

- P. M., and Cook, M. B., 1947, The Absorption of Radioactive Iron by Children 7-10 Years of Age, *J. Nutr.* 33, 107-119.
- Eve, I. S., 1966, A Review of the Physiology of the Gastrointestinal Tract in Relation to Radiation Doses from Radioactive Material, *Health Phys.* 12, 131-162.
- Garby, L. and Sjolín, S., 1959, Absorption of Labelled Iron in Infants Less than Three Months Old, *Acta Paediat.* 48 (Suppl.), 24-28.
- Gorten, M. K., Hepner, R., and Workman, J. B., 1963, Iron Metabolism in Premature Infants. I. Absorption and Utilization of Iron as Measured by Isotope Studies, *J. Pediat.* 63, 1063-1071.
- Hansard, S. L. and Crowder, H. M., 1957, The Physiological Behavior of Calcium in the Rat, *J. Nutr.* 62, 325-339.
- Harrison, H. E., Factors influencing calcium absorption, *Fed. Proc.* 18, 1959, 1085-1092.
- Harrison, J. D., 1982, *Gut Uptake Factors for Plutonium, Americium, and Curium*, National Radiological Protection Board Report NRPB-R129.
- Hofmann, W., Steinhausler, F., and Pohl, E., 1979, Dose Calculations for the Respiratory Tract from Inhaled Natural Radioactive Nuclides as a Function of Age, I. Compartment Deposition, Retention, and Resulting Dose, *Health Phys.* 37, 517-532.
- International Commission on Radiological Protection (ICRP), 1975, *Report of the Task Group on Reference Man*, ICRP Publication 23, Pergamon Press, Oxford, 375-376.
- International Commission on Radiological Protection, 1979, *Publication 30, Limits for Intakes by Workers*, Pergamon Press, Oxford.
- Kahn, B., Straub, C. P., Robbins, P. J., Wellman, H. N., Seltzer, R. A., and Telles, N. C., 1969, Retention of Radiostrontium, Strontium, Calcium, and Phosphorus by Infants, *Pediatrics* 43 (Suppl.), 651-756.
- Kirchgessner, M., Weigand, E., and Schwarz, F. J., 1981, Absorption of Zinc and Manganese in Relation to Age, in *Trace Element Metabolism in Man and Animals*, ed. by J. M. Gawthorne, J. Howell, and C. L. White, Springer, New York, pp. 125-128.
- Koldovsky, O., 1969, *Development of the Functions of the Small Intestine in Mammals and Man*, S. Karger, Basel.
- Leggett, R. W., Eckerman, K. F., and Williams, L. R., 1982, Strontium-90

- in Bone: a Case Study in Age-Dependent Dosimetric Modeling, *Health Phys.* 43, 307-322.
- Mewhinney, J. A. and Muggenburg, B. A., 1985, Comparison of Retention of  $^{241}\text{Am}$  in Immature, Young Adult, and Aged Dogs and in Monkeys after Inhalation of  $^{241}\text{AmO}_2$ , in *Annual Report of the Inhalation Toxicology Research Institute, 1984-1985*, ed. by M. A. Medinsky and B. A. Muggenburg, Lovelace Biomedical and Environmental Research Institute, Albuquerque, NM 87185, December 1985.
- Morrow, P. E., Bates, D. V., Fish, B. R., Hatch, T. F., and Mercer, T. T., 1966, Deposition and Retention Models for Internal Dosimetry of the Human Respiratory Tract, *Health Phys.* 12, 173-207.
- Muth, H. and Gloebel, B., 1983, Age Dependent Concentration of Ra-226 in Human Bone and Some Transfer Factors from Diet to Human Tissues, *Health Phys.* 44, 113-121.
- National Radiological Protection Board (NRPB), 1984, *Metabolic and Dosimetric Models for Application to Members of the Public. Recommended Models for the Metabolism of Iodine and Values for the Gut Transfer Fraction of Plutonium, Americium, Curium, and Neptunium*, NRPB Rep. NRPB-GS3.
- Schulz, J. and Smith, N. J., 1958, A Quantitative Study of the Absorption of Food Iron in Infants and Children, *J. Dis. Child.* 95, 109-119.
- Task Group on Metal Accumulation, 1973, Accumulation of Toxic Metals with Special Reference to Their Absorption, Excretion, and Biological Half-Times, *Environ. Physiol. Biochem.* 3, 65-107.
- Taylor, D. M., Bligh, P. H., and Duggan, M. H., 1962, The Absorption of Calcium, Strontium, Barium, and Radium from the Gastrointestinal Tract of the Rat, *Biochem. J.* 83, 25-29.
- Weigand, E. and Kirchgessner, M., 1979, Change in Apparent and True Absorption and Retention of Dietary Zinc with Age in Rats, *Biol. Trace Element Res.*, 1, 347-358.
- Ziegler, E. E., Edwards, B. B., Jensen, R. L., Mahaffey, K. R., and Fomon, S. J., 1978, Absorption and Retention of Lead by Infants, *Pediat. Res.* 12, 29-34.



PART 2. DOSIMETRIC MODELS

## SPECIFIC EFFECTIVE ENERGIES (SEE VALUES)

From a biokinetic model such as one of those discussed in Part 1 of this report, the distribution of activity in the body as a function of time after intake of a radionuclide is estimated. To convert from activity to dose-equivalent rates, we need a dosimetric quantity called the specific effective energy, SEE. We discuss in this section how the age-dependent SEE values are calculated; other sections in Part 2 discuss details of calculations on specific absorbed fractions, which are needed to calculate SEE. (For additional discussion of the computer code that combines the biokinetic and dosimetric data to generate dose-equivalent rates, see the first section in Part 3 of this report.) For simplicity, in the following discussion we sometimes refer to "dose" to mean "dose-equivalent" (the SEE values, defined below, include the quality factor that converts dose to dose-equivalent).

The activity of a radionuclide in a compartment is a measure of the energy being emitted in that compartment at time  $t$ . We now discuss briefly how one may relate the estimated activities of a radionuclide in all compartments at time  $t$  to the dose rate to a specific organ at time  $t$ . The problem is to estimate the fraction of the energy emitted by decay of the radionuclide in each compartment ("source organ") that is absorbed by the specified ("target") organ. This absorbed fraction is incorporated into the calculation through the use of the SEE values.

The dose-equivalent rate  $[\dot{H}_j(X)](t)$  to target organ  $X$  at time  $t$  due to radionuclide  $j$  in source organs  $Y_1, Y_2, \dots, Y_M$  is estimated to be

$$[\dot{H}_j(X)](t) = \sum_{k=1}^M [\dot{H}_j(X+Y_k)](t) ,$$

where

$$[\dot{H}_j(X+Y_k)](t) = c \cdot A_{jk}(t) \cdot \text{SEE}_j(X+Y_k) .$$

In the preceding equation  $A_{jk}(t)$  is the activity, at time  $t$ , of radionuclide  $j$  in source organ  $Y_k$ , and  $c$  is a constant that depends on the units of dose-equivalent rate, activity, and SEE. If dose-equivalent rate is in  $\text{Sv} \cdot \text{s}^{-1}$ , SEE is in  $\text{MeV} \cdot \text{kg}^{-1}$  per transformation, and

activity is in Bq, then  $c = 1.6 \times 10^{-13}$ . The SEE value refers only to radionuclide  $j$  and does not include any contribution from daughter radionuclides.

The SEE value for radionuclide  $j$  may be defined as

$$SEE_j(T+S) = \sum_i Y_i E_i \Phi_i(T+S) Q_i ,$$

where

$Y_i$  = yield of radiations of type  $i$  per transformation of radionuclide  $j$ ,

$E_i$  = average or unique energy of radiation  $i$  as appropriate,

$\Phi_i(X+Y)$  = specific absorbed fraction = fraction of emitted energy from source organ  $Y$  absorbed by target organ  $X$  per unit mass of  $X$ ,

$Q_i$  = the quality factor appropriate for radiation of type  $i$ ,

and where the summation is taken over all radiations of type  $i$ . In the following paragraphs we discuss briefly the estimation of the absorbed fractions  $\Phi_i(X+Y)$  for photon emissions and beta, electron, and alpha decays.

It should be evident that the value  $SEE_j(X+Y)$  is a function of the age of the individual, because the specific absorbed fractions  $\Phi_i(X+Y)$  used to calculate  $SEE_j(X+Y)$  may depend on the relative geometries of  $X$  and  $Y$  as well as the mass of the target organ  $X$  (Cristy 1980). We shall first discuss the determination of SEE values for various radiation types for a fixed age, and we later describe the introduction of age dependence into the SEE values.

#### PHOTON EMISSIONS

There are two principal computational procedures available for estimating specific absorbed fractions for photon emissions: the Monte Carlo method and the point-source kernel method. Each of these will be discussed briefly; references to the computer codes used to calculate these values are given in the following section.

The Monte Carlo method is an approach for estimating the probability of a photon interaction within target organ X after emission from source organ Y. This method is carried out as follows for all combinations of source and target organs and for several (usually 12) photon energies. The body is represented by an idealized phantom in which the internal organs are assigned masses, shapes, positions, and attenuation coefficients based on their chemical composition. A mass attenuation coefficient  $\mu_0$  is chosen, where  $\mu_0$  is greater than or equal to the mass attenuation coefficients for any region of the body. The photon begins its course from organ Y in a randomly chosen direction, and a potential site of an interaction is chosen by taking the distance traveled as  $-\ln r/\mu_0$ , where  $r$  is a random number distributed between 0 and 1. The point on the line at this distance from the photon's starting point and in the direction of the photon's path is tested to determine the region of the body containing this point. The computer randomly selects either a favorable or an unfavorable outcome; the probability of a favorable outcome is  $\mu_i/\mu_0$ , where  $\mu_i$  is the total mass attenuation coefficient for the  $i$ th region. If the outcome is unfavorable, then it is assumed that no interaction occurs, and the photon proceeds another randomly chosen distance along the same line of flight and the game is repeated. If the outcome is favorable, then it is assumed that an interaction occurs. With each interaction, an artificial "weight" of the photon (initially set at unity) is reduced by an amount equal to the expectation of absorption which the photon would have in the actual physical processes. The flight of the photon is terminated (1) if it escapes the body; (2) if its energy falls below a cutoff value -- typically 4 keV; or (3) if its weight falls below  $10^{-5}$ ; in the latter two cases, the energy is considered to be totally absorbed. The energy deposition for an interaction is determined according to a standard equation.

The second procedure for estimating specific absorbed fractions for photon emissions involves integration of a point-source kernel  $\Phi(x)$ , where  $x$  is the distance from the point source. The function  $\Phi$  is composed of inverse-square and exponential attenuation factors that reflect the loss of energy from photon interactions and a build-up factor that reflects the contribution of scattered photons to dose. One

must integrate this kernel over all distances  $x = |u - v|$  corresponding to pairs of points  $(u,v)$ , where  $u$  lies in the source organ  $Y$  and  $v$  lies in the target organ  $X$ . (The equation of the kernel is given in the following section.)

Both the Monte Carlo method and the point-source kernel method may involve significant sources of error, depending on the energy and the organs under consideration (Yalcintas, Eckerman, and Warner 1980). The Monte Carlo method is a probabilistic approach and produces significant errors in situations where few interactions are expected to occur, such as cases involving target organs which are relatively small or remote from important sources of activity. The point-source kernel method technically is valid only for a homogeneous, unbounded medium. Hence this method may lead to large errors in cases involving significant variations in composition or density of body tissue, or in cases where target organs or important sources of activity lie near a boundary of the body. We have been able to reduce errors in calculations of absorbed fractions by making extensive use of the geometrical reciprocity theorem and by developing correction factors for values generated by the point-source kernel method (see following section). That is, we use a weighted average of  $\Phi_i(X \leftarrow Y)$  and the reciprocal  $\Phi_i(Y \leftarrow X)$  produced by the Monte Carlo method, but replace this value with the corrected point-source kernel value if the former is statistically unreliable.

#### BETA, POSITRON, AND ELECTRON DECAY

Beta particles, positrons, and discrete electrons are usually not sufficiently energetic to contribute significantly to cross-irradiation doses of targets separated from a source organ (the photons produced upon annihilation of positrons are treated separately). Thus, it is generally assumed that  $\Phi_i(X \leftarrow X)$  is just the inverse of the mass of organ  $X$ , and if source and target are separated,  $\Phi_i(X \leftarrow Y) = 0$ . Exceptions occur when the source and target are in close proximity, which is the case, for example, with various skeletal tissues. Absorbed fractions for cross irradiations among skeletal tissues and walled organs were taken from ICRP Publication 30 (1979).

## ALPHA PARTICLE DECAY

The energy of alpha particles and their associated recoil nuclei is generally assumed to be absorbed in the source organ. Therefore,  $\Phi_{\alpha}(X \leftarrow X)$  is taken to be the inverse of the organ mass, and  $\Phi_{\alpha}(X \leftarrow Y) = 0$  if X and Y are separated. Special calculations are performed for active marrow and endosteal cells in bone, based on a method of Thorne (1977).

## CALCULATION OF SEE VALUES FOR DIFFERENT AGE GROUPS

For non-penetrating radiations the calculation of age-dependent specific absorbed fractions (and hence of SEE values) is straightforward. Since all emitted energy is assumed to be absorbed by the source organ, the only age-dependent variable in this case is the mass of the organ. Masses of organs vs age were taken from ICRP Publication 23 (1975) and are given in Cristy and Eckerman (1987).

The problem is considerably more complex for penetrating radiations, however, because the changing shapes and relative positions of the organs must be taken into account in this case in the development of specific absorbed fractions. Specific absorbed fractions for photon emissions of various energies have been calculated by us for age groups 0, 1, 5, 10, and 15 years and for adults (see following section). These absorbed fractions were calculated using a combination of the Monte Carlo and point-source kernel methods as described earlier, but using different mathematical phantoms of the human body for each age group. An external view of these mathematically represented phantoms, together with comparative cross-sections of the middle trunk regions of the newborn and adult phantoms, are shown in Fig. 1. Results of these calculations indicate that the specific absorbed fractions vary substantially with age for some energies, source organs, and target organs (see Fig. 2).

To avoid discontinuities in calculated doses, we calculate SEE values for any non-adult age from those for ages 0, 1, 5, 10, 15, and 20 (=adult) years by linear interpolation.

## REFERENCES

- Cristy, M., 1980, "Development of Mathematical Pediatric Phantoms for Internal Dose Calculations: Designs, Limitations, and Prospects," *Proceedings of the International Radiopharmaceutical Dosimetry Symposium*, U.S. Department of Health and Human Services, Rockville, Md., 496-517.
- Cristy, M. and Eckerman, K. F., 1987, *Specific Absorbed Fractions of Energy at Various Ages from Internal Photon Sources. I. Methods*, Oak Ridge National Laboratory Rep. ORNL/TM-8381:Vol. 1 (in press).
- International Commission on Radiological Protection, 1975, *Publication 23, Report of the Task Group on Reference Man*, Pergamon Press, Oxford.
- International Commission on Radiological Protection, 1979, *Publication 30, Limits for Intakes by Workers*, Pergamon Press, Oxford.
- Thorne, M. D., 1977. "Aspects of the Dosimetry of Alpha-emitting Radionuclides in Bone with Particular Emphasis on Ra-226 and Pu-239," *Phys. Med. Biol.* 22, 36-46.
- Yalcintas, M. G., Eckerman, K. F., and Warner, G. G., 1980, "Experimental Validation of Monte Carlo Calculations for Organ Dose," *Proceedings of the International Radiopharmaceutical Dosimetry Symposium*, U.S. Department of Health and Human Services, Rockville, Md., 482-495.

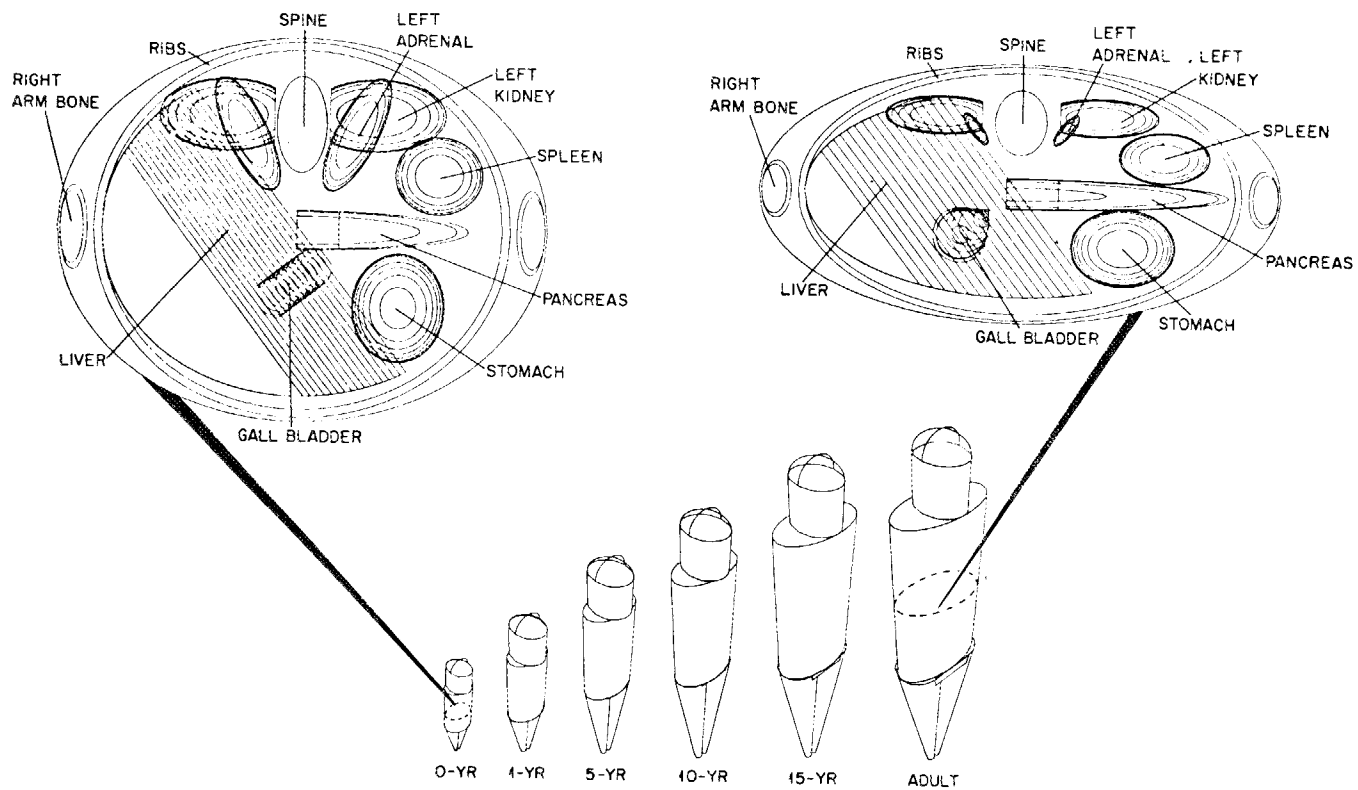
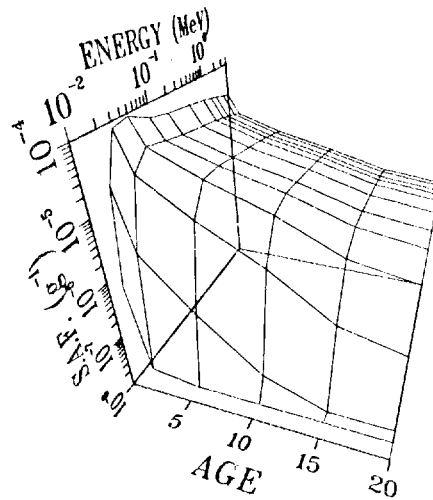
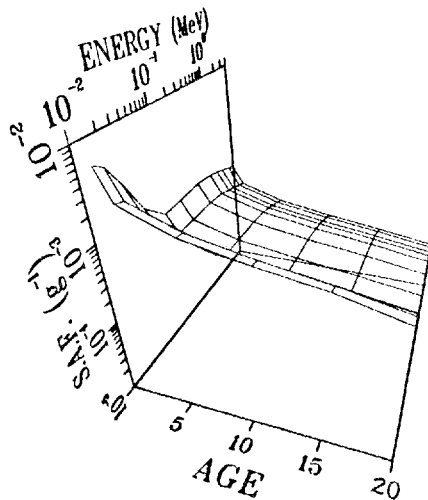


Figure 1. External views of the phantoms and superimposed cross-sections within the middle trunk of the newborn and adult phantoms, depicting the space from the bottom of the liver to the top of the liver. The geometry of the organs may change dramatically from birth to adulthood.

## LIVER -to- OVARIES



## LIVER -to- LIVER



## LUNGS -to- BREAST

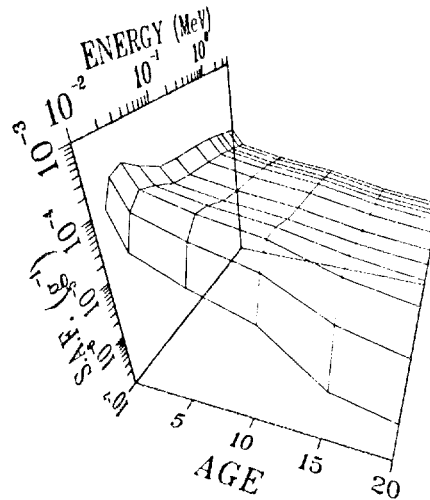


Figure 2. The notation "Y -to- X" indicates that Y is the source organ and X is the target organ. The figure shows the specific absorbed fractions (S.A.F.'s) for photons for various source and target organs, energies, and ages. A typical pattern at all energies is that the S.A.F. (the fraction of energy emitted from within Y that is absorbed by X per gram of X) decreases with age. The effects of the changes with age in the geometries and masses of organs are most marked for low-energy photons.

SPECIFIC ABSORBED FRACTIONS OF ENERGY  
AT VARIOUS AGES FROM INTERNAL PHOTON SOURCES

A series of reports tabulates specific absorbed fractions ( $\Phi$ 's) for monoenergetic photon sources uniformly distributed in organs of mathematical phantoms representing humans of various ages and describes the methods used to compute them (Cristy and Eckerman 1987a-g, in press; the tables are also available on diskettes for personal computers, by request). Procedures for choosing the "best" estimates of  $\Phi$  from the estimates generated by the various methods are described in the first volume, and the  $\Phi$ 's calculated by three methods and the "best" estimates recommended by us are tabulated in the remaining volumes for the newborn, for ages 1, 5, 10, and 15 years, for an adult female, and for an adult male. These  $\Phi$ 's can be used in calculating the photon component of dose equivalent from radionuclides in the body at various ages.

The methods used to calculate  $\Phi$ 's are similar to those used by Snyder, Ford, Warner, and Watson (1974) for their adult phantom. However, more use is made of the converse Monte Carlo estimate,  $\Phi(Y \leftarrow X)$  ( $Y$  = source organ,  $X$  = target organ), as an approximation to the direct Monte Carlo estimate,  $\Phi(X \rightarrow Y)$ . More extensive use is made of empirical correction factors for the estimates generated by the point-source kernel (or buildup factor) method. Also, a better method to calculate the fraction of energy deposited in the active marrow and the endosteal cells has been employed.

The phantoms described previously by Cristy (1980) are designed like the adult phantom of Snyder et al. (1974) and have different densities and chemical compositions for lung, skeletal, and soft tissues. ("Soft tissues" are all near-unit-density tissues, i.e., density  $\approx 1 \text{ g/cm}^3$ .) The age 15 phantom has been redesigned so that it represents both a 15-year-old male and an adult female. The current versions of all phantoms are reprinted in Appendix A of Cristy and Eckerman (1987a).

METHODS OF CALCULATING  $\Phi$ 

Three methods are used to calculate the  $\Phi$  for a given source organ-target organ pair at a given initial photon energy. (1)  $\Phi(X \leftarrow Y)$  is calculated with the Monte Carlo radiation transport computer program. (2)  $\Phi(Y \leftarrow X)$  is calculated with the Monte Carlo computer program, and this value is used to estimate  $\Phi(X \leftarrow Y)$ , sometimes after applying a correction factor. (3)  $\Phi(X \leftrightarrow Y)$  is calculated with the point-source kernel (or buildup factor) method. A correction factor may also be applied to this estimate. For the special case of the active marrow or the endosteal cells as the target organ,  $\Phi$  is calculated from methods described in the section "ESTIMATING DOSE IN ACTIVE MARROW AND OSTEOGENIC TISSUE FROM PHOTONS FROM INTERNAL OR EXTERNAL SOURCES" appearing later in Part 2 of this report.

## Monte Carlo Radiation Transport Computer Program

A radiation transport computer program employing Monte Carlo techniques, similar to that of Snyder et al. (1974), simulates the transport of photons of any given initial energy originating in a given organ (source organ). The photon emission is uniformly distributed in the source organ. The specific absorbed fraction, i.e., the energy absorbed in another organ (target organ), normalized as the fraction of emitted energy and per kilogram of target organ, is calculated, and the reliability of the  $\Phi$  is calculated as a coefficient of variation. The Monte Carlo method is outlined in the preceding section "SPECIFIC EFFECTIVE ENERGIES (SEE VALUES)"; details of the method and the computer program may be found in Ryman, Warner, and Eckerman (1987a).

For a given source-target pair, we obtain two numbers: the direct estimate,  $\Phi(X \leftarrow Y)$ , obtained when the photon emission is in the organ labeled "source," and the converse estimate,  $\Phi(Y \leftarrow X)$ , obtained when the photon emission is in the organ labeled "target." Each of these numbers is from a Monte Carlo computer run: what is labeled the direct estimate and what is labeled the converse estimate depend upon which organ we label the target organ. According to the reciprocal dose theorem, the converse estimate should be a good approximation to the direct estimate under ideal conditions. The usefulness of this theorem in providing

more reliable estimates of  $\Phi$  has been documented (Cristy 1983).

#### Point-source Kernel Method

In this method, the equation describing the absorption of energy at a distance  $r$  from a point source of monoenergetic photons in an infinite homogeneous medium (water) is employed:

$$\Phi(r) = \frac{\mu_{en}}{\rho} \cdot \frac{1}{4\pi r^2} \cdot e^{-\mu r} \cdot B(\mu r) ,$$

where

$\Phi(r)$  = point-isotropic specific absorbed fraction at  $r$ ,

$\mu_{en}$  = linear energy-absorption coefficient at the source energy,

$\mu$  = linear attenuation coefficient at the source energy,

$\rho$  = density of medium,

$B(\mu r)$  = energy absorption buildup factor, a factor which corrects for the contribution from scattered radiation.

Equations describing  $B(\mu r)$  for point photon sources in water have been published by Spencer and Simmons (1973); see also Berger (1968).

This equation is integrated over the volumes of the source and target organs, with numerical methods, to yield  $\Phi(X \leftrightarrow Y)$ . Note the double arrow: the conditions of the reciprocal dose theorem (Loevinger 1969) are met, and the reciprocal doses are exactly equal.

In this method, the phantoms are composed of water throughout and are embedded in an infinite water medium. In the Monte Carlo radiation transport method, the phantoms have different densities and chemical compositions for lung, skeletal, and soft tissue and are embedded in vacuum. Thus there may be systematic errors in the point-source kernel estimates of  $\Phi$ . These errors are reduced by applying empirical correction factors. Point-source kernel estimates are necessary when the Monte Carlo estimates are statistically unreliable.

Details of the point-source kernel computer program are given in Ryman, Warner, and Eckerman (1987b).

## REFERENCES

- Berger, M. J., 1968, "Energy Deposition in Water by Photons from Point Isotropic Sources," MIRD Pamphlet 2, *J. Nucl. Med.* 9, Suppl. No. 1, 15-25.
- Cristy, M., 1980, *Mathematical Phantoms Representing Children of Various Ages for Use in Estimates of Internal Dose*, U.S. Nuclear Regulatory Commission Rep. NUREG/CR-1159 (also Oak Ridge National Laboratory Rep. ORNL/NUREG/TM-367).
- Cristy, M., 1983, "Applying the Reciprocal Dose Principle to Heterogeneous Phantoms: Practical Experience from Monte Carlo Studies," *Phys. Med. Biol.* 28, 1289-1303.
- Cristy, M. and Eckerman, K. F., 1987a, *Specific Absorbed Fractions of Energy at Various Ages from Internal Photon Sources. I. Methods*, Oak Ridge National Laboratory Rep. ORNL/TM-8381:Vol. 1 (in press).
- 1987b, *Specific Absorbed Fractions of Energy at Various Ages from Internal Photon Sources. II. One-year-old*, Oak Ridge National Laboratory Rep. ORNL/TM-8381:Vol. 2 (in press).
- 1987c, *Specific Absorbed Fractions of Energy at Various Ages from Internal Photon Sources. III. Five-year-old*, Oak Ridge National Laboratory Rep. ORNL/TM-8381:Vol. 3 (in press).
- 1987d, *Specific Absorbed Fractions of Energy at Various Ages from Internal Photon Sources. IV. Ten-year-old*, Oak Ridge National Laboratory Rep. ORNL/TM-8381:Vol. 4 (in press).
- 1987e, *Specific Absorbed Fractions of Energy at Various Ages from Internal Photon Sources. V. Fifteen-year-old Male and Adult Female*, Oak Ridge National Laboratory Rep. ORNL/TM-8381:Vol. 5 (in press).
- 1987f, *Specific Absorbed Fractions of Energy at Various Ages from Internal Photon Sources. VI. Newborn*, Oak Ridge National Laboratory Rep. ORNL/TM-8381:Vol. 6 (in press).
- 1987g, *Specific Absorbed Fractions of Energy at Various Ages from Internal Photon Sources. VII. Adult Male*, Oak Ridge National Laboratory Rep. ORNL/TM-8381:Vol. 7 (in press).
- Loevinger, R., 1969, "Distributed Radionuclide Sources," *Radiation Dosimetry*, 2nd edition, Vol. III, (F. H. Attix and E. Tochilin,

Eds.) pp 51-90 (Academic Press; New York).

Ryman, J. C., Warner, G. G., and Eckerman, K. F., 1987a, *ALGAMP -- A Monte Carlo Radiation Transport Code for Calculating Specific Absorbed Fractions of Energy from Internal or External Photon Sources*, Oak Ridge National Laboratory Rep. ORNL/TM-8377 (in preparation).

---- 1987b, *Computer Codes for Calculating Specific Absorbed Fractions of Energy from Internal Photon Sources by the Point Kernel Method*, Oak Ridge National Laboratory Rep. ORNL/TM-8378 (in preparation).

Snyder, W. S., Ford, M. R., Warner, G. G., and Watson, S. B., 1974, *A Tabulation of Dose Equivalent per Microcurie-day for Source and Target Organs of an Adult for Various Radionuclides: Part 1*, Oak Ridge National Laboratory Rep. ORNL-5000.

Spencer, L. V. and Simmons, G. L., 1973, "Improved Moment Method Calculations of Gamma-Ray Transport: Application to Point Isotropic Sources in Water," *Nucl. Sci. Eng.* 50, 20-31.

## SPECIFIC ABSORBED FRACTIONS FOR THE PREGNANT FEMALE

During the last year Joel L. Davis, on sabbatical from the University of Tennessee at Chattanooga (UTC), has worked with our group to adapt the anatomical model of a pregnant female at the end of the first trimester for use with the code system used by our group to calculate specific absorbed fractions. The anatomical model was developed by M. G. Stabin of Oak Ridge Associated Universities (ORAU). These specific absorbed fractions are used in the MIRD schema of dosimetric estimates for internal gamma emitters (MIRD = Medical Internal Radiation Dosimetry Committee of the U.S. Society of Nuclear Medicine). In order to implement the MIRD system, one needs to know the fraction of the energy that is absorbed by one organ when it is emitted from another organ. One needs this information for all pairs of organs and a range of energies. This range of needs results in a total of 6,144 specific absorbed fractions required. Our work this year has resulted in recommendations for these values.

The phantom developed by Stabin is based on earlier work by R. J. Cloutier, S. A. Smith, and E. E. Watson of ORAU and W. S. Snyder and G. G. Warner of Oak Ridge National Laboratory. The uterus is represented by a right circular cone capped with a hemisphere. Room is made for this enlarged uterus in the lower abdomen by cutting out a section of a sphere from the lower front of the small intestine. A volume equal to the removed volume is added to the front of the small intestine. The urinary bladder is moved lower and flattened on top by its contact with the uterus. Also the ascending colon is moved to the right to miss the uterus. All of these geometrical changes were implemented in the Monte Carlo radiation transport code ALGAMP and the point kernel code and these codes were run to yield estimates of each specific absorbed fraction and 'best' estimates were chosen with methods discussed in the preceding section.

Similar work on a second and third trimester gravida will be undertaken in the future.

## ABSORBED FRACTION IN ACTIVE MARROW FOR ELECTRONS WITHIN TRABECULAR BONE

## INTRODUCTION

Because the structure of trabecular bone could not be described in simple geometrical terms, Spiers and coworkers (Spiers 1969; Whitwell and Spiers 1978) introduced a method of calculating the energy deposition in which the geometries of the trabeculae and marrow cavities are represented by measured distributions of the chord-lengths across them. If the track of a particle is assumed to be straight, then the total track in trabeculation is represented by path-lengths alternately selected in a random manner from the chord-length distribution for trabeculae and cavities. The energy loss of the electrons in the trabeculae and cavities can be computed from the range-energy relationship.

## DISTRIBUTION OF CHORD-LENGTHS

There are many ways in which randomness of chords may arise in convex bodies; however, only two are of interest here:

Mean-free-path randomness (or  $\mu$ -randomness). A chord of a convex body is defined by a point in space and a direction. The point and direction are chosen randomly from independent, uniform distributions. This kind of randomness results, for example, if a convex body is exposed to a uniform, isotropic field of straight lines.

Interior radiator randomness (or I-randomness). A chord is defined by a point within the interior of the convex body and a direction. The point and direction are chosen randomly from independent, uniform distributions. This kind of randomness results, for example, if the convex body contains a uniform distribution of point sources, each of which emits radiation isotropically.

If charged particles (electrons) originate in a uniform-isotropic manner outside of a convex body (trabeculae or marrow cavity) one is dealing with  $\mu$ -randomness, which is the situation under which chord-length distributions were measured by Spiers and coworkers (Spiers 1969; Beddoe et al. 1976; and Beddoe 1977). However, for particles

originating within a convex body I-randomness is applicable. The chord distributions under  $\mu$ - and I-randomness have been shown to be related as (Kellerer 1971);

$$f_I(x) = \frac{x}{\langle x \rangle_\mu} f_\mu(x) \quad , \quad (1)$$

where

$f_I(x)$  and  $f_\mu(x)$  denote the probability density functions for chord-lengths under I- and  $\mu$ -randomness, respectively, and  $\langle x \rangle_\mu$  denotes the mean value of the  $f_\mu(x)$  distribution.

Equation (1) refers to the full chord; however, we are interested in 'half-chords' or rays formed by particles originating within the convex body. The probability density function for the ray-length distribution,  $f_i(x)$ , can be shown to be given by

$$f_i(x) = \frac{1}{\langle x \rangle_\mu} \left\{ 1 - F_\mu(x) \right\} \quad , \quad (2)$$

where  $F_\mu(x)$  is the cumulative distribution function given as

$$F_\mu(x) = \int_0^x f_\mu(s) ds.$$

From the preceding it is apparent that the mean ray-length for particles emitted internally to a convex body is one-half the mean chord-length for I-randomness, i.e.,  $\langle x \rangle_i = \frac{1}{2} \langle x \rangle_I$ . The mean chord-length under  $\mu$ -randomness,  $\langle x \rangle_\mu$ , is related to the volume,  $V$ , and surface area,  $S$ , of a convex body by Cauchy's theorem:  $\langle x \rangle_\mu = 4 \frac{V}{S}$ .

As an example, consider a sphere whose chord-length distribution for  $\mu$ -randomness is simple and well-known, i.e.,  $f_\mu(x) = 2 \frac{x}{d^2}$ , with mean chord-length  $\langle x \rangle_\mu = \frac{2}{3} d$ . From Eq. (1), the distribution for I-randomness in a sphere is  $f_I(x) = \frac{3x^2}{d^3}$ , for which the mean chord length is  $\langle x \rangle_I = \frac{3}{4} d$ . The probability density function of ray-lengths, obtained from Eq. (2), is

$$f_i(x) = \frac{3}{2d} \left\{ 1 - (x/d)^2 \right\} \quad , \quad (3)$$

with mean ray-length of  $\langle x \rangle_i = \frac{3}{8} d$ . The various distributions of chord- and ray-lengths in a sphere are depicted in Fig. 1.

Mean chord- and ray-lengths for the trabeculae and marrow cavities of several trabecular bones of the skeleton of man are summarized in Table 1. Note that the parietal bone appears to be distinct from the other bones in that its thick trabeculae and small marrow cavities lead to a high  $\langle t \rangle_\mu : \langle c \rangle_\mu$  ratio.

#### ABSORBED FRACTIONS FOR MONOENERGETIC ELECTRONS

The absorbed fraction in  $v$  from  $r$ ,  $\phi(v+r)$ , is defined as

$$\phi(v+r) = \frac{\text{energy absorbed in target region } v}{\text{energy emitted by source region } r} \quad (4)$$

Thus  $\phi$  embodies the transport of the radiation under consideration as well as the geometric relationship of the regions. The absorbed fraction data developed here are for monoenergetic electrons emitted uniformly (by mass) and isotropically within the trabeculae and cavities of trabecular bone. The target region of interest is the active or red marrow (denoted as RM), for which we average the energy deposition over the marrow cavities.

The representation of paths for an electron of energy  $E$  and range in marrow  $R_{RM}$  are illustrated in Fig. 2. By use of chord-length distributions the three-dimensional geometry has been reduced to one dimension. Furthermore the two media (bone and marrow) nature of the problem can be reduced to a single medium as the ratio of the range of electrons in marrow (RM) to that of bone (TB) is nearly constant over electron energies of interest here, that is:  $R_{RM} \cong 1.75 R_{TB}$ .

For irradiation of the active marrow by electrons originating within trabeculae, Monte Carlo sampling is used to select a chord-length,  $t$ , from the probability density function,  $f_I(t)$ , for the bone under consideration. A ray-length,  $t'$ , is then determined as  $t' = \xi t$ , where  $\xi$  is a random number uniform on the region  $0 < \xi < 1$ . The electron is tracked as it alternately passes through marrow cavities along lengths  $c_1, c_2, \dots$ , and trabeculae along chords  $t_1, t_2, \dots$ , selected by Monte Carlo sampling of the probability density functions  $f_\mu(c)$  and  $f_\mu(t)$ , respectively. The electron is tracked until

$$1.75(t' + t_1 + t_2 + \dots) + (c_1 + c_2 + \dots) \geq R_{RM} \quad , \quad (5)$$

i.e., its energy has been deposited. The energy deposition in trabeculae (t's) and marrow cavities (c's) is calculated as the difference between the energy on entering and leaving a trabecula or cavity, in each case being determined from the residual range of the electron at that point in its track. The range-energy relationship was taken from Berger (1973). By tracking a large number of electrons in this manner, the absorbed fraction is obtained by dividing the total energy deposited in marrow cavities by the total energy of electrons simulated.

For electrons emitted within marrow cavities the calculations proceed as above, first with selection of a chord-length from the probability density function  $f_T(c)$  and determination of a ray-length  $c'$  as noted above. The electron is tracked until

$$(c' + c_1 + c_2 + \dots) + 1.75(t_1 + t_2 + \dots) \geq R_{RM} \quad . \quad (6)$$

The energy deposition in the marrow cavities and the absorbed fraction are determined as discussed above. Typically, ten- to seventy-thousand electrons were tracked in each of the two absorbed fraction calculations. The statistical errors in the Monte Carlo calculations were less than 1%.

## RESULTS

The absorbed fraction data for the parietal bone and lumbar vertebra of the skeleton of a 44-year-old male are shown in Fig. 3. At low electron energies,  $\phi(RM \leftarrow TB)$  approaches zero and  $\phi(RM \leftarrow RM)$  approaches unity. This limiting behavior reflects the fact that at low energy the range of electrons is small relative to the mean ray-lengths,  $\langle t \rangle_i$  and  $\langle c \rangle_i$ , and thus the energy is deposited locally. At high energies,  $\phi(RM \leftarrow RM) \cong \phi(RM \leftarrow TB)$  and the behavior is described as

$$\lim_{E \rightarrow \infty} \phi(RM \leftarrow TB) \cong \phi(RM \leftarrow RM) \cong \frac{\langle c \rangle}{\langle c \rangle + 1.75 \langle t \rangle} \quad , \quad (7)$$

i.e., the absorbed fraction is simply the fractional track length in the

marrow cavities. The equality of the absorbed fractions at high energy arises because electrons traverse multiple trabeculae and cavities thus establishing an energy deposition pattern which is largely independent of the electron's origin.

The results of the calculations for the parietal bone of the skull and the lumbar vertebra are given in Tables 2 and 3 for a 44-year-old male and a 20-month-old child, respectively. The atypical structure of the parietal bone is reflected in the absorbed fraction data for either the child or the adult; however, difference with age appears to be less pronounced.

#### REFERENCES

- Beddoe, A. H., Darley, P. J., and Spiers, F. W., 1976, "Measurements of Trabecular Bone Structure in Man," *Phys. Med. Biol.* 21, 589-607.
- Beddoe, A. H., 1977, "Measurements of the Microscopic Structure of Cortical Bone," *Phys. Med. Biol.* 22, 298-308.
- Berger, M. J., 1973, *Improved Point Kernals for Electron and Beta-Ray Dosimetry*, NBSIR 73-107.
- Kellerer, A. M., 1971, "Consideration on the Random Traversal of Convex Bodies and Solutions for General Cycliners," *Radiat. Res.* 47, 359-376.
- Spiers, F. W., 1969, "Transition-zone Dosimetry," *Radiation Dosimetry* Vol. 3, (E. H. Attix and E. Tochlin, Eds.), 809-867, (Academic Press) .
- Whitwell, J. R. and Spiers, F. W., 1978, "Calculated Beta-ray Dose Factors for Trabecular Bone," *Phys. Med. Biol.* 21, 16-38.
- Whitwell, J. R., 1973, *Theoretical Investigations of Energy Loss by Ionizing Particles in Bone*, Ph.D. Thesis, University of Leeds, Leeds, UK.

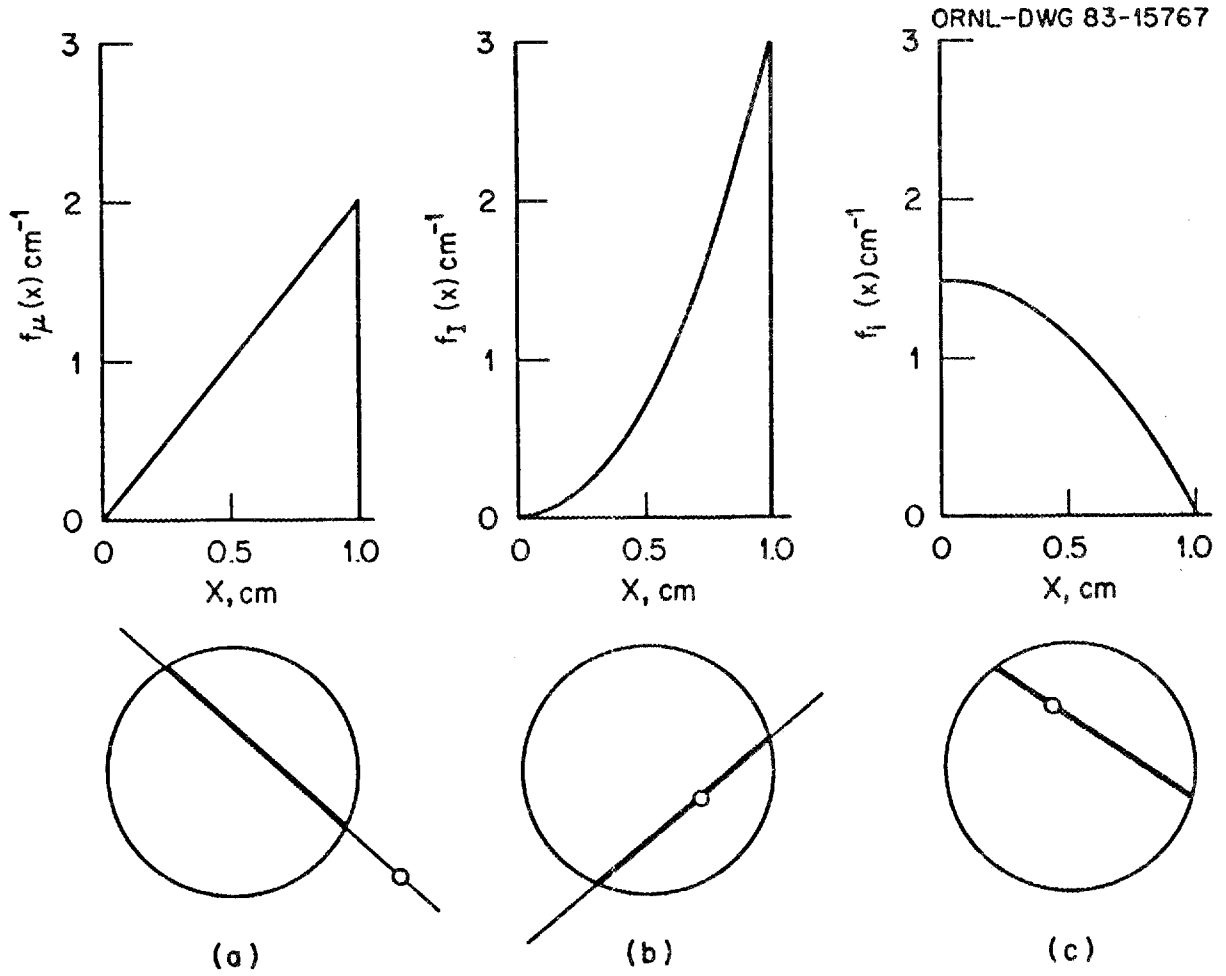


Figure 1. For a sphere of unit diameter, chord-length distributions for  $\mu$ -randomness (a), I-randomness (b), and ray-length distribution (c).

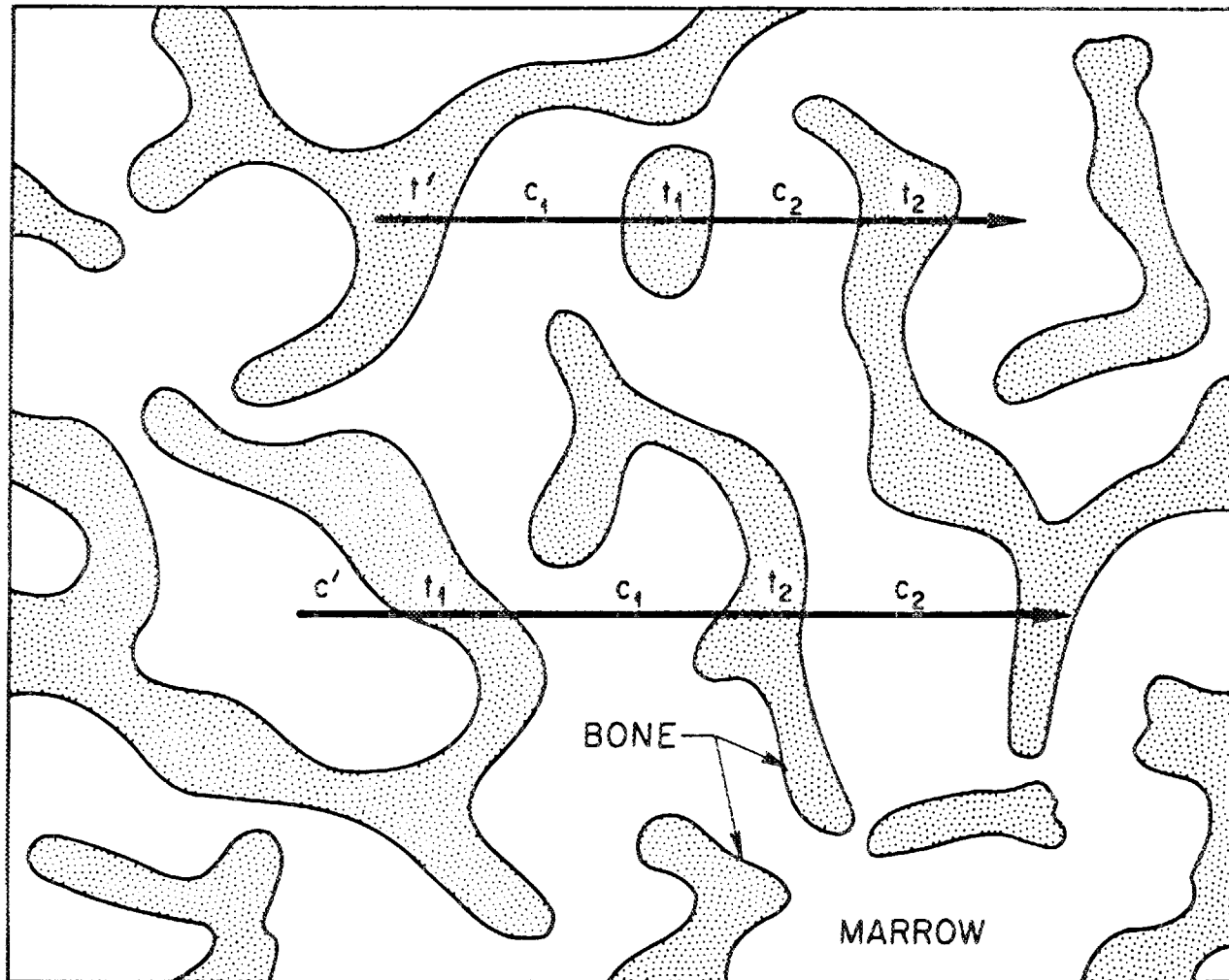


Figure 2. Schematic illustration of the track of an electron through trabecular bone. Monte Carlo sampling of chord-length distributions is used to determine the  $t$ 's and  $c$ 's defining the total track.

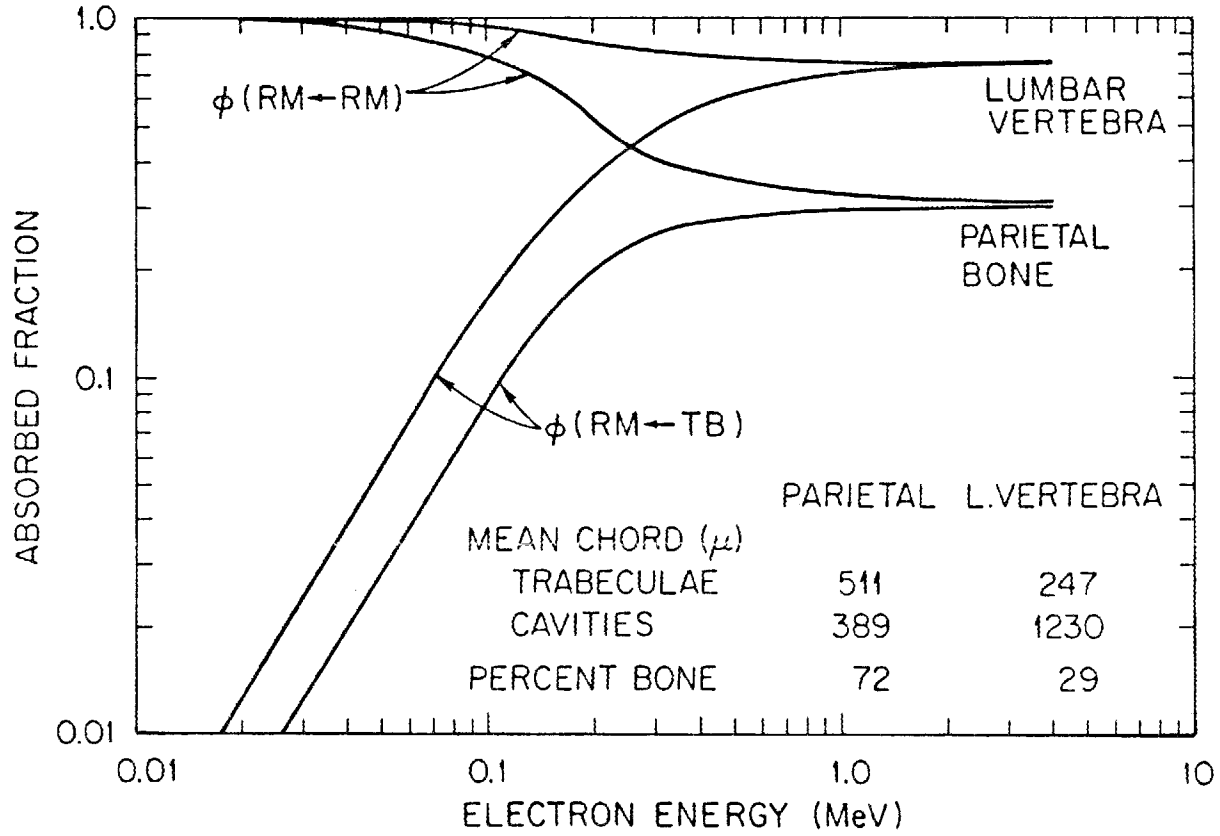


Figure 3. Absorbed fractions in active marrow RM for a monoenergetic electron source uniformly distributed in the trabeculae TB and the active marrow RM of the lumbar vertebra and parietal bone of the adult.

Table 1. Mean chord- and ray-lengths ( $\mu\text{m}$ ) for trabeculae and marrow cavities in various bones of man.

| Bones                           | Trabeculae <sup>a</sup>   |           |                       | Marrow Cavities <sup>a</sup> |           |                       |   |
|---------------------------------|---------------------------|-----------|-----------------------|------------------------------|-----------|-----------------------|---|
|                                 | $\langle t \rangle_{\mu}$ | $V_{\mu}$ | $\langle t \rangle_i$ | $\langle c \rangle_{\mu}$    | $V_{\mu}$ | $\langle c \rangle_i$ | $\langle t \rangle_{\mu} : \langle c \rangle_{\mu}$ |
| 44-year-old male <sup>b</sup>   |                           |           |                       |                              |           |                       |   |
| Parietal                        | 511                       | 0.570     | 401                   | 389                          | 0.784     | 347                   | 1.31  |
| Cervical vertebra               | 279                       | 0.719     | 240                   | 910                          | 0.894     | 861                   | 0.307   |
| Lumbar vertebra                 | 247                       | 1.11      | 260                   | 1228                         | 1.12      | 1299                  | 0.201   |
| Rib                             | 265                       | 1.49      | 330                   | 1706                         | 1.09      | 1786                  | 0.155   |
| Iliac crest                     | 242                       | 0.675     | 203                   | 904                          | 0.647     | 745                   | 0.268   |
| Femur head                      | 232                       | 0.665     | 193                   | 1157                         | 0.901     | 1099                  | 0.200   |
| Femur neck                      | 314                       | 0.914     | 301                   | 1655                         | 0.905     | 1576                  | 0.190   |
| 9-year-old child <sup>c</sup>   |                           |           |                       |                              |           |                       |   |
| Parietal                        | 539                       |           |                       | 306                          |           |                       | 0.272   |
| Cervical vertebra               | 162                       |           |                       | 906                          |           |                       | 0.179   |
| Lumbar vertebra                 | 168                       |           |                       | 857                          |           |                       | 0.196   |
| Rib                             | 231                       |           |                       | 1123                         |           |                       | 0.204   |
| Iliac crest                     | 180                       |           |                       | 744                          |           |                       | 0.242   |
| Femur, head & neck              | 249                       |           |                       | 616                          |           |                       | 0.404   |
| 20-month-old child <sup>b</sup> |                           |           |                       |                              |           |                       |   |
| Parietal bone                   | 566                       | 1.21      | 625                   | 255                          | 2.90      | 500                   | 2.22  |
| Lumbar vertebra                 | 188                       | 1.04      | 192                   | 736                          | 0.987     | 731                   | 0.255   |
| Rib                             | 191                       | 1.22      | 212                   | 559                          | 1.04      | 569                   | 0.342   |
| Iliac crest                     | 181                       | 1.43      | 206                   | 575                          | 0.873     | 539                   | 0.315   |
| Femur                           | 197                       | 0.865     | 184                   | 789                          | 1.10      | 830                   | 0.250   |

<sup>a</sup>Notation:  $(\langle t \rangle_{\mu}, V_{\mu})$  and  $(\langle c \rangle_{\mu}, V_{\mu})$  denote the mean and the fractional variance under  $\mu$ -randomness for the trabeculae and marrow cavities, respectively.  $\langle t \rangle_i$  and  $\langle c \rangle_i$  denote the mean ray-length for trabeculae and cavities, respectively. Lengths are in units of  $\mu\text{m}$ .

<sup>b</sup>Computed from the chord-length distributions of Whitwell (1973).

<sup>c</sup>See Tables 1 and 3 of Beddoe (1977).

Table 2. Absorbed fraction,  $\phi$ , in active marrow, RM, from a uniformly distributed source of monoenergetic electrons in trabeculae, TB, and marrow of the parietal bone and lumbar vertebrae of a 44-year-old male.

| Electron<br>energy<br>(MeV) | Parietal bone  |                | Lumbar Vertebrae |                |
|-----------------------------|----------------|----------------|------------------|----------------|
|                             | $\phi$ (RM+TB) | $\phi$ (RM+RM) | $\phi$ (RM+TB)   | $\phi$ (RM+RM) |
| 0.010                       | 1.95(-3)       | 0.994          | 3.94(-3)         | 0.999          |
| 0.015                       | 3.29(-3)       | 0.990          | 7.81(-3)         | 0.997          |
| 0.020                       | 5.77(-3)       | 0.983          | 1.29(-2)         | 0.996          |
| 0.030                       | 1.23(-2)       | 0.969          | 2.59(-2)         | 0.991          |
| 0.040                       | 1.98(-2)       | 0.950          | 4.34(-2)         | 0.985          |
| 0.050                       | 2.94(-2)       | 0.927          | 6.26(-2)         | 0.979          |
| 0.060                       | 4.03(-2)       | 0.901          | 8.25(-2)         | 0.971          |
| 0.080                       | 6.34(-2)       | 0.854          | 1.31(-1)         | 0.953          |
| 0.10                        | 8.80(-2)       | 0.794          | 1.83(-1)         | 0.935          |
| 0.15                        | 1.53(-1)       | 0.654          | 3.12(-1)         | 0.888          |
| 0.20                        | 1.99(-1)       | 0.538          | 4.17(-1)         | 0.848          |
| 0.30                        | 2.58(-1)       | 0.415          | 5.47(-1)         | 0.808          |
| 0.40                        | 2.71(-1)       | 0.376          | 5.97(-1)         | 0.793          |
| 0.50                        | 2.76(-1)       | 0.358          | 6.25(-1)         | 0.779          |
| 0.60                        | 2.82(-1)       | 0.346          | 6.48(-1)         | 0.767          |
| 0.80                        | 2.88(-1)       | 0.335          | 6.74(-1)         | 0.765          |
| 1.0                         | 2.93(-1)       | 0.327          | 6.90(-1)         | 0.757          |
| 2.0                         | 2.97(-1)       | 0.317          | 7.17(-1)         | 0.747          |
| 3.0                         | 3.00(-1)       | 0.311          | 7.22(-1)         | 0.747          |
| 4.0                         | 3.01(-1)       | 0.308          | 7.27(-1)         | 0.744          |

Table 3. Absorbed fraction,  $\phi$ , in active marrow, RM, from a uniformly distributed source of monoenergetic electrons in trabeculae, TB, and marrow of the parietal bone and lumbar vertebrae of a 20-month-old child.

| Electron energy (MeV) | Parietal Bone  |                | Lumbar Vertebrae |                |
|-----------------------|----------------|----------------|------------------|----------------|
|                       | $\phi$ (RM+TB) | $\phi$ (RM+RM) | $\phi$ (RM+TB)   | $\phi$ (RM+RM) |
| 0.01                  | 1.62(-3)       | 0.990          | 4.66(-3)         | 0.997          |
| 0.015                 | 3.44(-3)       | 0.981          | 9.90(-3)         | 0.995          |
| 0.02                  | 6.09(-3)       | 0.969          | 1.65(-2)         | 0.992          |
| 0.03                  | 1.24(-2)       | 0.947          | 3.39(-2)         | 0.984          |
| 0.04                  | 1.91(-2)       | 0.920          | 5.67(-2)         | 0.973          |
| 0.05                  | 2.80(-2)       | 0.889          | 8.01(-2)         | 0.962          |
| 0.06                  | 3.46(-2)       | 0.858          | 1.12(-1)         | 0.949          |
| 0.08                  | 5.12(-2)       | 0.789          | 1.74(-1)         | 0.922          |
| 0.10                  | 7.09(-2)       | 0.724          | 2.34(-1)         | 0.892          |
| 0.15                  | 1.06(-1)       | 0.591          | 3.74(-1)         | 0.829          |
| 0.20                  | 1.30(-1)       | 0.501          | 4.70(-1)         | 0.786          |
| 0.30                  | 1.54(-1)       | 0.401          | 5.58(-1)         | 0.750          |
| 0.40                  | 1.68(-1)       | 0.354          | 5.94(-1)         | 0.730          |
| 0.50                  | 1.76(-1)       | 0.328          | 6.26(-1)         | 0.722          |
| 0.60                  | 1.79(-1)       | 0.308          | 6.38(-1)         | 0.718          |
| 0.80                  | 1.81(-1)       | 0.283          | 6.51(-1)         | 0.706          |
| 1.0                   | 1.88(-1)       | 0.267          | 6.62(-1)         | 0.708          |
| 2.0                   | 1.96(-1)       | 0.238          | 6.78(-1)         | 0.698          |
| 3.0                   | 1.99(-1)       | 0.224          | 6.81(-1)         | 0.696          |
| 4.0                   | 2.01(-1)       | 0.221          | 6.84(-1)         | 0.696          |

ESTIMATING DOSE IN ACTIVE MARROW AND OSTEOGENIC TISSUE FROM PHOTONS  
FROM INTERNAL OR EXTERNAL SOURCES

The radiation transport computer program ALGAMP employs Monte Carlo techniques to simulate the transport of photons through the body (Ryman, Warner, and Eckerman 1987). It is used with any of a series of mathematical phantoms representing children and adults (see section "SPECIFIC ABSORBED FRACTIONS OF ENERGY AT VARIOUS AGES FROM INTERNAL PHOTON SOURCES" appearing earlier in Part 2 of this report) and can be used with photon sources either internal or external to the body. ALGAMP recognizes three different tissue types -- lung, skeletal, and soft tissues, each with its own density and chemical composition. Skeletal tissue in our phantoms is a homogenized mixture of mineral bone and the soft tissues within the skeleton, and in the past this has led to poor estimates of dose to the soft tissues within the skeleton.

In calculating the dose in an organ, we assume that the energy transferred to electrons by the photon interactions is absorbed by the organ in which the interaction occurred, i.e., the transport of energy by secondary electrons is not treated. This approach is reasonable if the amount of energy transported by secondary electrons out of the region of interest is balanced by transport into the region, i.e., electronic equilibrium exists. However, in the vicinity of discontinuities in tissue compositions, electronic equilibrium is not established and significant error in dose estimation may be introduced in assuming equilibrium. Examples of discontinuities in the body are the boundaries between skin and the surrounding air, between tissue and air voids within the respiratory tract, and between bone and soft tissue regions of the skeleton. It is this latter boundary we address here.

In each phantom the skeleton is represented as a uniform mixture of its component tissues, namely cortical bone, trabecular bone, fatty marrow, active (hematopoietic) marrow, and various connective tissues (see Table 1). The tissues of interest for dosimetric purposes (target regions) are the active marrow, which lies within the cavities of trabecular bone, and osteogenic cells adjacent to the surfaces of both cortical and trabecular bone; this latter target is referred to as endosteal tissue or "bone surfaces". To estimate the energy deposited

in these targets, one must consider the energy transported by secondary electrons arising from photon interactions within the target and from electrons entering the target from interactions occurring in the immediate vicinity, e.g., bone adjacent to the active marrow.

A number of investigators (Spiers 1949, 1953; Woodard and Spiers 1953; Charlton and Cormack 1962; Aspin and Johns 1963; Howarth 1965), using simple geometrical models (e.g., thin slabs, cylinders, and spherical cavities) to approximate the geometry, have demonstrated that for photon energies less than about 200 keV electronic equilibrium does not exist and electrons liberated in bone mineral contribute substantially to the absorbed dose in soft tissues of the skeleton. Snyder, Ford, and Warner (1978) encountered the intractable geometry of the skeleton in their Monte Carlo studies of photon transport and formulated their calculation of absorbed dose in marrow in a conservative manner. They partitioned the energy deposited in the skeleton to various skeletal tissues, including active marrow, according to the fraction of the skeletal mass attributed to the tissue. The potential for an overestimate of absorbed dose in the active marrow was noted by them (p. 20):

"... it is assumed that the marrow absorbs energy per gram as efficiently as does bone. This assumption is not grossly wrong at energies of 200 keV or more, but is increasingly inaccurate at energies below 100 keV. The effect is to somewhat overestimate the dose to marrow and to somewhat underestimate the dose to bone. This difficulty results from the failure to find ways to program the intricate mixture of bone and marrow spaces in a more realistic fashion."

The overestimate of the dose to active marrow with this assumption can be as much as 300-400% for photon energies less than 100 keV.

The consideration of osteogenic cells as the target tissue for bone cancer (ICRP 1977) and the overestimate of the dose to the active marrow required a new computational approach which formulated the absorbed dose in terms of the relevant physical and anatomical variables governing the energy deposition. The geometry problem, noted by Snyder and co-workers, is also encountered in the dosimetry of beta-emitting radionuclides incorporated in bone, for which Spiers and co-workers reduced the intractable three-dimensional geometry to one dimension

through use of measured distributions of chord lengths in trabeculae and marrow cavities of trabecular bone (Spiers 1969; Beddoe, Darley, and Spiers 1976; Beddoe 1977; and see preceding section). We have applied Spiers' methodology to secondary electrons liberated by photon interactions in the skeleton. Although the new computational approach uses information on the microscopic structure of bone to follow *electron transport*, it was possible to retain the homogeneous representation of the skeleton in the Monte Carlo calculations of *photon transport*. Thus, only minor revisions were made to the Monte Carlo transport code.

The absorbed dose from photon radiation varies, of course, with the number of photons passing through the region. In the discussion below we refer to the "dose per unit fluence" as a fluence-conversion function,  $R$ , and assume that such functions can be constructed to define the absorbed dose in the active marrow (or in the endosteal tissue) per unit fluence of photons in the skeleton. The derivation of the fluence-conversion functions is presented in an appendix which follows this section. The Monte Carlo transport code was modified to estimate the photon fluence and to "score or tally" the absorbed dose in the active marrow and endosteal tissues based on the fluence and the fluence-conversion functions. The photon fluence in a region of volume  $V$  can be related to the number of interactions occurring at energy  $E$ ,  $N(E)$ , calculated for the region;

$$\Psi(E) = \frac{N(E)}{\mu(E) V} \quad . \quad (1)$$

For an individual photon history,  $i$ , the contribution to the absorbed dose is scored as

$$D_i = \frac{1}{V} \sum_{j=1}^{N_i} \frac{wt_j}{\mu(E_j)} R(E_j) \quad , \quad (2)$$

where

$j$  indexes the collisions in region  $V$  experienced by the  $i$ th photon,  
 $V$  is the volume of the region over which the fluence is averaged,

$w_{jt}$  is the statistical weight\* of the photon entering the  $j$ th collision,

$\mu(E_j)$  is the linear attenuation coefficient at energy  $E_j$ , and

$R(E_j)$  is the absorbed dose per unit fluence.

In developing the above procedure we found it necessary to consider two fluence-conversion functions for the active marrow. One function pertains to marrow within the skull (a somewhat atypical trabecular bone) and the other addresses all other active marrow sites. A single fluence-conversion function was found to be adequate for the endosteal tissue.

#### REFERENCES

- Aspin, N. and Johns, H. E., 1963, "The Absorbed Dose in Cylindrical Cavities within Irradiated Bone," *Brit. J. Radiol.* 36, 350-362.
- Beddoe, A. H., 1977, "Measurements of the Microscopic Structure of Cortical Bone," *Phys. Med. Biol.* 22, 298-308.
- Beddoe, A. H., Darley, P. J., and Spiers, F. W., 1976, "Measurements of Trabecular Bone Structure in Man," *Phys. Med. Biol.* 21, 589-607.
- Charlton, D. E. and Cormack, D. V., 1962, "Energy Dissipation in Finite Cavities," *Radiat. Res.* 17, 34-49.
- Cristy, M. and Eckerman, K. F., 1987, *Specific Absorbed Fractions of Energy at Various Ages from Internal Photon Sources. I. Methods*, Oak Ridge National Laboratory Rep. ORNL/TM-8381:Vol. 1 (in press).
- Howarth, J. L., 1965, "Calculation of the Absorbed Dose in Soft-Tissue Cavities in Bone Irradiated by X-rays," *Rad. Res.* 24, 158-183.
- ICRP, 1977, *ICRP Publication 26, Recommendations of the International Commission on Radiological Protection* (Pergamon Press; Oxford).

---

\* In simulating the transport of photons it is useful to allow photons to continue undergoing scattering events rather than be absorbed. A statistical weight of one is initially assigned to the photon and at each collision the weight is reduced by the probability that the collision was a scattering event. Thus the statistical weight after  $j$  collision may be thought of as the probability of that particular photon existing. The number of collisions in region  $V$  for the  $i$ th photon history is simply  $\sum_j w_{jt}$ .

- Leggett, R. W., Eckerman, K. F., and Williams, L. R., 1982, "Strontium-90 in Bone: A Case Study in Age-dependent Dosimetric Modelling," *Health Phys.* 43, 307-322.
- Ryman, J. C., Warner, G. G., and Eckerman, K. F., 1987, *ALGAMP -- A Monte Carlo Radiation Transport Code for Calculating Specific Absorbed Fractions of Energy from Internal or External Photon Sources*, Oak Ridge National Laboratory Rep. ORNL/TM-8377 (in preparation).
- Snyder, W. S., Ford, M. R., and Warner, G. G., 1978, *Estimates of Specific Absorbed Fractions for Photon Sources Uniformly Distributed in Various Organs of a Heterogeneous Phantom*, MIRD Pamphlet No. 5, Revised (Society of Nuclear Medicine; New York).
- Spiers, F. W., 1949, "The Influence of Energy Absorption and Electron Range on Dosage in Irradiated Bone," *Brit. J. Radiol.* 12, 521-533.
- Spiers, F. W., 1951, "Dosage in Irradiated Soft Tissue and Bone," *Brit. J. Radiol.* 24, 365-369.
- Spiers, F. W., 1969, "Beta Dosimetry in Trabecular Bone," *Delayed Effects of Bone-Seeking Radionuclides* (C. W. Mays et al., Eds.) pp 95-108 (U. of Utah Press; Salt Lake City).
- Woodard, H. Q. and Spiers, F. W., 1953, "The Effect of X-Rays of Different Qualities on the Alkaline Phosphates of Living Mouse Bone," *Brit. J. Radiol.* 26, 38-46.

Table 1. Summary of Descriptive Parameters for the Skeleton of Man.

| Descriptive parameter                                | Age (yr) |       |       |       |       |       |
|--|----------|-------|-------|-------|-------|-------|
|  | 0        | 1     | 5     | 10    | 15    | Adult |
| <b>Skeleton<sup>a</sup></b>                          |          |       |       |       |       |       |
| Volume (cm <sup>3</sup> )                            | 288      | 813   | 1935  | 3309  | 5466  | 7155  |
| Mass (kg)  | 0.351    | 1.140 | 2.710 | 4.630 | 7.650 | 10.0  |
| Density (g/cm <sup>3</sup> )                         | 1.22     | 1.40  | 1.40  | 1.40  | 1.40  | 1.40  |
| <b>Bone mineral</b>                                  |          |       |       |       |       |       |
| Calcium <sup>b</sup> (g)                             | 28       | 99.8  | 219   | 396   | 806   | 1000  |
| Mass <sup>c</sup> (kg)                               | 0.140    | 0.499 | 1.095 | 1.980 | 4.030 | 5.000 |
| Fraction <sup>d</sup>                                | 0.399    | 0.438 | 0.404 | 0.427 | 0.527 | 0.500 |
| <b>Active marrow</b>                                 |          |       |       |       |       |       |
| Mass <sup>a</sup> (kg)                               | 0.047    | 0.150 | 0.320 | 0.610 | 1.050 | 1.120 |
| Fraction <sup>d</sup>                                | 0.134    | 0.132 | 0.118 | 0.132 | 0.137 | 0.112 |
| <b>Inactive marrow</b>                               |          |       |       |       |       |       |
| Mass <sup>a</sup> (kg)                               | -        | 0.020 | 0.140 | 0.590 | 1.550 | 2.380 |
| Fraction <sup>d</sup>                                | -        | 0.018 | 0.052 | 0.127 | 0.203 | 0.238 |
| <b>Other tissues<sup>e</sup></b>                     |          |       |       |       |       |       |
| Mass(kg)   | 0.164    | 0.469 | 1.154 | 1.453 | 1.022 | 1.5   |
| Fraction <sup>d</sup>                                | 0.467    | 0.412 | 0.426 | 0.314 | 0.133 | 0.150 |
| <b>Trabecular bone<sup>f</sup></b>                   |          |       |       |       |       |       |
| Mass (kg)  | 0.140    | 0.200 | 0.219 | 0.396 | 0.806 | 1.000 |
| Fraction <sup>d</sup>                                | 0.176    | 0.438 | 0.081 | 0.085 | 0.105 | 0.100 |
| S/V <sup>g</sup> (cm <sup>2</sup> /cm <sup>3</sup> ) | -        | 220   | -     | 225   | -     | 190   |
| <b>Cortical bone<sup>e</sup></b>                     |          |       |       |       |       |       |
| Mass (kg)  | -        | 0.299 | 0.875 | 1.584 | 3.224 | 4.000 |
| Fraction <sup>d</sup>                                | -        | 0.263 | 0.323 | 0.342 | 0.421 | 0.400 |
| <b>Surface area (m<sup>2</sup>)</b>                  |          |       |       |       |       |       |
| Trabecular <sup>h</sup>                              | 1.5      | 2.1   | 2.3   | 4.2   | 8.5   | 6.0   |
| Cortical <sup>i</sup>                                | -        | 0.45  | 1.3   | 2.4   | 4.8   | 6.0   |
| Total  | 1.5      | 2.6   | 3.6   | 6.6   | 13    | 12    |

<sup>a</sup> See Appendix B of Cristy and Eckerman (1987).

<sup>b</sup> See Leggett et al. 1982.

<sup>c</sup> Computed assuming 0.2 g-Ca per g bone mineral.

<sup>d</sup> Mass fraction in the skeleton.

<sup>e</sup> Difference between skeletal mass and identified tissues.

<sup>f</sup> All bone is trabecular at birth; 40% at one year, 20% thereafter.

<sup>g</sup> Surface to volume ratio (Beddoe et al. 1976).

<sup>h</sup> Based on trabecular bone mass and S/V ratio of 220 through age 10, 190 at age 15, and 120 for the adult.

<sup>i</sup> The adult S/V ratio for cortical bone was applied to all ages.

ESTIMATING DOSE IN ACTIVE MARROW AND OSTEOGENIC TISSUE FROM PHOTONS.  
FLUENCE-CONVERSION FUNCTIONS.

Calculations of absorbed dose to soft tissues within the skeleton have been hampered by difficulties in modeling the geometry of the bone-soft tissue mixture. In this Appendix the absorbed dose in the soft tissue of the skeleton per unit photon fluence is formulated in terms of the physical and anatomical parameters governing the energy deposition. We refer to the resulting relationships as fluence-conversion functions, and we can estimate the absorbed dose by applying them to estimates of photon fluence in the skeleton derived from Monte Carlo transport calculations.

ABSORBED DOSE PER UNIT FLUENCE

Consider the trabeculation of a bone experiencing a fluence,  $\Psi(E)$ , of photons of energy  $E$ . Let  $m(TB)$ ,  $m(RM)$ , and  $m(BS)$  denote the mass of trabecular bone (TB), active (red) marrow (RM), and endosteal tissue (or "bone surface," BS) adjacent to the surface of the trabeculae. If we index the type of interaction by  $i$  and the region in which it occurred by  $r$ , where  $r = TB$  or  $RM$ , then the absorbed dose in active marrow,  $D(RM)$ , and in endosteal tissue,  $D(BS)$ , per unit fluence can be expressed as

$$\frac{D(RM)}{\Psi(E)} = \sum_r \frac{m(r)}{m(RM)} \sum_i \int_0^{\infty} \phi(RM \leftarrow r, T_i) (i/\rho)_r n_r(T_i) T_i dT_i \quad (1)$$

$$\frac{D(BS)}{\Psi(E)} = \sum_r \frac{m(r)}{m(BS)} \sum_i \int_0^{\infty} \phi(BS \leftarrow r, T_i) (i/\rho)_r n_r(T_i) T_i dT_i \quad (2)$$

where

$\phi(RM \leftarrow r, T_i)$  is the absorbed fraction in RM from  $r$  for electrons of energy  $T_i$ ,

$\phi(BS \leftarrow r, T_i)$  is the absorbed fraction in BS from  $r$  for electrons of energy  $T_i$ ,

$(i/\rho)_r$ ,  $i = \tau, \sigma$ , and  $\kappa$ , denotes the mass attenuation coefficients in medium  $r$  for the photoelectric, Compton, and pair-production

interactions, respectively, and

$n_r(T_i)dT_i$  denotes the number of electrons of energy between  $T_i$  and  $T_i + dT_i$  liberated in region  $r$  per interaction  $i$ .

The mass ratios appearing in the above equations can be related to the mean chord lengths of the trabeculae,  $\langle t \rangle$ , and marrow space,  $\langle c \rangle$ , as measured by scanning the trabeculation in an isotropic manner (Beddoe, Darley, and Spiers 1976). Information on the mean chord lengths for various trabecular bones of the body as a function of age is given in Table 1 of the section "ABSORBED FRACTION IN ACTIVE MARROW FOR ELECTRONS WITHIN TRABECULAR BONE" appearing earlier in Part 2 of this report. Note that for all ages the parietal bone of the skull appears to be distinct from other trabecular bones, as indicated by the ratios of the mean chord-lengths. The mass ratios in Eq. (1) and (2) can be expressed in terms of the measured chord lengths:

$$\frac{m(\text{TB})}{m(\text{RM})} = \frac{\rho_{\text{TB}} \langle t \rangle}{\rho_{\text{RM}} \langle c \rangle} \quad (3)$$

$$\frac{m(\text{TB})}{m(\text{BS})} = \frac{\rho_{\text{TB}} \langle t \rangle}{\rho_{\text{RM}} 4 d} \quad (4)$$

$$\frac{m(\text{RM})}{m(\text{BS})} = \frac{\langle c \rangle}{4 d} \quad (5)$$

where  $\rho_{\text{TB}}$  and  $\rho_{\text{RM}}$  denote the density of bone and marrow and  $d$  is the distance over which the dose to endosteal tissue is averaged. We use a value for  $d$  of 10  $\mu\text{m}$  from Publication 30 of the International Commission on Radiological Protection (ICRP 1979).

About one-half of the mass of soft tissue within 10  $\mu\text{m}$  of the surfaces of bone is associated with trabecular bone (ICRP 1975). The soft tissue of cortical bone is contained within small cavities (mostly the Haversian canals of about 50  $\mu\text{m}$  diameter) within the bone matrix. The fluence-conversion function for this component of the endosteal tissue is computed as the dose to a small tissue-filled cavity in an infinite extent of bone. The fluence-conversion function for the endosteal tissue of cortical bone is given as

$$\frac{D(BS)}{\Psi(E)} = \sum_i \int_0^{\infty} (i/\rho)_r n_r(T_i) T_i S(T_i) dT_i, \quad (6)$$

where  $S(T_i)$  denotes the ratio of the mass stopping power for soft tissue to that of bone at energy  $T_i$ . Stopping power data were computed with the procedures of Seltzer and Berger (1982a,b) and the elemental composition of marrow and bone from Kerr (1982). The dose to endosteal tissues is taken as the average of that indicated by equations 2 and 3, since trabecular and cortical bone each contributes equally to the skeletal endosteal tissue.

#### ABSORBED FRACTIONS FOR MONOENERGETIC ELECTRONS

Because the geometry of trabecular bone could not be described in simple terms, Spiers and co-workers (Spiers 1969; Whitwell and Spiers 1976; Spiers et al. 1978) introduced a method of calculating energy deposition using the path-lengths traversed by particles. These path-lengths are based on chord-length distributions for trabeculae and marrow cavities obtained by optically scanning the trabeculation (Beddoe et al. 1976). Absorbed fraction data for monoenergetic electrons, as required in Eq. (1), were computed (Eckerman 1986) following the methods outlined by Whitwell (1973) and Whitwell and Spiers (1976); see also the section "ABSORBED FRACTION IN ACTIVE MARROW FOR ELECTRONS WITHIN TRABECULAR BONE" appearing earlier in Part 2 of this report. These absorbed fraction data, for active marrow and for endosteal tissue, are tabulated in Table 1 for the parietal bone and lumbar vertebra of the skeleton of a 44-year-old male; corresponding data for a child (age 20 months) are presented in Table 2. (The data for active marrow for the 44-year-old male is also presented in Fig. 1 of the section mentioned above.) In both subjects the absorbed fraction data for other marrow sites were similar to that for the lumbar vertebra. Although some age dependence is indicated, it appears to be weak. (It should be remembered, however, that the data for each age are from only one person; it would be useful to have data from additional persons.)

## ENERGY DISTRIBUTION OF SECONDARY ELECTRONS

Photons transfer energy to electrons through three major interactions: the photoelectric effect, the Compton effect, and pair-production. Photon cross sections from Hubbell (1982) and elemental composition of tissue from Kerr (1982) were used in evaluating the energy transfer. Photoelectrons were assumed to be of discrete energy corresponding to the incident photon energy. The energy distribution of Compton electrons was calculated from the Klein-Nishina relationship (Evans 1969), and the positron-electron energy distribution was derived from the Bethe-Heitler theory of pair-production (Heitler 1964).

## DOSE PER UNIT FLUENCE

A complete set of fluence-conversion functions for the active marrow of each trabecular bone of the adult is given in Table 3. The contributions of electrons arising from photon interactions in bone and marrow to the absorbed dose in the active marrow are shown in Fig. 1. The fluence-conversion function for the active marrow of the parietal bone is different from the fluence-conversion functions for the other sites. Considering the highly stylized model of the skeleton used in photon transport calculations, we recommend that the skull be treated as a separate bone region and data for the parietal bone in Table 3 be applied to estimate marrow dose. The lumbar vertebra appears to be representative of other trabecular sites. Furthermore, we note that the age dependence in the microstructure of trabecular bone appears not to strongly influence the absorbed dose estimates for the active marrow. We thus recommend that the fluence-conversion functions of Table 4 be used for all ages. These data can be applied to estimates of photon fluence from the Monte Carlo transport calculations in a phantom to estimate absorbed dose. Variations with incident photon energy in the ratio of absorbed dose in active marrow to the equilibrium dose (kerma) in soft tissue are indicated in Fig. 2. The ratios are largest at photon energies to 50 to 60 keV and are higher for the thick trabeculae and small marrow cavities of the parietal bone than for the thinner trabeculae and larger marrow cavities of other bones. The ratios at low energies conform to the general features indicated by Spiers (1969).

However, the parietal bone exhibits a substantially higher enhancement of the marrow dose than other trabecular bones. This enhancement should be considered in deriving skeletal average values for the diagnostic x-ray region. Enhancement of dose in the high-energy (pair-production) region is also indicated by our calculations. Enhancement is small, about 5%, for most trabecular sites but approaches 20% for the parietal bone.

## REFERENCES

- Beddoe, A. H., 1977, "Measurements of the Microscopic Structure of Cortical Bone," *Phys. Med. Biol.* 22, 298-308.
- Beddoe, A. H., Darley, P. J., and Spiers, F. W., 1976, "Measurements of Trabecular Bone Structure in Man," *Phys. Med. Biol.* 21, 589-607.
- Eckerman, K. F., 1986, "Aspects of the Dosimetry of Radionuclides Within the Skeleton with Particular Emphasis on the Active Marrow," *Fourth International Radiopharmaceutical Dosimetry Symposium* (A. T. Schlafke-Stelson and E. E. Watson, Eds.) pp 514-534, CONF-85113 NTIS; Springfield, Virginia, USA).
- Evans, R. D., 1969, *The Atomic Nucleus* (Academic Press; New York).
- Heitler, W., 1964, *The Quantum Theory of Radiation*, 3rd edition Oxford Press: London).
- Hubbell, J. H., 1982, "Photon Mass Attenuation and Energy-absorption Coefficients for 1 keV to 20 MeV," *Int. J. Appl. Radiat. Isot.* 33, 1269-1290.
- ICRP, 1977, *ICRP Publication 26. Recommendations of the International Commission on Radiological Protection* (Pergamon Press; Oxford).
- ICRP, 1979, *ICRP Publication 30. Recommendations of the International Commission on Radiological Protection*. (Pergamon Press; Oxford).
- Kerr, G. D., 1982, *Photon and Neutron-to-Kerma Conversion Factors for ICRP- 1975 Reference Man Using Improved Element Compositions for Bone and Marrow of the Skeleton*, Oak Ridge National Laboratory Report ORNL/TM-8318.
- Leggett, R. W., Eckerman, K. F., and Williams, L. R., 1982, "Strontium-90 in Bone: A Case Study in Age-dependent Dosimetric Modelling," *Health Phys.* 43, 307-322.

- Seltzer, S. M. and Berger, M. J., 1982a, "Evaluation of the Collision Stopping Power of Elements and Compounds for Electrons and Positrons," *Int. J. Appl. Radiat. Isot.* 33, 1189-1218.
- Seltzer, S. M. and Berger, M. J., 1982b, "Procedure for Calculating the Radiation Stopping Power for Electrons," *Int. J. Appl. Radiat. Isot.* 33, 1219-1226.
- Snyder, W. S., Ford, M. R., and Warner, G. G., 1978, *Estimates of Specific Absorbed Fractions for Photon Sources Uniformly Distributed in Various Organs of a Heterogeneous Phantom*, MIRD Pamphlet No. 5, Revised (Society of Nuclear Medicine; New York).
- Spiers, F. W., 1969, "Transition-zone Dosimetry," *Radiation Dosimetry* (F. H. Attix and E. Tochlin, Eds.) pp 809-867 (Academic Press; New York).
- Spiers, F. W., Whitwell, J. R., and Beddoe, A. H., 1978, "Calculated Dose Factors for Radiosensitive Tissues in Bone Irradiated by Surface-deposited Radionuclides," *Phys. Med. Biol.* 23, 481-494.
- Whitwell, J. R., and Spiers, F. W., 1976, "Calculated Beta-ray Dose Factors for Trabecular Bone," *Phys. Med. Biol.* 21, 16-38.
- Whitwell, J. R., 1973, *Theoretical Investigations of Energy Loss by Ionizing Particles in Bone*, Ph.D. Thesis, University of Leeds, Leeds, UK.

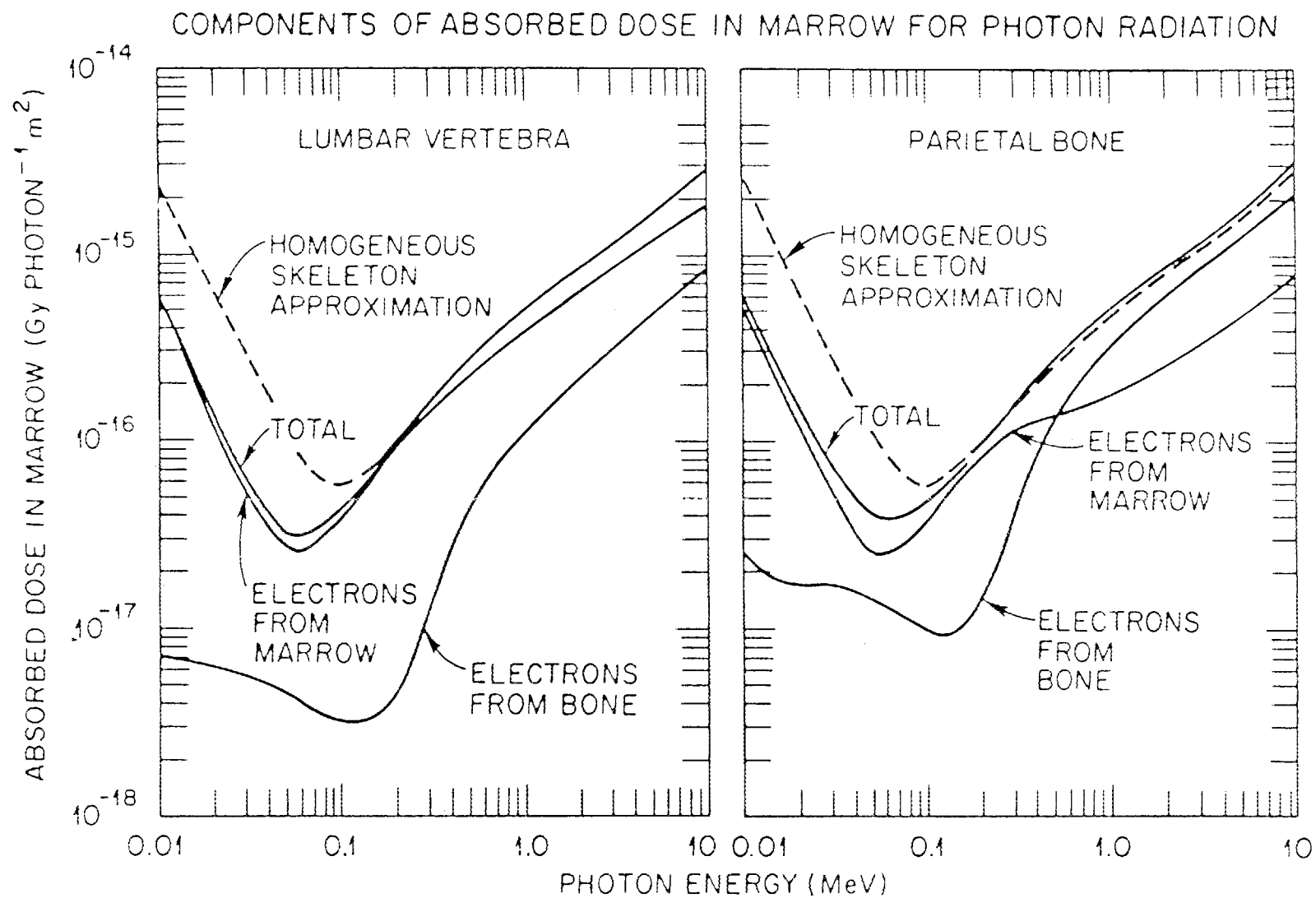


Figure 1. Components of the absorbed dose in marrow from photon radiations. The dotted curve shows the dose with the assumption that the active marrow absorbs energy per unit mass at the rate for the homogeneous skeleton approximation, as in Snyder et al. (1978).

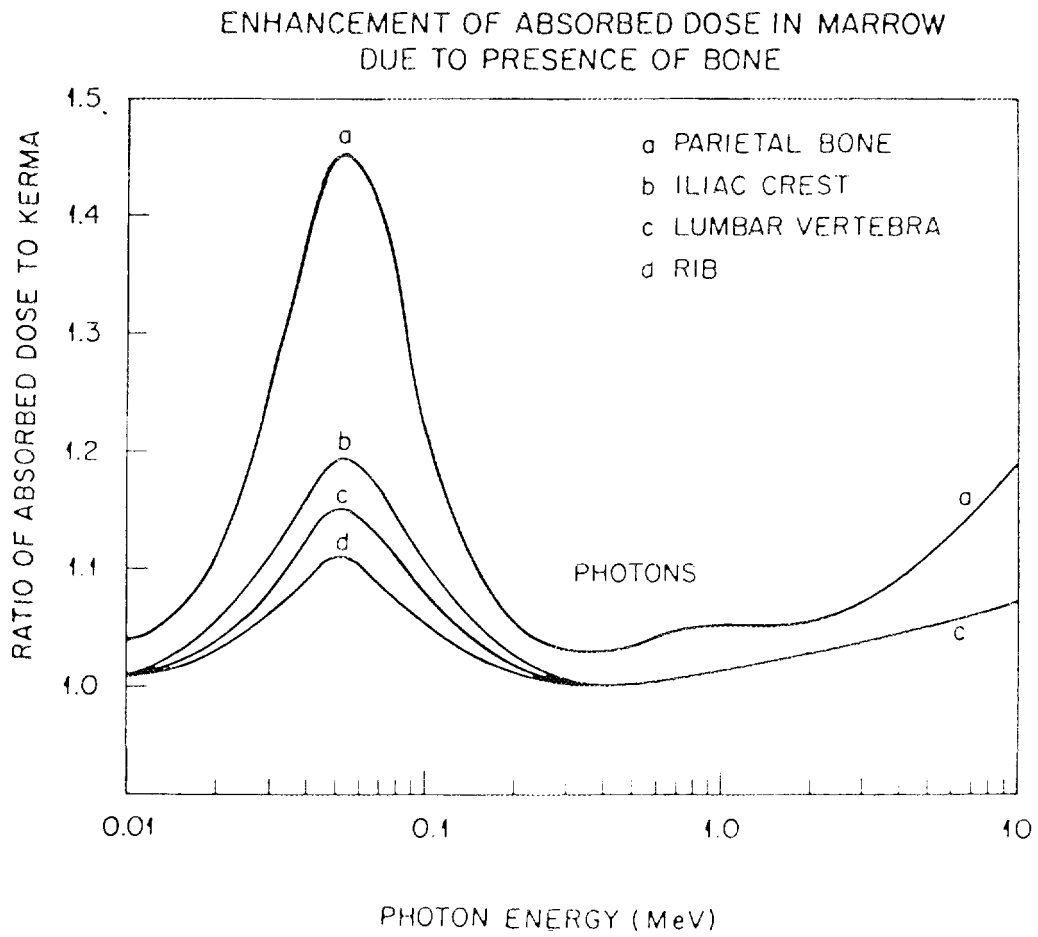


Figure 2. Illustration of the effects of the microstructure of trabecular bone on energy deposition in active marrow for various bones of the adult skeleton.

Table 1. Absorbed fraction,  $\phi$ , in active marrow, RM, and bone surface, BS, from a uniformly distributed source of monoenergetic electrons in trabeculae, TB, and marrow of the parietal bone and lumbar vertebra of a 44-year-old male.

| Electron<br>energy<br>(MeV) | Parietal bone  |                |                |                | Lumbar Vertebra |                |                |                |
|-----------------------------|----------------|----------------|----------------|----------------|-----------------|----------------|----------------|----------------|
|                             | $\phi$ (RM+TB) | $\phi$ (RM+RM) | $\phi$ (BS+RM) | $\phi$ (BS+TB) | $\phi$ (RM+TB)  | $\phi$ (RM+RM) | $\phi$ (BS+RM) | $\phi$ (BS+TB) |
| 0.010                       | 1.95(-3)       | 0.994          | 1.05(-1)       | 1.95(-3)       | 3.94(-3)        | 0.999          | 3.87(-2)       | 2.94(-3)       |
| 0.015                       | 3.29(-3)       | 0.990          | 9.67(-2)       | 3.29(-3)       | 7.81(-3)        | 0.997          | 3.77(-2)       | 6.56(-3)       |
| 0.020                       | 5.77(-3)       | 0.983          | 9.11(-2)       | 5.77(-3)       | 1.29(-2)        | 0.996          | 3.51(-2)       | 1.17(-2)       |
| 0.030                       | 1.23(-2)       | 0.969          | 7.88(-2)       | 1.14(-2)       | 2.59(-2)        | 0.991          | 3.06(-2)       | 2.08(-2)       |
| 0.040                       | 1.98(-2)       | 0.950          | 6.97(-2)       | 1.54(-2)       | 4.34(-2)        | 0.985          | 2.82(-2)       | 2.90(-2)       |
| 0.050                       | 2.94(-2)       | 0.927          | 6.55(-2)       | 1.85(-2)       | 6.26(-2)        | 0.979          | 2.75(-2)       | 3.32(-2)       |
| 0.060                       | 4.03(-2)       | 0.901          | 6.10(-2)       | 2.04(-2)       | 8.25(-2)        | 0.971          | 2.68(-2)       | 3.56(-2)       |
| 0.080                       | 6.34(-2)       | 0.854          | 5.28(-2)       | 2.18(-2)       | 1.31(-1)        | 0.953          | 2.51(-2)       | 3.91(-2)       |
| 0.10                        | 8.80(-2)       | 0.794          | 5.09(-2)       | 2.37(-2)       | 1.83(-1)        | 0.935          | 2.58(-2)       | 4.24(-2)       |
| 0.15                        | 1.53(-1)       | 0.654          | 4.52(-2)       | 2.65(-2)       | 3.12(-1)        | 0.888          | 2.82(-2)       | 4.24(-2)       |
| 0.20                        | 1.99(-1)       | 0.538          | 4.08(-2)       | 2.84(-2)       | 4.17(-1)        | 0.848          | 2.78(-2)       | 3.87(-2)       |
| 0.30                        | 2.58(-1)       | 0.415          | 3.87(-2)       | 2.98(-2)       | 5.47(-1)        | 0.808          | 2.84(-2)       | 3.44(-2)       |
| 0.40                        | 2.71(-1)       | 0.376          | 3.60(-2)       | 2.96(-2)       | 5.97(-1)        | 0.793          | 2.90(-2)       | 3.23(-2)       |
| 0.50                        | 2.76(-1)       | 0.358          | 3.50(-2)       | 3.00(-2)       | 6.25(-1)        | 0.779          | 2.86(-2)       | 3.32(-2)       |
| 0.60                        | 2.82(-1)       | 0.346          | 3.35(-2)       | 3.05(-2)       | 6.48(-1)        | 0.767          | 2.85(-2)       | 3.30(-2)       |
| 0.80                        | 2.88(-1)       | 0.335          | 3.37(-2)       | 3.09(-2)       | 6.74(-1)        | 0.765          | 2.87(-2)       | 3.32(-2)       |
| 1.0                         | 2.93(-1)       | 0.327          | 3.30(-2)       | 3.09(-2)       | 6.90(-1)        | 0.757          | 2.88(-2)       | 3.23(-2)       |
| 2.0                         | 2.97(-1)       | 0.317          | 3.19(-2)       | 3.11(-2)       | 7.17(-1)        | 0.747          | 2.94(-2)       | 3.26(-2)       |
| 3.0                         | 3.00(-1)       | 0.311          | 3.18(-2)       | 3.11(-2)       | 7.22(-1)        | 0.747          | 2.90(-2)       | 3.23(-2)       |
| 4.0                         | 3.01(-1)       | 0.308          | 3.15(-2)       | 3.11(-2)       | 7.27(-1)        | 0.744          | 2.88(-2)       | 3.22(-2)       |

Table 2. Absorbed fraction,  $\phi$ , in active marrow, RM, and in bone surface, BS, from a uniformly distributed source of monoenergetic electrons in the trabeculae, TB, and marrow space of the parietal bone and lumbar vertebra of a 20-month old child.

| Electron<br>energy<br>(MeV) | Parietal Bone  |                |                |                | Lumbar Vertebra |                |                |                |
|-----------------------------|----------------|----------------|----------------|----------------|-----------------|----------------|----------------|----------------|
|                             | $\phi$ (RM+TB) | $\phi$ (RM+RM) | $\phi$ (BS+TB) | $\phi$ (BS+RM) | $\phi$ (RM+TB)  | $\phi$ (RM+RM) | $\phi$ (BS+TB) | $\phi$ (BS+RM) |
| 0.01                        | 1.62(-3)       | 0.990          | 1.62(-3)       | 1.40(-1)       | 4.66(-3)        | 0.997          | 4.66(-3)       | 5.99(-2)       |
| 0.015                       | 3.44(-3)       | 0.981          | 3.44(-3)       | 1.33(-1)       | 9.90(-3)        | 0.995          | 9.90(-3)       | 5.68(-2)       |
| 0.02                        | 6.09(-3)       | 0.969          | 6.09(-3)       | 1.21(-1)       | 1.65(-2)        | 0.992          | 1.65(-2)       | 5.26(-2)       |
| 0.03                        | 1.24(-2)       | 0.947          | 1.14(-2)       | 1.01(-1)       | 3.39(-2)        | 0.984          | 3.16(-2)       | 4.62(-2)       |
| 0.04                        | 1.91(-2)       | 0.920          | 1.47(-2)       | 9.04(-2)       | 5.67(-2)        | 0.973          | 4.24(-2)       | 4.19(-2)       |
| 0.05                        | 2.80(-2)       | 0.889          | 1.74(-2)       | 7.98(-2)       | 8.01(-2)        | 0.962          | 4.83(-2)       | 3.94(-2)       |
| 0.06                        | 3.46(-2)       | 0.858          | 1.79(-2)       | 6.97(-2)       | 1.12(-1)        | 0.949          | 5.37(-2)       | 3.75(-2)       |
| 0.08                        | 5.12(-2)       | 0.789          | 2.00(-2)       | 6.28(-2)       | 1.74(-1)        | 0.922          | 5.83(-2)       | 3.49(-2)       |
| 0.10                        | 7.09(-2)       | 0.724          | 2.28(-2)       | 5.73(-2)       | 2.34(-1)        | 0.892          | 5.68(-2)       | 3.52(-2)       |
| 0.15                        | 1.06(-1)       | 0.591          | 2.44(-2)       | 4.67(-2)       | 3.74(-1)        | 0.829          | 5.30(-2)       | 3.65(-2)       |
| 0.20                        | 1.30(-1)       | 0.501          | 2.61(-2)       | 4.21(-2)       | 4.70(-1)        | 0.786          | 4.78(-2)       | 3.95(-2)       |
| 0.30                        | 1.54(-1)       | 0.401          | 2.67(-2)       | 3.76(-2)       | 5.58(-1)        | 0.750          | 4.37(-2)       | 4.11(-2)       |
| 0.40                        | 1.68(-1)       | 0.354          | 2.79(-2)       | 3.49(-2)       | 5.94(-1)        | 0.730          | 4.20(-2)       | 4.23(-2)       |
| 0.50                        | 1.76(-1)       | 0.328          | 2.80(-2)       | 3.34(-2)       | 6.26(-1)        | 0.722          | 4.16(-2)       | 4.25(-2)       |
| 0.60                        | 1.79(-1)       | 0.308          | 2.75(-2)       | 3.26(-2)       | 6.38(-1)        | 0.718          | 4.12(-2)       | 4.11(-2)       |
| 0.80                        | 1.81(-1)       | 0.283          | 2.79(-2)       | 3.18(-2)       | 6.51(-1)        | 0.706          | 4.09(-2)       | 4.12(-2)       |
| 1.0                         | 1.88(-1)       | 0.267          | 2.80(-2)       | 3.09(-2)       | 6.62(-1)        | 0.708          | 4.18(-2)       | 4.19(-2)       |
| 2.0                         | 1.96(-1)       | 0.238          | 2.82(-2)       | 2.96(-2)       | 6.78(-1)        | 0.698          | 4.12(-2)       | 4.13(-2)       |
| 3.0                         | 1.99(-1)       | 0.224          | 2.82(-2)       | 2.92(-2)       | 6.81(-1)        | 0.696          | 4.12(-2)       | 4.13(-2)       |
| 4.0                         | 2.01(-1)       | 0.221          | 2.82(-2)       | 2.89(-2)       | 6.84(-1)        | 0.696          | 4.09(-2)       | 4.10(-2)       |

Table 3. Absorbed dose in active marrow,  $D(RM)$ , per unit fluence,  $\Psi(E)$ , of monoenergetic photons in trabecular bones of the skeleton of a 44-year-old male.

| Photon<br>energy<br>(MeV) | $D(RM)/\Psi(E)$ , Gy per photon/m <sup>2</sup> |                      |                    |           |                |                  |                  |
|---------------------------|--|----------------------|--------------------|-----------|----------------|------------------|------------------|
|                           | Parietal<br>bone                               | Cervical<br>vertebra | Lumbar<br>vertebra | Rib       | Iliac<br>crest | Head of<br>femur | Neck of<br>femur |
| 0.010                     | 6.30(-16)                                      | 6.157(-16)           | 6.14(-16)          | 6.12(-16) | 6.16(-16)      | 6.12(-16)        | 6.12(-16)        |
| 0.015                     | 2.71(-16)                                      | 2.62(-16)            | 2.61(-16)          | 2.59(-16) | 2.63(-16)      | 2.60(-16)        | 2.59(-16)        |
| 0.020                     | 1.53(-16)                                      | 1.45(-16)            | 1.43(-16)          | 1.41(-16) | 1.45(-16)      | 1.42(-16)        | 1.41(-16)        |
| 0.030                     | 7.49(-17)                                      | 6.60(-17)            | 6.44(-17)          | 6.29(-17) | 6.61(-17)      | 6.39(-17)        | 6.31(-17)        |
| 0.040                     | 5.04(-17)                                      | 4.27(-17)            | 4.11(-17)          | 3.99(-17) | 4.28(-17)      | 4.08(-17)        | 3.99(-17)        |
| 0.050                     | 4.18(-17)                                      | 3.45(-17)            | 3.31(-17)          | 3.20(-17) | 3.45(-17)      | 3.27(-17)        | 3.21(-17)        |
| 0.060                     | 3.93(-17)                                      | 3.26(-17)            | 3.11(-17)          | 3.01(-17) | 3.24(-17)      | 3.08(-17)        | 3.01(-17)        |
| 0.080                     | 4.15(-17)                                      | 3.58(-17)            | 3.45(-17)          | 3.36(-17) | 3.57(-17)      | 3.44(-17)        | 3.37(-17)        |
| 0.10                      | 4.79(-17)                                      | 4.33(-17)            | 4.22(-17)          | 4.14(-17) | 4.33(-17)      | 4.21(-17)        | 4.15(-17)        |
| 0.15                      | 7.16(-17)                                      | 6.83(-17)            | 6.74(-17)          | 6.68(-17) | 6.83(-17)      | 6.72(-17)        | 6.70(-17)        |
| 0.20                      | 9.88(-17)                                      | 9.63(-17)            | 9.57(-17)          | 9.52(-17) | 9.64(-17)      | 9.53(-17)        | 9.53(-17)        |
| 0.30                      | 1.57(-16)                                      | 1.54(-16)            | 1.54(-16)          | 1.53(-16) | 1.54(-16)      | 1.52(-16)        | 1.53(-16)        |
| 0.40                      | 2.15(-16)                                      | 2.12(-16)            | 2.10(-16)          | 2.10(-16) | 2.12(-16)      | 2.07(-16)        | 2.10(-16)        |
| 0.50                      | 2.72(-16)                                      | 2.67(-16)            | 2.66(-16)          | 2.65(-16) | 2.68(-16)      | 2.60(-16)        | 2.65(-16)        |
| 0.60                      | 3.28(-16)                                      | 3.20(-16)            | 3.19(-16)          | 3.17(-16) | 3.20(-16)      | 3.10(-16)        | 3.18(-16)        |
| 0.80                      | 4.28(-16)                                      | 4.17(-16)            | 4.15(-16)          | 4.14(-16) | 4.17(-16)      | 4.04(-16)        | 4.14(-16)        |
| 1.0                       | 5.19(-16)                                      | 5.06(-16)            | 5.03(-16)          | 5.01(-16) | 5.06(-16)      | 4.88(-16)        | 5.02(-16)        |
| 1.5                       | 7.12(-16)                                      | 6.95(-16)            | 6.90(-16)          | 6.88(-16) | 6.94(-16)      | 6.69(-16)        | 6.90(-16)        |
| 2.0                       | 8.77(-16)                                      | 8.52(-16)            | 8.45(-16)          | 8.43(-16) | 8.50(-16)      | 8.19(-16)        | 8.45(-16)        |
| 3.0                       | 1.16(-15)                                      | 1.11(-15)            | 1.10(-15)          | 1.09(-15) | 1.11(-15)      | 1.06(-15)        | 1.10(-15)        |
| 4.0                       | 1.41(-15)                                      | 1.33(-15)            | 1.31(-15)          | 1.29(-15) | 1.32(-15)      | 1.26(-15)        | 1.30(-15)        |
| 5.0                       | 1.64(-15)                                      | 1.52(-15)            | 1.49(-15)          | 1.46(-15) | 1.51(-15)      | 1.43(-15)        | 1.48(-15)        |
| 6.0                       | 1.87(-15)                                      | 1.69(-15)            | 1.65(-15)          | 1.62(-15) | 1.68(-15)      | 1.58(-15)        | 1.64(-15)        |
| 8.0                       | 2.33(-15)                                      | 2.02(-15)            | 1.94(-15)          | 1.89(-15) | 1.99(-15)      | 1.86(-15)        | 1.93(-15)        |
| 10.0                      | 2.79(-15)                                      | 2.32(-15)            | 2.21(-15)          | 2.14(-15) | 2.29(-15)      | 2.10(-15)        | 2.19(-15)        |

Table 4. Absorbed dose in active marrow, D(RM), and in bone surface, D(BS), per unit fluence,  $\Psi(E)$ , of monoenergetic photons in the skeleton.

| Photon<br>energy<br>(MeV) | D(RM or BS)/ $\Psi(E)$ , Gy per photon/m <sup>2</sup> |           |                 |           |           |                    |
|---------------------------|---|-----------|-----------------|-----------|-----------|--------------------|
|                           | Parietal Bone   |           | Lumbar Vertebra |           | Cortical  | Total <sup>a</sup> |
|                           | D(RM)   | D(BS)     | D(RM)           | D(BS)     | D(BS)     | D(BS)              |
| 0.010                     | 6.30(-16)   | 8.47(-16) | 6.14(-16)       | 9.43(-16) | 5.32(-15) | 3.13(-15)          |
| 0.015                     | 2.71(-16)   | 4.17(-16) | 2.61(-16)       | 4.98(-16) | 2.45(-15) | 1.47(-15)          |
| 0.020                     | 1.53(-16)   | 2.98(-16) | 1.43(-16)       | 3.39(-16) | 1.39(-15) | 8.65(-16)          |
| 0.030                     | 7.49(-17)   | 2.00(-16) | 6.44(-17)       | 2.12(-16) | 6.11(-16) | 4.12(-16)          |
| 0.040                     | 5.04(-17)   | 1.42(-16) | 4.11(-17)       | 1.51(-16) | 3.41(-16) | 2.46(-16)          |
| 0.050                     | 4.18(-17)   | 1.09(-16) | 3.31(-17)       | 1.10(-16) | 2.20(-16) | 1.65(-16)          |
| 0.060                     | 3.93(-17)   | 8.75(-17) | 3.11(-17)       | 8.69(-17) | 1.57(-16) | 1.22(-16)          |
| 0.080                     | 4.15(-17)   | 6.61(-17) | 3.45(-17)       | 7.03(-17) | 1.03(-16) | 8.67(-17)          |
| 0.10                      | 4.79(-17)   | 6.32(-17) | 4.22(-17)       | 6.76(-17) | 8.51(-17) | 7.64(-17)          |
| 0.15                      | 7.16(-17)   | 7.96(-17) | 6.74(-17)       | 8.90(-17) | 8.80(-17) | 8.85(-17)          |
| 0.20                      | 9.88(-17)   | 1.05(-16) | 9.57(-17)       | 1.22(-16) | 1.10(-16) | 1.16(-16)          |
| 0.30                      | 1.57(-16)   | 1.65(-16) | 1.54(-16)       | 1.98(-16) | 1.67(-16) | 1.83(-16)          |
| 0.40                      | 2.15(-16)   | 2.26(-16) | 2.10(-16)       | 2.65(-16) | 2.24(-16) | 2.45(-16)          |
| 0.50                      | 2.72(-16)   | 2.85(-16) | 2.66(-16)       | 3.30(-16) | 2.80(-16) | 3.05(-16)          |
| 0.60                      | 3.28(-16)   | 3.38(-16) | 3.19(-16)       | 3.94(-16) | 3.34(-16) | 3.64(-16)          |
| 0.80                      | 4.28(-16)   | 4.37(-16) | 4.15(-16)       | 5.09(-16) | 4.33(-16) | 4.71(-16)          |
| 1.0                       | 5.19(-16)   | 5.29(-16) | 5.03(-16)       | 6.12(-16) | 5.22(-16) | 5.67(-16)          |
| 1.5                       | 7.13(-16)   | 7.23(-16) | 6.91(-16)       | 8.37(-16) | 7.09(-16) | 7.73(-16)          |
| 2.0                       | 8.79(-16)   | 8.89(-16) | 8.50(-16)       | 1.03(-15) | 8.69(-16) | 9.49(-16)          |
| 3.0                       | 1.17(-15)   | 1.18(-15) | 1.12(-15)       | 1.36(-15) | 1.15(-15) | 1.26(-15)          |
| 4.0                       | 1.43(-15)   | 1.44(-15) | 1.37(-15)       | 1.65(-15) | 1.42(-15) | 1.54(-15)          |
| 5.0                       | 1.69(-15)   | 1.70(-15) | 1.59(-15)       | 1.93(-15) | 1.68(-15) | 1.81(-15)          |
| 6.0                       | 1.94(-15)   | 1.95(-15) | 1.82(-15)       | 2.20(-15) | 1.94(-15) | 2.07(-15)          |
| 8.0                       | 2.46(-15)   | 2.46(-15) | 2.26(-15)       | 2.74(-15) | 2.47(-15) | 2.61(-15)          |
| 10.0                      | 2.99(-15)   | 2.99(-15) | 2.70(-15)       | 3.28(-15) | 3.03(-15) | 3.16(-15)          |

<sup>a</sup>Total represents the bone surface response of the skeleton and is computed as the average of the lumbar vertebra and cortical responses.

ELECTRON DOSE-RATE CONVERSION FACTORS FOR EXTERNAL EXPOSURE OF THE  
SKIN FROM UNIFORMLY DEPOSITED ACTIVITY ON THE BODY SURFACE

INTRODUCTION

Compilation of electron dose-rate conversion factors for external exposure of radiosensitive tissues of the skin from radionuclides dispersed in the environment are available in the literature (Kocher 1981a; Kocher and Eckerman 1981). In this paper we described methods implemented to calculate electron dose-rate factors for the skin from radionuclides deposited uniformly on the body surface. The calculations are based on the point kernel method (Foderaro 1968) and use electron scaled point kernels in water developed by Berger (1971; 1973; 1974). Similar calculations were presented previously by Henson (1972), but results were reported for only a few radionuclides.

ELECTRON DOSE-RATE FACTORS FOR SKIN FROM  
MONOENERGETIC SOURCES ON THE BODY SURFACE

We assume that radioactivity is deposited uniformly on the body surface; i.e., the source region is an infinite, uniformly contaminated plane surface at the boundary of a semi-infinite tissue medium. This assumption is justifiable for most exposure situations because the electron range in soft tissue (NAS 1964) is less than 2 cm for most electron energies that occur in radioactive decay (Kocher 1981b), and thus a contaminated area on the body surface as small as  $15 \text{ cm}^2$  is effectively infinite with regard to estimating electron dose to skin along the centroid of the contamination.

Electron dose-rate factors are calculated at four locations below the body surface. First, we assume that the radiosensitive tissue is located at depths of 4, 8, or  $40 \text{ mg/cm}^2$  below the body surface, as recommended by Whitton (1973). The smallest of these depths corresponds to an average epidermal thickness for the head, trunk, upper arm, and upper leg; the intermediate value applies to the lower arm, wrist, back of the hand, lower leg, ankle, and upper foot; and the largest value

applies to the palm of the hand and sole of the foot (Whitton 1973). Thus, for contamination of any part of the body surface, the dose-rate factors for the appropriate depth may be selected. In addition, dose-rate factors have been calculated at a depth of  $7 \text{ mg/cm}^2$ , which is the average value recommended by the ICRP (1977).

The dose-rate at a depth  $x$  in tissue ( $t$ ) from a source ( $1 \text{ Bq/cm}^2$ ) of monoenergetic electrons of energy  $E$  deposited uniformly on the body surface, denoted by  $D^t(x,E)$ , is calculated as

$$D^t(x,E) = kE \int_{\sigma} \Phi^t(r,E) d\sigma \quad (1)$$

In this equation, the dose-rate factor is in units of  $\text{Gy/s per Bq/cm}^2$ ;  $k$  is a constant that converts energy absorption in  $\text{MeV/kg}$  to absorbed dose in  $\text{Gy}$ , and is equal to  $1.6 \times 10^{-13} \text{ kg-Gy/MeV}$ ;  $E$  is in units of  $\text{MeV}$  per emitted electron;  $\Phi^t$  is the specific absorbed fraction for electrons in tissue, defined as the fraction of the emitted energy  $E$  that is absorbed per unit mass of tissue at a distance  $r$  from an isotropic point source, in units of  $\text{kg}^{-1}$ ; and  $\sigma$  denotes the source region, which is an infinite planar surface at the boundary of the tissue medium.

Since an analytical expression for the specific absorbed fraction for electrons has not been developed, Eq. (1) must be solved by numerical integration over the source region. We use the electron scaled point kernel developed by Berger (1973), in which scaling of the specific absorbed fraction is accomplished by expressing the source-to-receptor distance  $r$  in terms of the scaled distance  $r/r_0$ , where  $r_0$  is the mean electron range in tissue for emitted energy  $E$  evaluated in the continuous-slowing-down approximation. The electron scaled point kernel in tissue,  $F^t(r/r_0, E)$ , is defined by the equation

$$F^t(r/r_0, E) d(r/r_0) = 4\pi\rho_t \Phi^t(r,E)r^2 dr \quad (2)$$

where  $\rho_t$  is the density of tissue. Solving Eq. (2) for the specific absorbed fraction  $\Phi^t$  and expressing the element of area for a plane source,  $d\sigma$ , as  $d\sigma = 2\pi r dr$ , we obtain the dose-rate factor in Eq. (1) in the form

$$D^t(x, E) = \frac{kE}{2\rho_t r_o} \Omega(x, E) \quad , \quad (3)$$

where

$$\Omega(x, E) = \int_{x/r_o}^{\infty} \frac{1}{u} \Phi^t(u, E) du \quad . \quad (4)$$

In evaluating Eq. (3), we assume that the electron scaled point kernels in tissue are the same as the values in water, and we obtain these values from Berger's tabulation (Berger 1973). Because of the finite range of electrons in tissue, the integrand in Eq. (4) is zero for values of the scaled distance greater than about 1.25 (Berger 1973).

The electron dose-rate factors at depths of 4, 8, and 40 mg/cm<sup>2</sup> as a function of emitted energy for sources deposited uniformly on the body surface, as obtained from eqs. (3) and (4), are shown in Fig. 1. The conversion from absorbed dose in Gy to dose equivalent in Sv assumes a quality factor of one.

#### DOSE-RATE FACTORS FOR ELECTRON SPECTRA FROM RADIOACTIVE DECAY

For a given radionuclide deposited uniformly on the body surface, the dose-rate factor as a function of depth in tissue is obtained by applying eqs. (3) and (4) for monoenergetic sources to the particular energy spectrum of emitted electrons. In general, radionuclides may emit discrete Auger and internal conversion electrons and a continuous spectrum of electrons from beta decay. The energy distribution for a given beta transition ranges from zero energy to the maximum endpoint energy. We define  $f_{ie}$  as the intensity of the  $i$ th discrete electron ( $e$ ) in number per decay,  $E_{ie}$  as the energy of the  $i$ th discrete electron in MeV,  $f_{j\beta}$  as the intensity of the  $j$ th continuous beta transition ( $\beta$ ) in number per decay,  $E_{j\beta}^{\max}$  as the endpoint energy in MeV for the  $j$ th beta transition, and  $N_{j\beta}(E)$  as the energy distribution function for the  $j$ th beta transition. The energy distribution function is assumed to be normalized so that

$$\int_0^{E_{j\beta}^{\max}} N_{j\beta}(E) dE = 1 \quad (5)$$

Then, for a given electron spectrum, the dose-rate factor as a function of depth in tissue is given by

$$D^t(x) = \sum_i f_{ie} D^t(x, E_{ie}^{\max}) + \sum_j f_{j\beta} \int_0^{E_{j\beta}^{\max}} N_{j\beta}(E) D^t(x, E) dE \quad (6)$$

where the summations over  $i$  and  $j$  include all discrete and continuous electron radiations in the decay of the radionuclide, respectively.

## RESULTS

Electron dose-rate factors for the skin from radionuclides deposited uniformly on the body surface were calculated for about 500 radionuclides using a modified version of the DOSFACTER computer code (Kocher 1981a). The energies and intensities of the discrete and continuous electrons emitted by each radionuclide were obtained from a compilation of evaluated nuclear decay data (Kocher 1981b). The energy distribution function  $N_{\beta}(E)$  for beta decay was calculated from the Fermi theory (Wu and Moskowski 1966) using an approximation technique described previously (Kocher and Eckerman 1981). Integrals over scaled distance and energy in eqs. (4) and (6) were evaluated by numerical methods.

The calculated electron dose-rate factors in skin for selected radionuclides are given in Table 1. The tabulation includes only the contributions from electrons; i.e., contributions from alpha particles and photons are not included. Possible contributions to the dose-rate factor from radioactive daughter products are not included in the values for a given radionuclide. In each such case (e.g.,  $^{90}\text{Sr}$ ,  $^{106}\text{Ru}$ , and  $^{137}\text{Cs}$ ), the dose-rate factors for radioactive daughter products are also listed in the table. The contributions from short-lived daughter products can be combined with the dose-rate factors for the parent using known branching fractions for the particular decay chain (Kocher 1981b).

## REFERENCES

- Berger, M. J., 1971, "Distribution of Absorbed Dose Around Point Sources of Electrons and Beta Particles in Water and Other Media," MIRD Pamphlet 7, *J. Nucl. Med.* 12, Suppl. No. 5, 5.
- Berger, M. J., 1973, "Improved Point Kernels for Electron and Beta-ray Dosimetry," National Bureau of Standards Report NBSIR 73-107.
- Berger, M. J., 1974, "Beta-ray Dose in Tissue-equivalent Material Immersed in a Radioactive Cloud," *Health Phys.* 26, 1.
- Foderaro, A., 1968, "Point Kernel Methods," in: *Engineering Compendium on Radiation Shielding*, Vol. I (R. G. Jaeger, Ed.), p 124 (Springer-Verlag: New York).
- Henson, P. W., 1972, "A Note on Some Aspects of Skin Contamination by Certain Radionuclides in Common Use," *Brit. J. Radiol.* 45, 938.
- ICRP 1977, International Commission on Radiological Protection, "Recommendations of the International Commission on Radiological Protection," ICRP Publication 26, *Ann. ICRP* 1, No. 3.
- ICRP 1978, International Commission on Radiological Protection, "Statement from the 1978 Stockholm Meeting of the ICRP," ICRP Publication 28, *Ann. ICRP* 2, No. 1.
- Kocher, D. C., 1981a, "Dose-Rate Conversion Factors for External Exposure to Photons and Electrons," Oak Ridge National Laboratory Report NUREG/CR-1918, ORNL/NUREG-79.
- Kocher, D. C. and Eckerman, K. F., 1981, "Electron Dose-Rate Conversion Factors for External Exposure of the Skin," *Health Phys.* 40, 467; erratum, *Health Phys.* 41, 567.
- Kocher, D. C., 1981b, "Radioactive Decay Data Tables," U.S. Department of Energy Report DOE/TIC-11026.
- Kocher, D. C., 1983, "Dose-Rate Conversion Factors for External Exposure to Photons and Electrons," *Health Phys.* 45, 665.
- NAS 1964, National Academy of Sciences-National Research Council, "Studies in Penetration of Charged Particles in Matter," *NAS-NRC Publication* 1133 (NAS-NRC: Washington, DC).
- Whitton, J. T., 1973, "New Values for Epidermal Thickness and Their Importance," *Health Phys.* 24, 1.
- Wu, C. S. and Moskowski, S. A., 1966, *Beta Decay* (Interscience: New York).

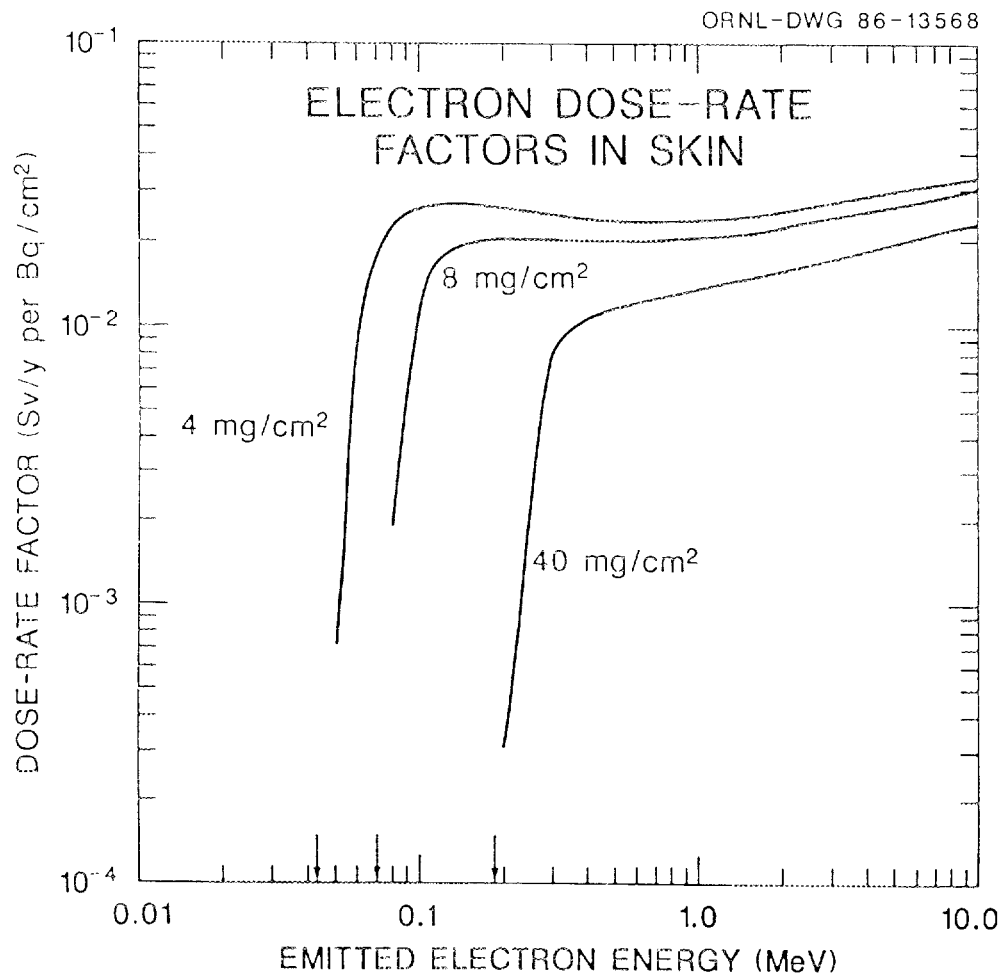


Figure 1. Electron dose-rate factors in skin at various depths vs emitted energy for sources deposited uniformly on the body surface; the arrows at the bottom of the figure give the energies below which the dose-rate factors are zero.

Table 1. Electron dose-rate factors in skin from radionuclides deposited uniformly on the body surface

| Nuclide | Dose-rate factor vs depth in tissue <sup>a</sup> |                      |                      |                       |                     |
|---------|--|----------------------|----------------------|-----------------------|---------------------|
|         | Half-life  | 4 mg/cm <sup>2</sup> | 8 mg/cm <sup>2</sup> | 40 mg/cm <sup>2</sup> | 7mg/cm <sup>2</sup> |
| C-14    | 5.73E3 y   | 7.9E-3               | 2.1E-3               | 0.0                   | 2.9E-3              |
| P-32    | 14.29 d  | 2.4E-2               | 2.0E-2               | 1.1E-2                | 2.1E-2              |
| Co-60   | 5.271 y  | 1.6E-2               | 8.7E-3               | 2.5E-4                | 9.9E-3              |
| Zn-65   | 244.4 d  | 3.3E-4               | 2.1E-4               | 1.0E-5                | 2.3E-4              |
| Sr-90   | 28.6 y   | 2.1E-2               | 1.5E-2               | 3.4E-3                | 1.6E-2              |
| Y-90    | 64.1 h   | 2.4E-2               | 2.0E-2               | 1.2E-2                | 2.1E-2              |
| Zr-95   | 64.02 d  | 1.7E-2               | 1.0E-2               | 7.4E-4                | 1.2E-2              |
| Nb-95   | 35.06 d  | 6.4E-3               | 1.7E-3               | 1.8E-5                | 2.3E-3              |
| Ru-106  | 368.2 d  | 0.0                  | 0.0                  | 0.0                   | 0.0                 |
| Rh-106  | 29.92 s  | 2.5E-2               | 2.1E-2               | 1.4E-2                | 2.2E-2              |
| Te-131  | 25.0 m   | 2.8E-2               | 2.2E-2               | 1.0E-2                | 2.3E-2              |
| Te-132  | 78.2 h   | 1.3E-2               | 5.9E-3               | 4.7E-5                | 7.0E-3              |
| I-123   | 13.13 h  | 4.3E-3               | 2.9E-3               | 0.0                   | 3.2E-3              |
| I-129   | 1.57E7 y   | 5.7E-3               | 1.3E-3               | 0.0                   | 1.9E-3              |
| I-131   | 8.04 d   | 2.1E-2               | 1.4E-2               | 3.0E-3                | 1.5E-2              |
| I-132   | 2.30 h   | 2.3E-2               | 1.8E-2               | 8.2E-3                | 1.9E-2              |
| I-133   | 20.8 h   | 2.3E-2               | 1.8E-2               | 7.6E-3                | 1.9E-2              |
| I-135   | 6.61 h   | 2.2E-2               | 1.7E-2               | 6.5E-3                | 1.8E-2              |
| Cs-134  | 2.062 y  | 1.6E-2               | 1.1E-2               | 2.7E-3                | 1.2E-2              |
| Cs-137  | 30.17 y  | 2.0E-2               | 1.3E-2               | 2.3E-3                | 1.4E-2              |
| Ba-137m | 2.552 m  | 2.4E-3               | 2.0E-3               | 1.2E-3                | 2.1E-3              |
| Ba-140  | 12.789 d   | 2.2E-2               | 1.6E-2               | 5.0E-3                | 1.7E-2              |
| La-140  | 40.22 h  | 2.4E-2               | 1.9E-2               | 9.2E-3                | 2.0E-2              |
| Ce-144  | 284.3 d  | 1.5E-2               | 7.6E-3               | 1.7E-4                | 8.9E-3              |
| Pr-144  | 17.28 m  | 2.4E-2               | 2.1E-2               | 1.3E-2                | 2.2E-2              |
| Hg-203  | 46.60 d  | 1.6E-2               | 8.5E-3               | 3.7E-4                | 9.6E-3              |
| Pb-210  | 22.26 y  | 1.8E-5               | 0.0                  | 0.0                   | 0.0                 |
| Bi-210  | 5.013 d  | 2.3E-2               | 1.8E-2               | 7.4E-3                | 1.9E-2              |
| Bi-214  | 19.9 m   | 2.3E-2               | 1.9E-2               | 9.6E-3                | 2.0E-2              |
| Ra-224  | 3.62 d   | 2.9E-4               | 2.2E-4               | 1.5E-5                | 2.4E-4              |
| Ra-226  | 1600 y   | 5.9E-4               | 3.7E-4               | 0.0                   | 4.2E-4              |
| U-234   | 2.445E5 y  | 6.5E-5               | 1.6E-5               | 0.0                   | 2.1E-5              |
| U-235   | 7.038E8  | 3.1E-3               | 8.0E-4               | 2.9E-7                | 1.1E-3              |
| U-238   | 4.468E9 y  | 3.7E-5               | 9.8E-6               | 0.0                   | 1.6E-5              |
| Np-237  | 2.14E6 y   | 4.3E-3               | 4.3E-4               | 0.0                   | 6.8E-4              |
| Np-238  | 2.117 d  | 1.8E-2               | 1.1E-2               | 3.5E-3                | 1.2E-2              |
| Np-239  | 2.355 d  | 3.6E-2               | 2.0E-2               | 1.2E-3                | 2.3E-2              |

<sup>a</sup>Values in units of Sy/y per Bq/cm<sup>2</sup>.



PART 3. APPLICATIONS OF THE BIOKINETIC AND DOSIMETRIC MODELS

## HOW COMPUTATIONS ARE PERFORMED

The biokinetic and dosimetric models discussed in this report are implemented using a computer code called NEWAGE, which is an updated version of our original code called AGEDOS (Leggett et al. 1984). NEWAGE generates a matrix of dose equivalent rates  $MATRIX(B,T)$  for selected "basic beginning ages" B, that is, ages at acute exposure, and for subsequent times T chosen by the user. (In the following we will use the shorter phrase "dose rate" in place of "dose equivalent rate".) The standard set of basic beginning ages is B=0, 100, 365, 1825, 3650, 5475, and 7300 days, but NEWAGE will soon be modified to treat selected adult ages in addition to 7300 days. The generated matrix of dose rates is based on a unit intake, U, of a radionuclide by inhalation, ingestion, or injection. Dose rates for arbitrary intake patterns occurring over any age interval(s) may be estimated from this matrix by convoluting against any specified intake function. The method of convolution is described in the original AGEDOS report (Leggett et al. 1984).

The computational approach may be summarized in terms of three operations: (1) The user supplies a model for the time-dependent uptake and distribution of the parent nuclide and any dosimetrically significant progeny. It is preferable that the compartments in this model be physically identifiable entities, but provisions have been made to consider hypothetical compartments if needed. Parameter values must be given for the adult and should be supplied for as many of the additional basic beginning ages as information allows. (2) For each of the basic beginning ages, the NEWAGE code performs simple mathematical operations on the supplied age-dependent parameter values. The purpose is to approximate the redistribution of activity, including recycling of material released from compartments, that should occur within the specified compartments during a period of aging that is relatively short compared with the entire time span considered. (3) The NEWAGE code converts the estimated activities in selected compartments to dose rates using stored age-dependent SEE values (see the first section in Part II of this report) that account for radiation transport and energy deposition. Integrated doses are also calculated.

Movement of activity from one compartment to another generally is assumed to be a first order process. For removal of activity from bone volume, a temporary delay may be imposed by the user. Flow rates must be supplied for each of the compartments for adults (persons at least 7300 days of age), and age-specific flow rates may be defined for as many of the other six basic beginning ages as information allows. When input information is lacking for a basic beginning age, the code defaults to the data for the next higher basic beginning age.

Data bases of dose rates generated by NEWAGE are for acute unit intakes at each age. Differences with age in the amount of material inhaled or ingested are taken into account in applications of these data bases to exposure scenarios. Differences with age in the fraction of ingested material absorbed into blood are considered within the NEWAGE code whenever age-specific absorption fractions are supplied. Provisions have been made to use age-specific values for behavior of material within the respiratory and gastrointestinal tracts, but for all age groups we currently apply parameter values specified for the reference adult in the ICRP respiratory and GI tract models (Eve 1966, Morrow et al. 1966, ICRP 1979). As indicated earlier, we believe that present information on variation with age in fractional deposition and rate of transport of material in the respiratory tract or movement of material through the GI tract is still too uncertain to be of benefit in reducing uncertainties involved in applying the ICRP models to all age groups. We will amend our treatment of the respiratory and gastrointestinal tracts as more supportable age-dependent biokinetic models for these regions become available.

NEWAGE proceeds in a sequence of "time steps" or "intervals", with each step being defined by a beginning time  $t_1$  and an ending time  $t_2$ . These steps may be altered by the user but ideally should start out short and gradually increase in length, from a fraction of a day immediately after intake to perhaps one year at times remote from intake. Such a pattern is needed to obtain a reasonably accurate and efficient approximation of both the typically rapid changes in activity in organs soon after exposure and the relatively slow changes that occur at extended times after exposure.

Suppose that calculations are being made for the basic beginning age  $B$ , that the code has made calculations up to some time  $t_1$ , and that the next time step is from time  $t_1$  to time  $t_2$ . The age of the exposed person at time  $t_1$  is  $B+t_1$ . If  $B+t_1$  is 7300 days or greater, input parameters for the adult are used during the present time step. If not, the code finds closest basic beginning ages  $B_1$  and  $B_2$  bounding  $B+t_1$ , assigns age-specific rate constants and/or deposition fractions for age  $B+t_1$  by linearly interpolating input data for ages  $B_1$  and  $B_2$ , and applies the interpolated data to this entire time step.

For the time step from  $t_1$  to  $t_2$ , the code defines an initial activity, an inflow rate, and an outflow rate for each compartment. The initial activity for a given compartment at time  $t_1$  is the activity remaining in the compartment at the end of the preceding time step, if any. The rate of inflow of activity into the compartment is estimated using the length of the time step together with the portion of the total amount of outflow of material from all other compartments destined for the given compartment during the preceding time step. The rate of outflow from the compartment is the rate interpolated from the age-specific input data. The inflow rate and outflow rate are assumed to be constant during a time step but may vary from one time step to the next. The constant inflow and outflow rates during the time step and the initial activity at the beginning of the time step are used to calculate the activity at the end of the time step as well as the integrated activity during the time step, based on standard methods for first-order differential equations. The code advances to the next compartment in its list and proceeds in this way until all compartments have been addressed during the time step from  $t_1$  to  $t_2$ .

After activity at the right endpoint of the time step (time  $t_2$ ) has been calculated for all compartments, age-specific SEE values are retrieved by the code from a permanent library and used to convert instantaneous activities to dose rates to selected tissues at time  $t_2$ . For a given tissue, the SEE values are used to account for all energy deposited in the tissue from radiation emitted within the tissue as well as from penetrating radiations emitted from other regions of the body. These SEE values have been calculated using mathematical phantoms of the human body, one for each of the ages 0, 365, 1825, 3650, 5475, and 7300

days (Cristy 1980; Cristy and Eckerman, to appear). For a given age, the phantom has been constructed using volumes, masses, and geometries of organs that appear typical for that age. As with metabolic parameters, SEE values for age  $B+t_1$  are determined using linear interpolation of SEE values for closest bounding basic beginning ages.

## REFERENCES

- Cristy, M., 1980, *Mathematical Phantoms Representing Children of Various Ages for Use in Estimates of Internal Dose*, NUREG/CR-1159, ORNL/NUREG/TM-367.
- Cristy, M. and Eckerman, K. F., to appear, *Specific Absorbed Fractions of Energy at Various Ages from Internal Photon Sources. I. Methods*, ORNL/TM-8381:Vol.1.
- Eve, I. S., 1966, A Review of the Physiology of the Gastrointestinal Tract in Relation to Radiation Doses from Radioactive Material, *Health Phys.* 12, 131-162.
- International Commission on Radiological Protection, 1979, *Publication 30, Limits for Intakes by Workers*, Pergamon Press, Oxford.
- Leggett, R. W., Eckerman, K. F., Dunning, D. E., Jr., Cristy, M., Crawford-Brown, D. J., and Williams, L. R., 1984, *On Estimating Dose Rates to Organs as a Function of Age Following Internal Exposure to Radionuclides*, ORNL/TM-8265.
- Morrow, P. E., Bates, D. V., Fish, B. R., Hatch, T. F., and Mercer, T. T., 1966, Deposition and Retention Models for Internal Dosimetry of the Human Respiratory Tract, *Health Phys.* 12, 173-207.

COMPARISON OF OUR AGE-SPECIFIC DOSE COMMITMENT FACTORS  
WITH VALUES PRODUCED BY OTHER APPROACHES

In the absence of age-specific biokinetic models for most radionuclides, two main approaches have arisen for evaluating internal exposures to the general public. (1) The assumption often is made that all age groups receive the same organ doses as does a reference adult, usually as currently depicted in models of the ICRP (e.g., Sullivan et al. 1981). This approach is thought by some to be justified on the basis that potential increases in dose due to smaller organ masses in children might be expected to be offset by more rapid turnover of the radionuclide at younger ages. (2) Others have taken the apparently more conservative approach of assigning biokinetic models for a reference adult to all age groups (except in scattered cases where age-specific biokinetic models are available) but considering the smaller organ masses of younger persons in calculation of organ doses (e.g. Hoenes and Soldat 1977; Greenhalgh, Fell, and Adams 1985). As discussed in this report, our approach is to consider not only the smaller organ masses of younger persons in calculations of dose but also to employ a framework for biokinetic modeling that allows incorporation of pertinent age-specific radiobiological or physiological information as well as physiologically based assumptions where blind assumptions might have to be made in more conventional approaches.

In Table 1 we compare our estimated 50-year dose commitment factors with factors based on the other two approaches. Dose commitments from acute inhalation of a unit activity of Th-230, U-238, or Pu-239 (AMAD=1.0 micron) or from acute ingestion of a unit activity of Cs-134, Cs-137, or U-238 at ages 0, 1, 5, 10, and 15 years or during adulthood are considered for selected target organs. All values are normalized to the value produced using the models and methods for a reference adult as described in ICRP Publication 30. Thus, for comparison with the approach of applying ICRP "reference adult" dose commitments to all age groups, we need only read the values on the lines labeled "ORNL". For comparison with the second approach we have used age-specific dose commitment factors published in Report NRPB-R162 (1985), where this approach was used. Note that the NRPB values for the adult are nearly

the same as the ICRP reference man values, since essentially the same models are used in the two cases.

#### INHALATION OF THORIUM-230

Our estimates of dose to bone surface and active marrow from inhalation of Th-230 are not strongly age dependent, for two reasons. First, the smaller denominator in the calculations (mass of irradiated tissue) is offset largely by a smaller numerator (deposited energy) because of more rapid burial of activity into bone volume at younger ages. Second, thorium is removed so slowly from the skeleton that a substantial portion of the 50-year dose commitment arises from energy deposited during adulthood, regardless of age at intake.

A stronger dependence on age is estimated for liver. This results from our assumption of independence of age in liver uptake and turnover, and the faster movement of material from skeleton to liver during younger ages.

Our values for bone surface and active marrow do not differ greatly from those generated by the other two methods, but the reasonably close agreement is fortuitous. In the ICRP (and hence the NRPB) biokinetic model, thorium is assumed to be uniformly distributed on bone surface at all times following its deposition in the skeleton, so that reduction in dose to bone surface and active marrow due to burial in bone volume is ignored. On the other hand, in the ICRP model the potential overestimate from ignoring burial is offset by what we believe to be an underestimate in the apparent half-time for removal from the skeleton to excretion. The higher dose commitments to liver at all ages estimated by our methods results largely from considerations of recycling of activity between skeleton and liver.

#### INHALATION OR INGESTION OF URANIUM-238

It is almost certain that much of the uranium deposited in the skeleton does not move quickly to bone volume or plasma but resides a few weeks, months, or longer on or near bone surfaces (see the discussion in ICRP Publication 30, 1979). In ICRP Publication 30 fairly short-lived isotopes of uranium are assumed to reside on bone surface at all times after deposition in the skeleton, but residence on bone

surface is ignored for long-lived isotopes such as U-238. For consideration of young age groups it is critical that residence on bone surface be considered. If more than a few days are actually required for uranium to move from bone surface to bone volume and/or plasma in young children, then very large doses to bone surface will result. This is suggested by our values in Table 1, where large factors are estimated for inhalation or ingestion of U-238 at early ages. The larger values for ingestion are due to our assumption of enhanced absorption from the small intestine in children. We have assumed that movement from bone surfaces to bone volume occurs faster in young children than in adults, but we can find no reason to assume a faster removal from bone surface to plasma at younger ages. We regard our parameter values for bone surface and the resulting estimates of dose to bone surface as very uncertain, but we believe that our estimates are more strongly supported than those derived using the ICRP biokinetic model.

Elevated estimates for kidney at younger ages result from our assumption that removal from kidney is independent of age. This assumption may be modified somewhat after further investigations into the physiological literature.

#### INHALATION OF PLUTONIUM-239

It is interesting that the three approaches yield fairly similar estimates at all ages in this case for bone surface, active marrow, and liver. Despite the large apparent differences between our biokinetic model and that of the ICRP, the net retention in liver and near bone surfaces (including residence in marrow in our model) in adults is not much different in the two models. The effect of smaller organ masses at younger ages is largely offset in our estimates by the greater remodeling rates for bone. As in the case of inhalation of thorium, age dependence in 50-year dose commitments is reduced considerably by the fact that much of the intake at younger ages is still available for recycle to bone surfaces after adulthood.

## INGESTION OF CESIUM-134 OR CESIUM-137

There do not appear to be any large uncertainties in our estimates for Cs-134 and Cs-137. Cesium should be fairly completely absorbed from the small intestine at all ages, so that no problem is introduced by having to estimate age-specific values for  $f_1$ . Our biokinetic model for cesium appears to be well founded, although more investigation of behavior in the skeleton is needed. There may be some escape of the decay product Ba-137m from Cs-137, but this is limited by the short radiological half-life of Ba-137m. For the types of radiations and energies involved our SEE values should involve only small uncertainties.

The more rapid turnover of cesium at younger ages may more than offset the effects of smaller organ masses except for infants, so that the ICRP value for adults may be an overestimate for most non-adults and the NRPB approach may yield even greater overestimates for all non-adults. Recall that our biokinetic model for cesium includes a reduction in the biological half-time during the first 6 months of life and an increase after age 1 year; we believe the initial reduction in half-time is a result of a reduction of the ratio of slow to fast muscle fiber after birth. (See the report by Leggett, 1983, for a discussion of the different rates of transport of cesium from fast and slow muscle.)

## REFERENCES

- Greenhalgh, J. R., Fell, T. P., and Adams, N., 1985, *Doses from Intakes of Radionuclides by Adults and Young People*, Report of the National Radiological Protection Board, NRPB-R162, Chilton, Didcot, Oxon OX11 0RQ.
- Hoenes, G. R. and Soldat, J. K., 1977, *Age-Specific Radiation Dose Commitment Factors for a One-Year Chronic Intake*, U.S. Nuclear Regulatory Commission Report NUREG-0172.
- International Commission on Radiological Protection, 1979, *Publication 30, Limits for Intakes by Workers*, Pergamon Press, Oxford.
- Leggett, R. W., 1983, *Metabolic Data and Retention Functions for the*

*Intracellular Alkali Metals*, NUREG/CR-3245, ORNL/TM-8630.  
Sullivan, R. E., Nelson, N. S., Ellett, W. H., Dunning, D. E., Leggett,  
R. W., Yalcintas, M. G., and Eckerman, K. F., 1981, *Estimates of  
Health Risk from Exposure to Radioactive Pollutants*, Oak Ridge  
National Laboratory Report ORNL/TM-7745.

Table 1. Comparison of our age-specific estimates of 50-year dose commitment with age-specific estimates of NRPB, for intake of various nuclides. Values are normalized to the ICRP value for Reference Man.

| Case                                 | Organ         | Age at acute intake (y) |      |      |      |      | Adult | Source |
|--------------------------------------|---------------|-------------------------|------|------|------|------|-------|--------|
|                                      |               | 0                       | 1    | 5    | 10   | 15   |       |        |
| Inhalation of<br>Th-230<br>(Class W) | Bone surface  | 2.0                     | 1.6  | 1.4  | 1.3  | 1.2  | 1.4   | ORNL   |
|                                      |               |                         | 2.1  |      | 1.1  |      | 1.0   | NRPB   |
|                                      | Active marrow | 2.3                     | 1.7  | 1.1  | 0.77 | 0.59 | 0.62  | ORNL   |
|                                      |               |                         | 2.1  |      | 1.2  |      | 0.98  | NRPB   |
|                                      | Liver         | 15.                     | 11.  | 6.4  | 4.0  | 2.7  | 2.5   | ORNL   |
|                                      |               |                         | 5.0  |      | 1.7  |      | 1.0   | NRPB   |
| Inhalation of<br>U-238<br>(Class D)  | Bone surface  | 53.                     | 10.  | 2.7  | 2.1  | 2.1  | 0.88  | ORNL   |
|                                      |               |                         | 2.7  |      | 1.2  |      | 0.99  | NRPB   |
|                                      | Kidney        | 11.                     | 3.6  | 1.8  | 1.2  | 0.88 | 0.65  | ORNL   |
|                                      |               |                         | a    |      | a    |      | a     | NRPB   |
| Ingestion of<br>U-238                | Bone surface  | 160.                    | 20.  | 3.7  | 3.5  | 3.7  | 0.88  | ORNL   |
|                                      |               |                         | 2.6  |      | 1.2  |      | 1.0   | NRPB   |
|                                      | Kidney        | 34.                     | 7.2  | 2.5  | 2.0  | 1.6  | 0.65  | ORNL   |
|                                      |               |                         | a    |      | a    |      | a     | NRPB   |
| Inhalation of<br>Pu-239<br>(Class Y) | Bone surface  | 0.83                    | 0.77 | 0.74 | 0.77 | 0.80 | 0.83  | ORNL   |
|                                      |               |                         | 1.4  |      | 1.0  |      | 1.0   | NRPB   |
|                                      | Active marrow | 0.89                    | 0.75 | 0.57 | 0.50 | 0.50 | 0.50  | ORNL   |
|                                      |               |                         | 1.4  |      | 1.0  |      | 1.0   | NRPB   |
|                                      | Liver         | 1.2                     | 1.1  | 0.92 | 0.82 | 0.79 | 0.83  | ORNL   |
|                                      |               |                         | 1.4  |      | 1.1  |      | 0.96  | NRPB   |
| Ingestion of<br>Cs-134               | Kidney        | 2.4                     | 0.81 | 0.66 | 0.74 | 1.0  | 1.0   | ORNL   |
|                                      |               |                         | a    |      | a    |      | a     | NRPB   |
|                                      | Liver         | 2.5                     | 0.83 | 0.68 | 0.76 | 1.0  | 1.0   | ORNL   |
|                                      |               |                         | 4.2  |      | 1.8  |      | 1.0   | NRPB   |
|                                      | Ovary         | 3.0                     | 1.0  | 0.82 | 0.93 | 1.2  | 0.99  | ORNL   |
|                                      |               |                         | 4.1  |      | 1.8  |      | 0.94  | NRPB   |
| Ingestion of<br>Cs-137               | Kidney        | 2.9                     | 0.87 | 0.68 | 0.76 | 1.0  | 1.0   | ORNL   |
|                                      |               |                         | a    |      | a    |      | a     | NRPB   |
|                                      | Liver         | 2.9                     | 0.89 | 0.69 | 0.77 | 1.1  | 1.1   | ORNL   |
|                                      |               |                         | 5.1  |      | 2.0  |      | 1.0   | NRPB   |
|                                      | Ovary         | 3.2                     | 0.98 | 0.77 | 0.87 | 1.2  | 1.0   | ORNL   |
|                                      |               |                         | 5.1  |      | 1.9  |      | 1.0   | NRPB   |

<sup>a</sup>NRPB did not include kidney as a target organ in their report NRPB-R162 (1985).

A CLOSER LOOK AT AGE-SPECIFIC ESTIMATES OF DOSE TO  
BONE SURFACES FOLLOWING INHALATION OF THORIUM-230

In the previous section we looked at dose commitment factors based on a unit intake at certain ages. In this section we consider the case of inhalation of Th-230 in more detail. In particular, we examine how dose (equivalent) rates as well as dose commitments vary with age at intake, how values are affected by folding in age-specific intake rates, and how estimates vary with variation in the most uncertain parameter value, the removal rate from bone surface.

The inhaled activity is assumed to be class W material with an activity median aerodynamic diameter of 1.0 microns, in the language of Publication 30 of the ICRP. It is assumed that each adult inhales one microcurie of Th-230 over a short period and that each pre-adult of age A inhales  $f(A)$  microcuries, where  $f(A)$  is the typical daily air intake at age A divided by the typical daily air intake of an adult.

The amounts of thorium inhaled at ages 0, 1, 5, 10, 15, and 20 y are assumed to be 0.04, 0.15, 0.45, 0.70, 0.85, and 1.0 units of activity. These are based on data from various references (e.g., see ICRP 1975; Hofmann, Steinhausler, and Pohl 1979) and include consideration of relative amounts of resting, light, and heavy activities at different ages. Thorium intakes for intermediate ages are assigned by linear interpolation of values for nearest bounding ages from this list; all adults are assumed to inhale 1.0 microcurie.

Dose rates to bone surfaces, based on the models described earlier, are indicated in Fig. 1 for three ages at exposure: 1 y, 10 y, and 20 y. The curves in Fig. 1 include only high-LET radiation; the contribution from low-LET radiation is negligible. Since the deposition fraction on bone surfaces is assumed to depend only weakly on age, differences in dose rates as a function of age at intake result primarily from differences in the amount of activity inhaled, in the mass of irradiated tissue, and in the bone turnover rate. Persons of age 10 y at exposure are estimated to experience the greatest dose rates to bone surfaces at early times. Dose rates to the bone surfaces of children are estimated to be smaller than those for adults at times longer than a few years after exposure. This is due to the faster

removal of thorium from bone surfaces in the immature skeleton.

Much of the uncertainty in our estimates of relative values of dose rates and committed dose to bone surfaces for different ages at inhalation of Th-230 appears to stem from the paucity of information on the age-specific rate of removal of thorium from bone surfaces. We shall examine how relative estimates are affected as removal rates from bone surfaces in adults are left fixed and those in children are varied within reasonable bounds.

As discussed in earlier sections, it is well known that bone turnover occurs at a much higher rate in children than in adults, although the rates have never been quantified with much certainty. At one extreme we will assume that, through age 15 years, the removal of Th-230 from bone surfaces occurs at a rate ten times our preferred values given in the table of parameter values for the biokinetic model for thorium; all other parameter values in that table are assumed to be correct. This will be referred to as the RRS assumption (Rapid Removal from Surfaces). At age one year, for example, the RRS assumption implies a removal rate from cortical bone surfaces that is 700 times the adult rate, and at age ten years the removal rate would be 220 times the adult rate. At the other extreme we will assume that the removal rate for Th-230 from bone surfaces in nonadults is only two times the rate in adults, and all other removal rates assumed in our model for thorium will be left unaltered. This will be referred to as the SRS assumption (Slow Removal from Surfaces). The parameter values for removal from bone surfaces as given in the section on biokinetics of thorium will be referred to as the BRS assumption (Baseline Removal from Surfaces). For age one year the removal rate from cortical bone is varied by a factor of 350 between the RRS and SRS assumptions; for age ten years it is varied by a factor of 110.

Estimates of dose rates corresponding to the RRS and SRS assumptions are indicated in Figs. 2 and 3, respectively, for 1-year-olds, 10-year-olds, and adults at exposure. The relative patterns are similar in the first few weeks after exposure in the two extreme cases, but dose rates fall more rapidly after that time under the RRS than the SRS assumption.

Comparative age-specific lifetime dose commitments to bone surfaces under the different assumptions are listed in Table 1. Note that the integrated dose commitments vary somewhat less from one assumption to the other than do the assumed bone turnover rates. Also note that in each case dose commitment is an increasing function of age up to adulthood. This is a result of the increasing inhalation rate from birth to adulthood. Recall that these calculations are based on the assumption that the fraction of inhaled material deposited in various regions of the lung and the clearance time to blood are both independent of age. Present indications are that this assumption does not lead to a serious error in most cases, but better information certainly is needed.

#### REFERENCES

- Hofmann, W., Steinhausler, F., and Pohl, E., 1979, Dose Calculations for the Respiratory Tract from Inhaled Natural Radioactive Nuclides as a Function of Age, I. Compartment Deposition, Retention, and Resulting Dose, *Health Phys.* 37, 517-532.
- International Commission on Radiological Protection, 1975, *Publication 23, Report of the Task Group on Reference Man*, Pergamon Press, Oxford.

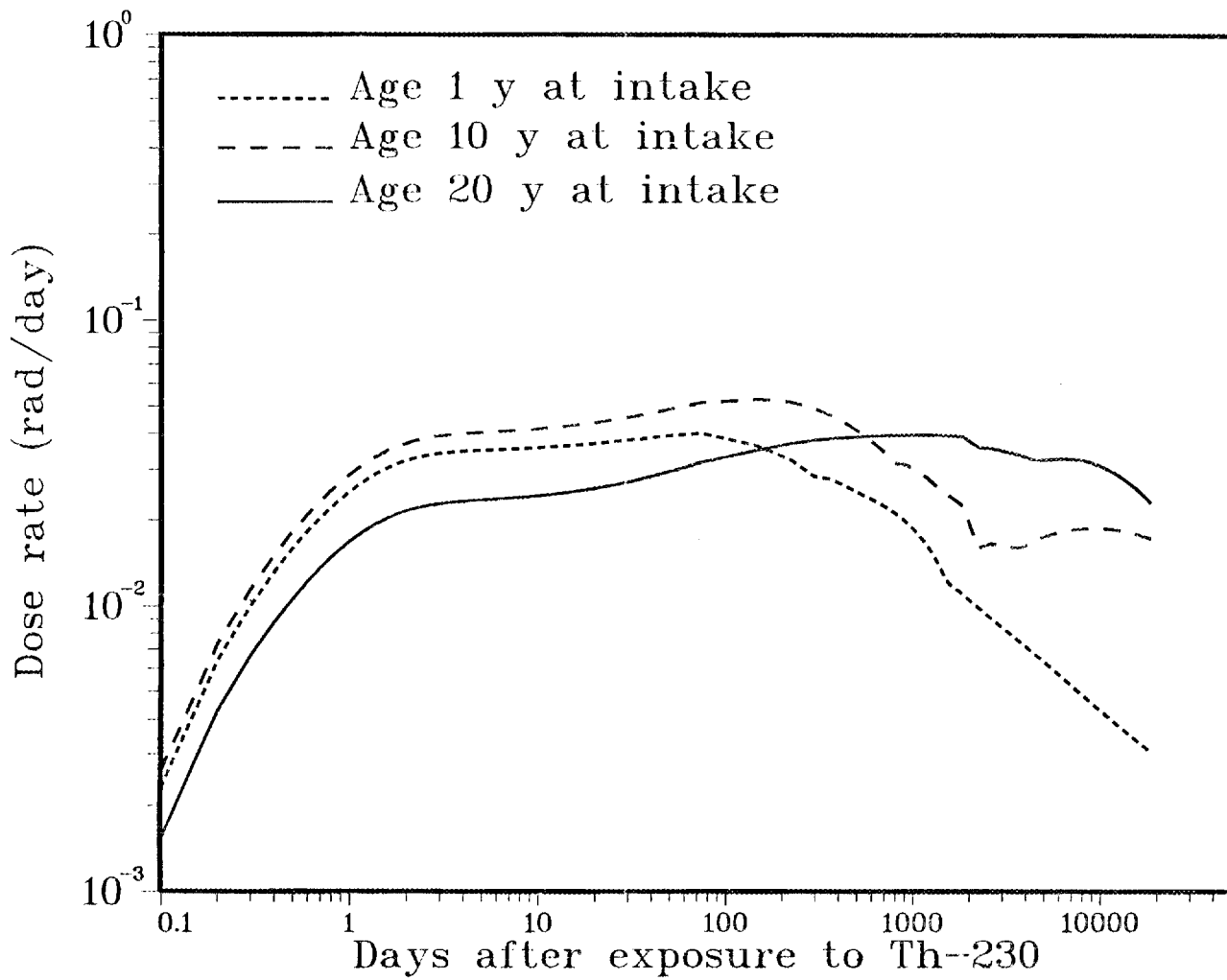


Fig. 1. Estimated dose rates to bone surfaces after acute inhalation of Th-230 at age 1, 10, or 20 y (BRS assumption).

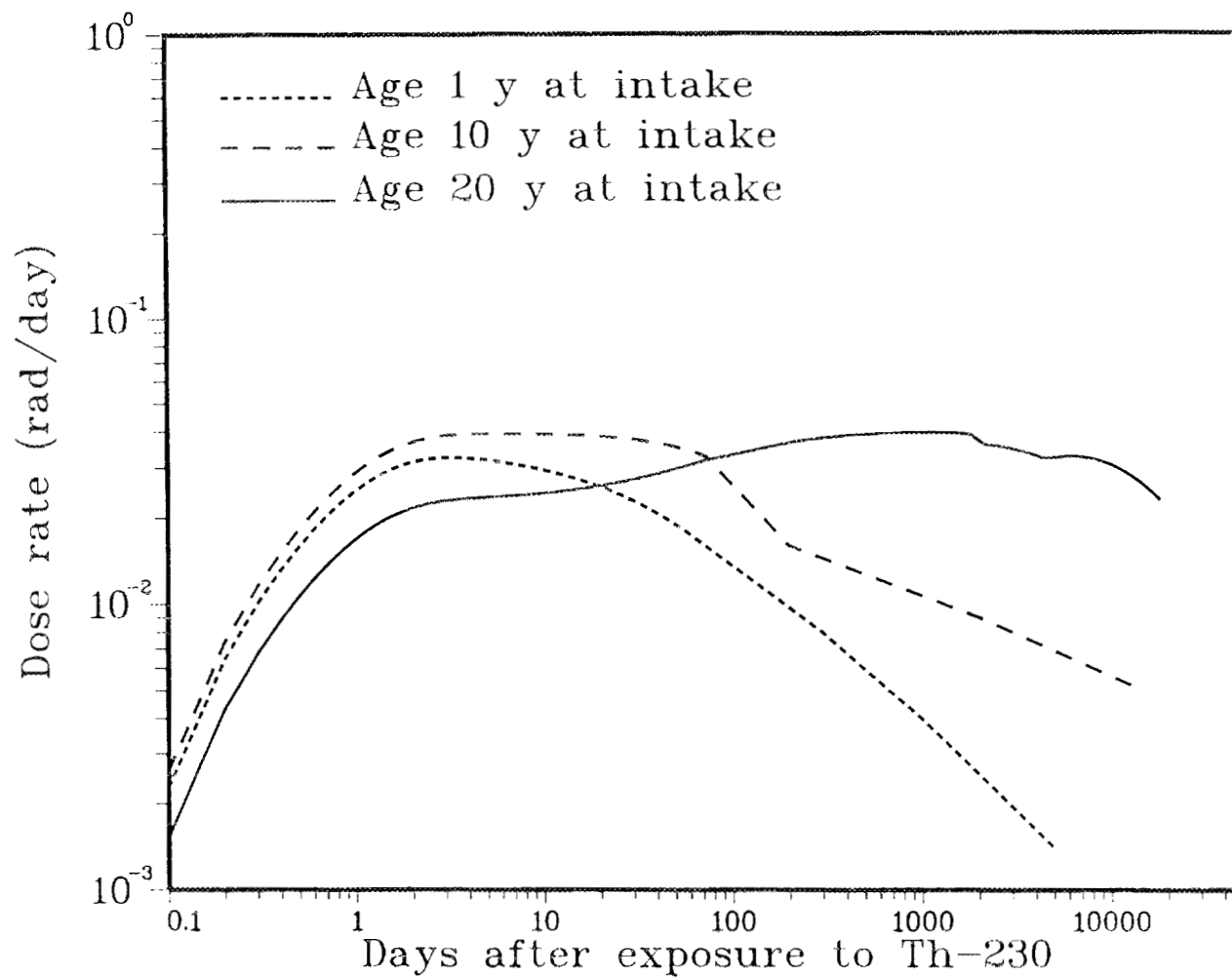


Fig. 2. Estimated dose rates to bone surfaces after acute inhalation of Th-230 at age 1, 10, or 20 y, assuming very rapid removal from bone surfaces in children (RRS assumption).

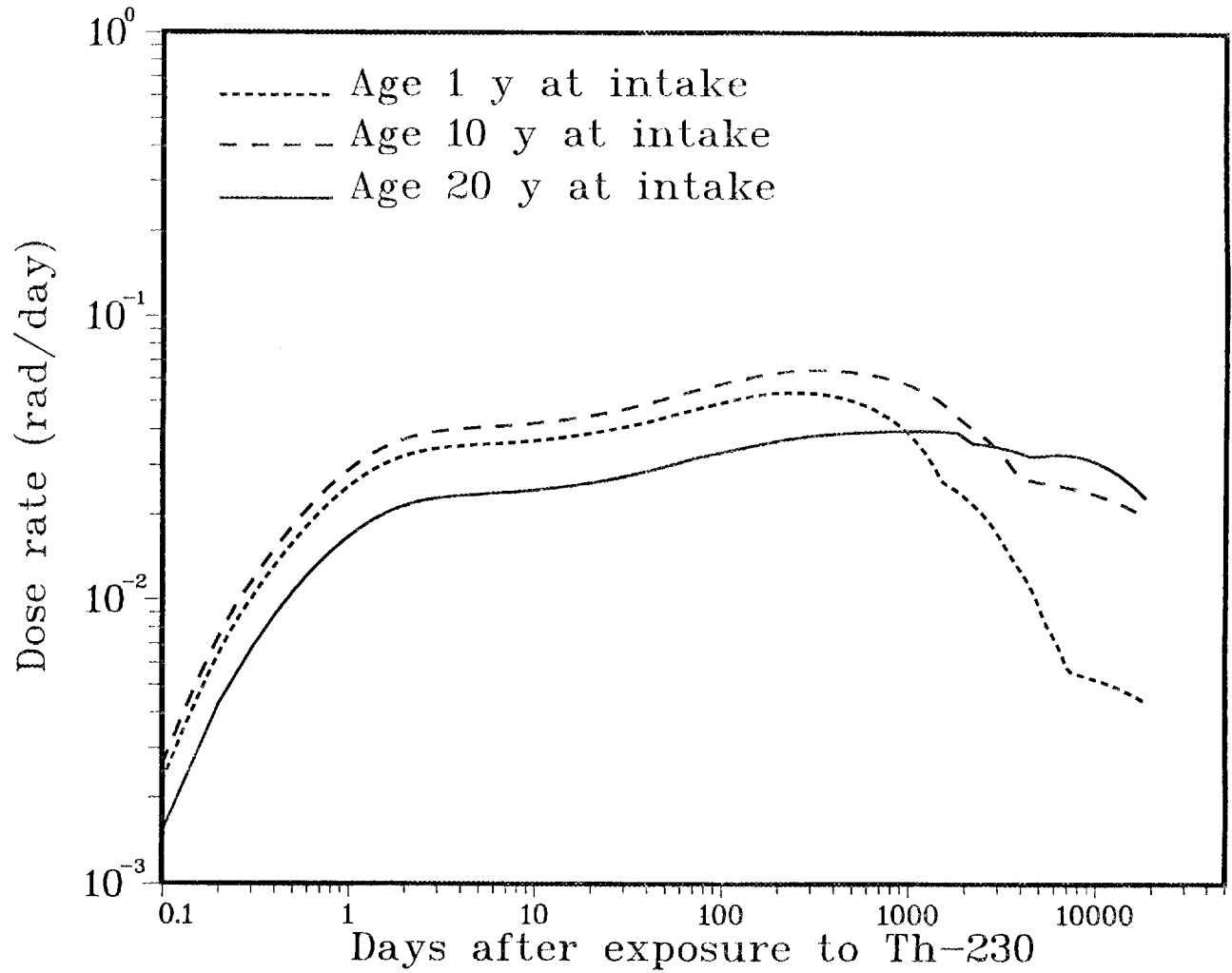


Fig. 3. Estimated dose rates to bone surfaces after acute inhalation of Th-230 at age 1, 10, or 20 y, assuming very slow removal from bone surfaces in children (SRS assumption).

Table 1. Age-specific estimates of lifetime\* dose commitment to bone surfaces following acute inhalation of Th-230, under different assumptions concerning residence on bone surfaces. Values are relative to the value for an adult. Differences with age in amounts inhaled have been included.

| Age<br>(years) | Assumption  |  |   |
|----------------|---|--|---|
|                | Baseline removal<br>from surfaces<br>at all ages<br>(BRS) | Rapid removal<br>from surfaces<br>in children<br>(RRS) | Slow removal<br>from surfaces<br>in children<br>(SRS) |
| 0              | 0.05  | 0.01   | 0.08  |
| 1              | 0.2   | 0.03   | 0.3   |
| 5              | 0.4   | 0.09   | 0.7   |
| 10             | 0.7   | 0.2  | 0.9   |
| 15             | 0.8   | 0.5  | 1.0   |
| Adult          | 1.0   | 1.0  | 1.0   |

\*Relative values are similar for integration over any period of at least 50 years.

A CLOSER LOOK AT AGE-SPECIFIC ESTIMATES OF DOSE TO BONE SURFACES  
FOLLOWING ACUTE INHALATION OR INGESTION OF URANIUM-238

In a previous section we considered age dependence in dose commitment factors based on acute ingestion or inhalation of a unit activity of U-238. In this section we examine how dose (equivalent) rates as well as dose commitments vary with age at intake, how values are affected by folding in age-specific intake rates, and how estimates vary if we impose different assumptions concerning residence or uranium on bone surfaces.

ACUTE INHALATION OF U-238

Suppose that persons of all age groups are exposed briefly to soluble U-238 in air, with the inhaled material being in the form of class D material with an activity median aerodynamic diameter of 1.0 microns. Assume that adults inhale one microcurie of U-238 over a short period and that nonadults of age A inhale  $f(A)$  microcuries, where  $f(A)$  is the typical daily air intake at age A divided by the typical daily air intake of an adult. As in the example for Th-230, the relative intakes of U-238 at ages 0, 1, 5, 10, 15, and 20 y are assumed to be 0.04, 0.15, 0.45, 0.70, 0.85, and 1.0 units of activity. Intakes for intermediate ages are assigned by linear interpolation of values for nearest bounding ages in the list; all adults are assumed to inhale 1.0 microcurie.

Dose rates to bone surface, based on the age-specific biokinetic model for uranium and SEE values described earlier, are indicated in Fig. 1 for three ages at exposure: 1 y, 10 y, and 20 y. Note that persons of age 1 y at exposure are estimated to experience higher dose rates than the other age groups at early times, despite the much smaller amount of uranium inhaled. This is a result of the larger fraction of systemic uranium assumed to go to skeleton surfaces, combined with the much smaller mass of irradiated tissue at younger ages. Dose rates to the bone surface of children are estimated to be smaller than those for adults at times longer than a few hundred days after exposure. This results from the faster removal of uranium assumed for the surfaces and volume of the bones of children.

We next examine how estimates of dose rate to bone surface would be affected by using the assumption, as in ICRP 30, that long-lived uranium is uniformly distributed in bone mineral at all times after its deposition in the skeleton. This will be called the RUD assumption (Rapid Uniform Distribution); our previous, preferred assumption will be referred to as the TRS assumption (Temporary Residence on Surfaces). The RUD assumption was implemented in our modeling scheme by increasing the removal rates from bone surfaces to blood and from bone surfaces to bone volume by a factor of 100 and keeping all other parameter values as before.

Estimates of dose rates to bone surface generated using the RUD assumption are indicated in Fig. 2 for 1-year-olds, 10-year-olds, and adults at exposure. Note that dose rates to bone surface are much lower in the first few months after exposure than was the case with the TRS assumption (see Fig. 1), and that the dose rates for a person of age 1 year at exposure decrease below the level for adult much more quickly for the RUD assumption.

Comparative age-specific lifetime dose commitments to bone surface under the alternate assumptions are listed in Table 1. Dose rates were integrated over 110 years to cover the maximum lifetime in essentially any population; because almost all activity has been removed from the body by 50 years, approximately the same relative values would be obtained by integrating over any period of 50 years or greater. For exposed newborns and children, the estimated lifetime dose commitments were 1.3-2.3 times higher than for adults under the TRS assumption, despite the smaller amounts inhaled. On the other hand, under the RUD assumption, lifetime dose commitments to persons less than age 10 y at exposure were considerably smaller than for adults.

In the remainder of this section we restrict attention to estimates based on the TRS assumption.

#### INGESTION OF U-238

Assume that each adult ingests one microcurie of U-238 in drinking water over a short period and that each nonadult of age A ingests  $f(A)$  microcuries, where  $f(A)$  is the daily intake of water at age A divided by the typical intake by an adult. We assume relative intakes at ages 0,

1, 5, 10, 15, and 20 y of 0.45, 0.6, 0.7, 0.7, 0.7, and 1.0 units of activity. This is based on "maximally exposed" individuals, that is, persons in each age group with high intakes of water. For consideration of average intakes at each age, values of  $f(A)$  for young ages  $A$  probably should be reduced. Absorption fractions from the small intestine to blood for these six ages are assumed to be 0.16, 0.10, 0.07, 0.08, 0.09, and 0.05 (see Cristy et al. 1986). Note that there is not much variation with age in the product of the intake and the absorption fraction, that is, in the amount of ingested uranium assumed to reach the bloodstream.

The temporal pattern for dose rate to bone surface for a given intake age, 1, 10, or 20 years, is not too different from that shown for the inhalation case in Fig. 1. However, the relative magnitudes of dose rates and integrated doses for different ages at intake is much different in the case of ingestion of U-238 in drinking water, as is indicated in Table 2. This difference stems from the fact that in the case of ingestion of U-238 in drinking water, the amount of environmental contamination reaching the blood is not assumed to vary substantially with age to offset the substantial age dependence in estimated dose to bone surface per unit intake.

#### REFERENCES

- Cristy, M., Leggett, R. W., Dunning, D. E., and Eckerman, K. F., 1986, *Relative Age-Specific Radiation Dose Commitment Factors for Major Radionuclides Released from Nuclear Fuel Facilities*, NUREG/CR-4628, ORNL/TM-9890.

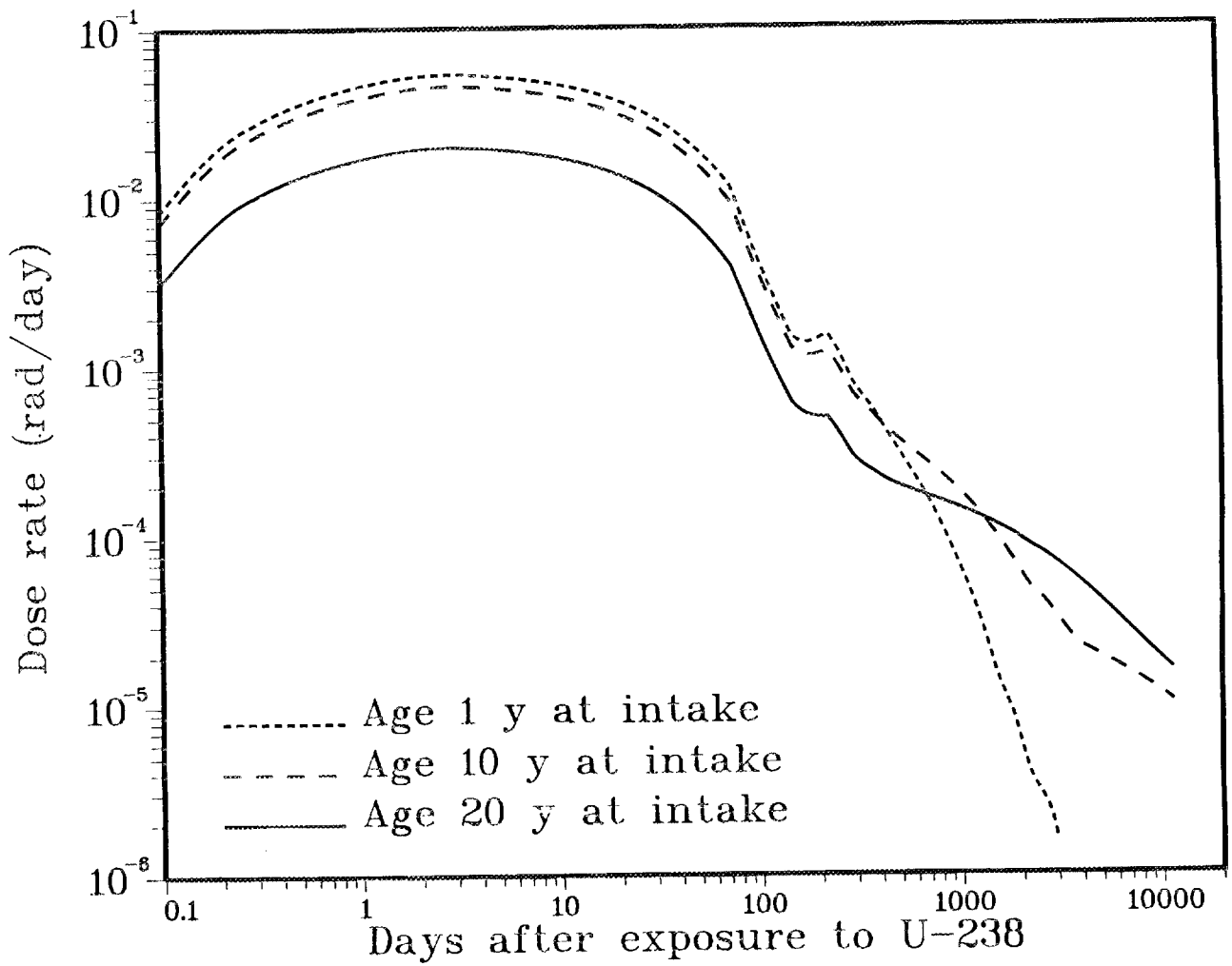


Fig. 1. Estimated dose rates to bone surfaces after acute inhalation of U-238 at age 1, 10, or 20 y, assuming temporary residence on bone surfaces (TRS assumption).

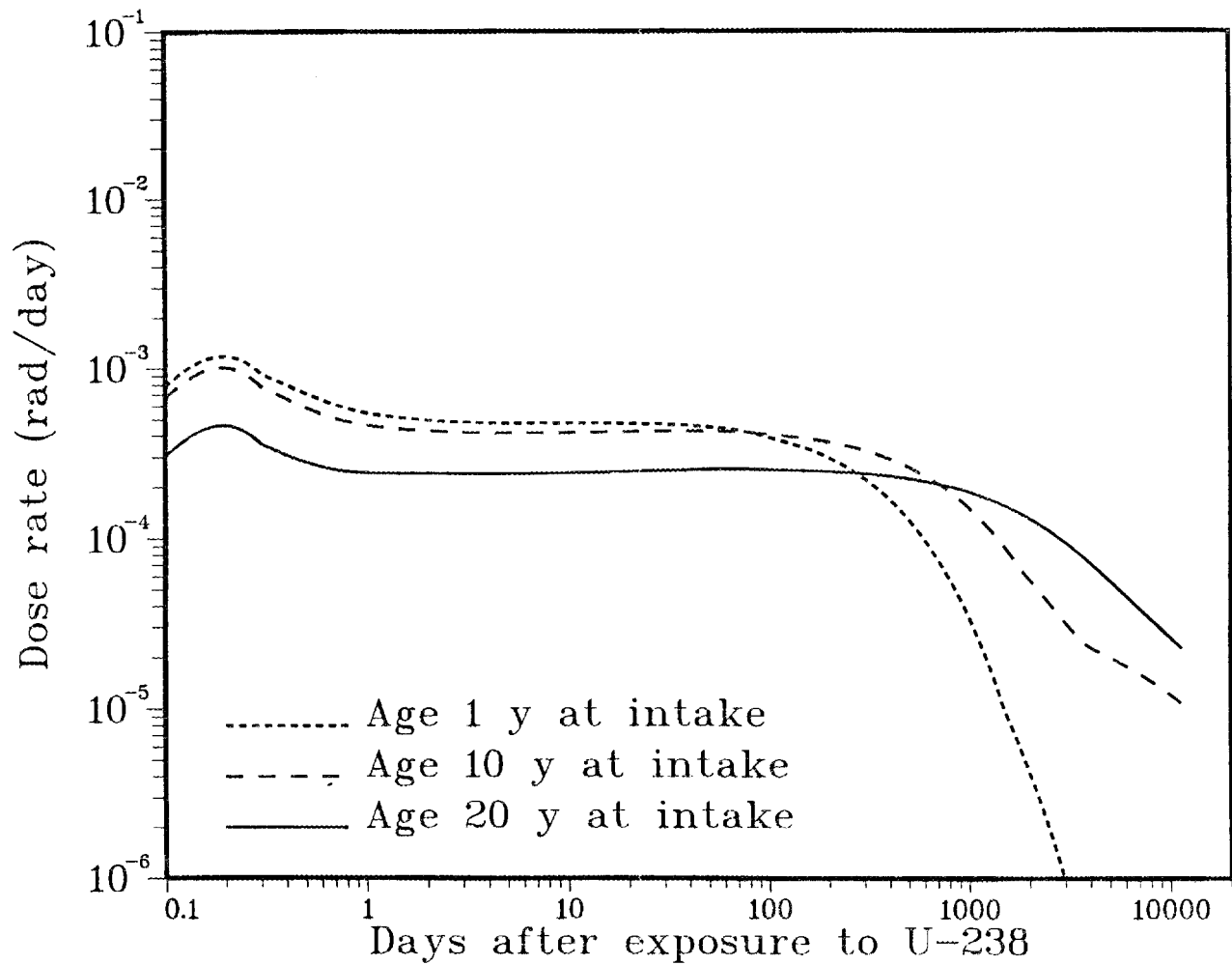


Fig. 2. Estimated dose rates to bone surfaces after acute inhalation of U-238 at age 1, 10, or 20 y, assuming rapid uniform distribution in bone (RUD assumption).

Table 1. Age-specific estimates of lifetime\* dose commitment to bone surfaces following acute inhalation of U-238, under alternate assumptions concerning residence on bone surfaces. Values are relative to the value for an adult. Differences with age in amounts inhaled have been included.

| Age<br>(years) | Assumption  |   |
|----------------|---|---|
|                | Baseline case:<br>temporary residence<br>on surfaces<br>(TRS) | ICRP 30 assumption:<br>rapid uniform<br>distribution in bone<br>(RUD) |
| 0              | 2.3   | 0.1   |
| 1              | 1.6   | 0.2   |
| 5              | 1.3   | 0.3   |
| 10             | 1.6   | 0.6   |
| 15             | 2.1   | 1.6   |
| Adult          | 1.0   | 1.0   |

\*Relative values are similar for integration over any period of at least 50 years.

Table 2. Age-specific estimates of lifetime\* dose commitment to bone surface following acute ingestion of U-238 using our biokinetic model. Values are relative to the value for an adult. Differences with age in amounts ingested have been included.

| Age (years) | Relative dose commitment |
|-------------|--------------------------|
| 0           | 79                       |
| 1           | 13                       |
| 5           | 2.8                      |
| 10          | 2.6                      |
| 15          | 3.1                      |
| Adult       | 1.0                      |

\*Relative values are similar for integration over any period of at least 50 years.



PART 4. THE NEXT STEP: CALCULATION OF RADIOGENIC RISK

## FACTORS CONSIDERED IN CALCULATIONS OF RISK

We have developed the computer code RISKAP (Leggett 1986) to estimate risk to a heterogeneous population exposed to a contaminant for which organ dose (or accumulation) per unit exposure and a dose-response (or accumulation-response) model are available. Risk is measured in terms of expected incidence or number of premature deaths resulting from the exposure, the number of years of life lost, if any, as a result of these deaths, and the average number of years of life lost per premature death. In the special case that the population consists of a single birth cohort, the decrease in life expectancy of the cohort is also computed. In the following it will be assumed that the exposure is to a radioactive contaminant and risk is measured in terms of premature death.

The user defines a population by specifying its size and age distribution at reference time 0, its subsequent age-specific mortality rates assuming no radiogenic deaths, and its subsequent birth rates. Age-specific dose rates generated by NEWAGE (or by any other means) for acute intakes are read by a "hook-up" subroutine that converts these rates to an average dose rate for each year of age, based on an intake function specified by the user. For example, the user may wish to consider an intake which is chronic and which varies with age and time. RISKAP uses a history of these average yearly dose rates to compute an annual, age-specific risk of premature cancer death, based on a dose-response function selected by the user. Calculations of premature radiation deaths, deaths from all causes, and the new age distribution of the population are performed for one-year intervals. The population is tracked over any specified period.

For many applications it is reasonable to assume that competing risks (as defined by mortality rates for all causes of death not related to the radiation exposure--called "non-radiogenic" in the following) do not change a great deal during the period of radiogenic risk. Depending on the dose-response hypothesis, however, observed or anticipated changes in non-radiogenic risks during the period of interest may have significant impact on the estimate of the number of incremental (radiogenic) deaths. In particular, if the assumption is made that the

risk of incurring a certain radiogenic health effect is related to the natural incidence of that health effect, then changes with time in the incidence of the health effect could be large enough over a few years to alter estimates of premature deaths substantially. A case in point is lung cancer, whose incidence has changed dramatically in some populations during the last few decades. To handle such situations, the code has been designed to allow the use of time-dependent mortality rates. The birth rate is also allowed to vary with time.

The dose-response function or "risk function" for a radiation exposure is usually expressed in terms of a latency period in which no radiogenic cancers are expected to occur, followed by a so-called "plateau" or "expression" period in which the risk of radiogenic cancer persists. It is usually assumed that the risk is uniformly distributed across the plateau period (as the name suggests), but RISKAP has been designed to accommodate latency and plateau periods that vary with age at exposure and risk functions that vary with age at exposure as well as time after exposure.

The general forms of dose-response functions commonly used are a purely linear function, a purely quadratic function, or a sum of linear and quadratic terms; these are sometimes multiplied by an exponential factor that accounts for reduced risk at very high doses due to a cell-killing effect. The version of RISKAP listed in the report by Leggett (1986) allows the use of a linear, quadratic, or linear-quadratic dose-response function. The user simply supplies the coefficients to the linear and quadratic terms. The code is structured, however, so that the user may include an exponential factor or substitute any preferred dose-response function by editing a few lines that define the function.

#### REFERENCE

Leggett, R. W., 1986, *RISKAP, a Computer Code for Analysis of Increased Risk to Arbitrary Populations*, ORNL/TM-9910.

POTENTIAL VARIATION WITH AGE AT INTAKE  
IN RADIOGENIC RISK: SOME EXAMPLES

The concepts of dose commitment and committed effective dose equivalent are frequently used as surrogates for radiogenic risk. However, it is often questioned whether long-term integrated dose suitably reflects the potential expression of risk, even in the context of the reference adult. The suitability of these concepts seems particularly questionable when we consider changes in susceptibility to various types of radiogenic risk at different stages of life. For example, depending somewhat on the type of dose-response hypothesis applied, the use of long-term integrated dose as a surrogate for risk sometimes appears to mask potentially multiplicative effects of elevated response and elevated dose rates during some stages of life.

In this section we apply our computation approach to risk analysis (see the discussion of the RISKAP computer code in the preceding section) to various exposure scenarios to estimate variation of certain radiogenic risks as a function of age at acute intake or beginning of chronic intake. We also discuss one epidemiological study of persons internally exposed to a radionuclide; in this case some fairly definitive statements concerning age dependence of radiogenic risk can be made, independently of theoretical dosimetry and dose-response models.

In each of our hypothetical cases we assume that mortality rates for all causes (competing risks) are similar to those of the entire U. S. population in the early 1980's. Differences with sex are ignored. The mortality rates and risk factors used represent averages of values that have been estimated for males and females.

EXAMPLE 1.

We return to the scenario discussed in an earlier section in which persons of all ages are exposed briefly to the same concentration of Th-230 in air. All assumptions used earlier concerning solubility class, AMAD, and inhalation rate at different ages are assumed to hold. We examine the risk of dying prematurely from a radiogenic bone sarcoma and the expected number of years of life lost as a function of age at

acute intake. Since we are interested only in comparative values, we will express our estimates only as a multiple of the value for a young adult, which will mean a person in his/her early 20's.

We assume that response is linear with dose and has no threshold level. For adults we use the following risk-rate coefficient for high LET radiation:

$$1 \times 10^{-6} \text{ sarcoma/person-year-rad.}$$

This is based on observations of persons receiving protracted injections of Ra-224 and applies over a period of 27 years following a latency period of 4 years (BEIR 1980). For persons less than 20 years of age we assume that incidence per unit dose is 1.3 times higher than in adults (cf. Mays, Spiess, and Gerspach 1978); latency periods and periods of expression of risk (or "plateau" periods) are assumed to be independent of age.

This dose-response function, the age-specific dose rates for a unit inhalation of Th-230, and the age-specific inhalation rates described earlier were used to estimate, for different ages at intake, the risk of premature death from bone sarcoma and the expected number of years of life lost. We estimate that a person of age 1 year at intake may be about 0.3 times as likely as a young adult to experience a bone sarcoma and has a reduced life expectancy about half that of a young adult. A person of age 10 years at intake may be about 0.6 times as likely as a young adult to experience a radiogenic bone sarcoma and has about the same reduced life expectancy as a young adult. Of course, the uncertainty in these comparative values is large, even for fairly high levels of intake, primarily because of uncertainties involved in the dose-response function. Still, we believe they represent best available estimates at this time.

#### EXAMPLE 2.

We assume that persons of all ages are exposed briefly to soluble U-238 in drinking water. The assumptions used earlier concerning the amount of water consumed at different ages are assumed to hold. We again consider the comparative risk at different ages at intake of dying prematurely from a radiogenic bone sarcoma, using the same dose-function

as in Example 1.

This dose-response function, the age-specific dose rates for a unit ingestion of soluble U-238, and the age-specific intakes of drinking water described earlier were used to estimate, for different ages at intake, the risk of premature death from bone sarcoma and the expected number of years of life lost. We estimate that a person in the first year of life at intake may be 20-100 times as likely as a young adult to experience a bone sarcoma and may have a reduced life expectancy about 30-200 times that of a young adult. A person of age 10 years at intake may be about 4 times as likely as a young adult to experience a radiogenic bone sarcoma and may have a reduced life expectancy about 5 times higher than a young adult. Note that in this case not only the dose-response function but also the dose rates underlying these estimates involve large uncertainties.

For consideration of environmental exposures we are often interested in chronic rather than acute intakes. We assume that the intakes of U-238 in drinking water are chronic and that the concentration remains constant over the lifetime of the population after some initial time, and we examine how risk of a radiogenic bone sarcoma varies as a function of age at beginning of intake. Of course, variation in risk with age at beginning of chronic intake may be expected to be considerably smaller than variation in risk as a function of age at acute intake, because in the chronic intake scenario the intake during adulthood represents a large portion of the total intake. For the case of chronic intake of U-238 in drinking water we estimate that the risk of experiencing a radiogenic bone sarcoma is about 4-6 times as high and the expected years of life lost is about 8-12 times as high for a person who begins intake during the first year of life as for a person who begins intake as a young adult.

#### EXAMPLE 3.

Several authors have estimated age-specific doses to the thyroid from intake of I-131 (see Table 6 of Killough and Eckerman 1986). There is general agreement that the dose is higher in infants, young children, and adolescents than in adults; in fact, estimates for the first year or two of life are generally an order of magnitude higher than those for an

adult. Recent information indicates that children may be much more likely than adults to experience thyroid cancer from a given radiation dose (NIH 1985). Thus, short-term exposure to I-131 might be expected to result in a much greater risk of thyroid cancer in young children than adults due to a multiplicative effect of elevated dose per unit intake and elevated response per unit dose. This is in contrast to the two preceding examples in which the dose response function varied little with age; in those cases differences with age at intake in risk resulted mainly from differences in dose rates as a function of age and time after intake and in mortality rates from all competing causes.

We examine a scenario in which persons are exposed briefly to elevated levels of I-131 in milk, and we examine the risk of eventually experiencing a radiogenic thyroid cancer as a function of age at intake. We assume that the intake of milk is about the same at all ages.

We assume that response is linear with dose and has no threshold level. The risk-rate coefficient for adults is

$$1 \times 10^{-6} \text{ thyroid cancer/person-year-rad,}$$

and that for persons less than 20 years of age is assumed to be 3.3 times as great (NIH 1985). A latency period of 10 years and a lifetime plateau period are used here.

Using this risk function and dose rates generated by NEWAGE and based on the biokinetic model of Killough and Eckerman (1986), we estimate that the risk to an infant is on the order of 100 times greater than that to a young adult, assuming equal intakes of contaminated milk. The risk to a 10-year-old child may be about 20 times greater than that to a young adult.

#### EXAMPLE 4

Numerous measurements of Sr-90 in bone over the last three decades indicate that infants, young children, and teenagers accumulate considerably higher concentrations of this bone-seeking nuclide from the environment than do adults (Leggett, Eckerman, and Williams 1982). Studies of the Japanese atomic bomb survivors indicate that persons very young or very old at the time of exposure may be more likely to experience radiogenic leukemia from a given dose to active marrow than

are intermediate age groups (NAS 1980). Thus, for the case of environmental contamination with Sr-90, it seems likely that persons very young at exposure may be at much higher risk of radiogenic leukemia because of the potentially multiplicative effect of elevated dose to active marrow per unit exposure and elevated risk of leukemia per unit dose to active marrow.

We examine a scenario in which persons of all ages are acutely exposed to Sr-90 in drinking water. Assumptions concerning the amount of water taken in as a function of age are the same as in the scenario for U-238. The age-specific dose-response function was based on an average of the values for males and females given in the L-L model for leukemia in the BEIR III document (1980, p. 204).

We estimate that a person in the first year of life at intake may be 2-5 times as likely as a young adult to experience radiogenic leukemia and may have a reduced life expectancy about 4-9 times that of a young adult. Little difference in risk, including decreased life expectancy, is estimated for persons 5-30 years of age at intake.

#### EXAMPLE 5

Follow-up studies of about 900 persons of all ages who were injected with Ra-224 for medical purposes provide a valuable data set for the study of age and sex dependence in radiogenic risk (Mays, Spiess, and Gerspach 1978; Leggett and Crawford-Brown 1983). There have been over fifty observed cases of bone sarcoma in the follow-up group, compared with an expected incidence of 0.2. Age dependence in these supposedly radiogenic bone sarcomas is indicated in Fig. 1, where it becomes evident that the interpretation of the term "age dependence" depends strongly on the unit of measure applied. Bone sarcomas have occurred much more frequently in those exposed as children than as adults; this difference with age appears even more enhanced if one considers the relative likelihood of a bone sarcoma per unit of injected Ra-224. On the other hand, young children generally received a much larger amount of Ra-224 per unit of body mass than did adults, so that the difference with age is not as marked if one considers the probability of a bone sarcoma per unit activity of Ra-224 per unit of body mass. Mays and coworkers (1978) attribute the higher incidence of

bone sarcomas in young children to a higher dose to bone surfaces at young ages and suggest that the risk per unit dose is nearly independent of age. Their analysis is based on a rather crude bone dosimetry; a more detailed examination of the age-specific dose to bone surfaces from injection of Ra-224 will be made later in this report.

Other difference with age in deleterious effects from Ra-224 were found (Fig. 2). As with bone sarcomas, it is difficult to unravel the extent to which these differences stem from variation with age in dose to pertinent tissues or variation in effect per unit dose. A pattern somewhat similar to that for bone sarcomas was seen for exostoses (benign cartilaginous tumors of bone) except that this effect did not occur in adult patients. Exostoses occurred about 3 times more frequently in males than females (in agreement with the pattern seen in the hereditary form of the disease), indicating that there can also be significant sex-related differences in radiogenic risk. As with bone sarcomas and exostoses, the incidence of growth retardation also fell with age to adulthood. The age distribution of deleterious effects in teeth was somewhat different, with the peak frequency of tooth breakage occurring between 16 and 20 years of age.

The hypothetical examples given above are some of the many instances in which a marked age dependence in risk from intake of radionuclides is suggested but not confirmed by available information. The epidemiological study of the Ra-224 patients provides an example in which it can be established with reasonable confidence that exposed children were at much higher risk of radiogenic bone sarcoma than were adults, whatever the definition of "age dependence of radiogenic risk"; it cannot be established with any certainty, however, whether the reason was a greater dose per unit exposure, a greater risk per unit dose, or a combination of both.

#### REFERENCES

- Killough, G. G. and Eckerman, K. F., 1986, *Age- and Sex-Specific Estimation of Dose to a Normal Thyroid from Clinical Administration of Iodine-131*, NUREG/CR-3955, ORNL/TM-9800.

- Leggett, R. W. and Crawford-Brown, D. J., 1983, The Role of Age in Human Susceptibility to Radiation, *Sci. Prog., Oxford* 68, 227-258.
- Leggett, R. W., Eckerman, K. F., and Williams, L. R., 1982, Strontium-90 in Bone: a Case Study in Age-Dependent Dosimetric Modeling, *Health Phys.* 43, 307-322.
- Mays, C. W., Spiess, H., and Gerspach, A., 1978, Skeletal Effects following Ra-224 Injections into Humans, *Health Phys.* 35, 83-90.
- National Academy of Sciences, Advisory Committee of the Effects of Ionizing Radiation, 1980, *The Effects on Populations of Exposure to Low Levels of Ionizing Radiation*, (BEIR III Report), Washington, D. C., National Academy of Science.
- NIH, 1985, *Report of the National Institutes of Health Ad Hoc Working Group to Develop Radioepidemiological Tables*, U. S. Department of Health and Human Services, NIH Publication 85-2748.

ORNL-DWG 82C-12101

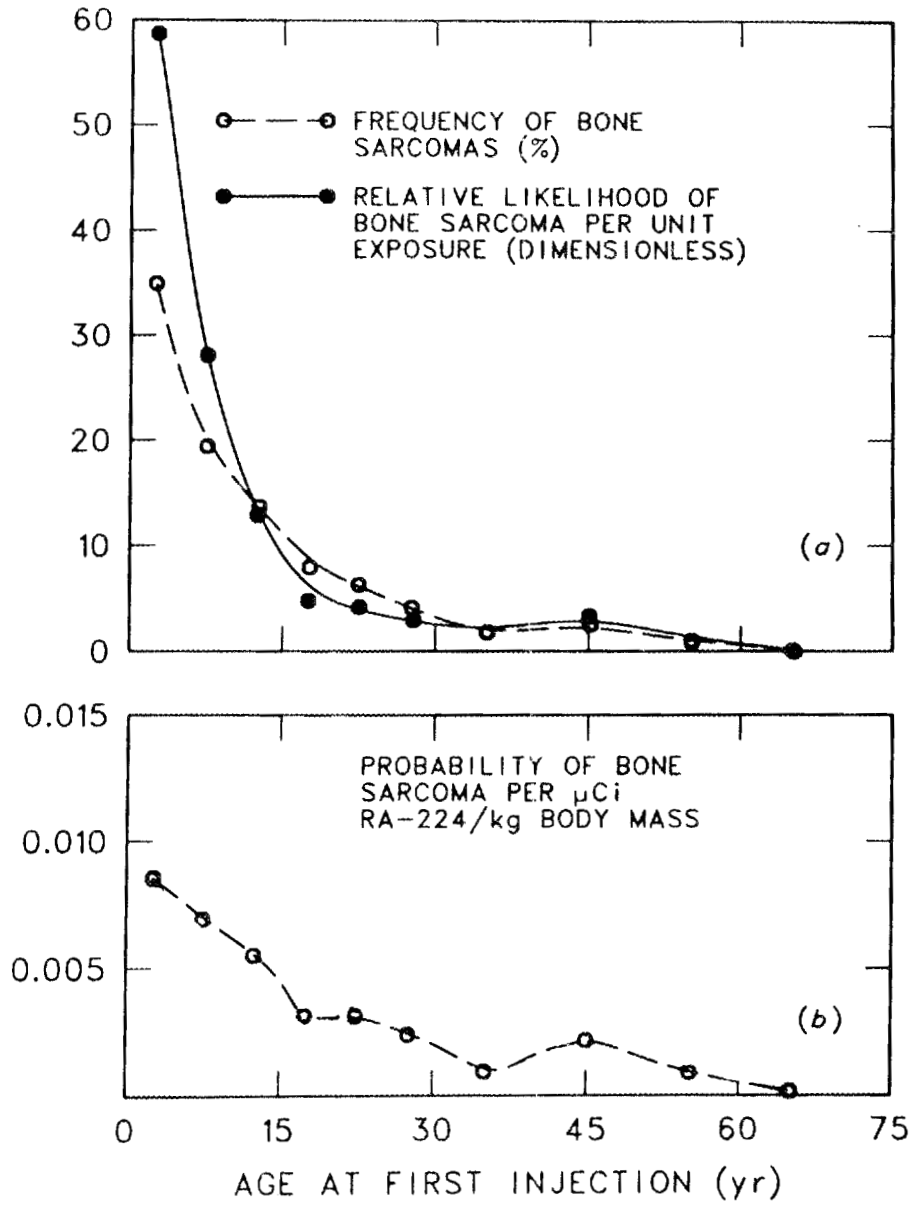


Figure 1. Age-specific risk of bone sarcoma in Ra-224 patients.

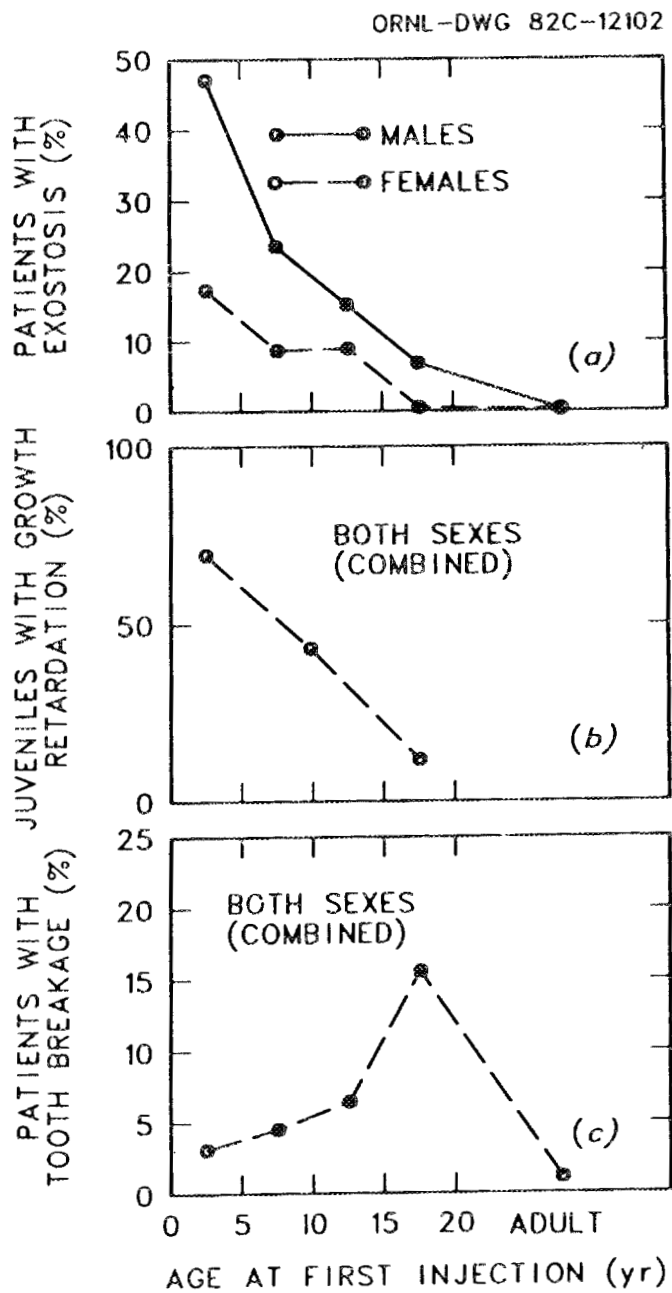


Figure 2. Frequencies of some other deleterious effects suffered by the Ra-224 patients.

## INTERNAL DISTRIBUTION

1. B. A. Berven
- 2-3. R. O. Chester
- 4-8. M. Cristy
9. J. L. Davis
- 10-14. K. F. Eckerman
15. R. J. M. Fry
16. W. R. Garrett
17. A. R. Hawthorne
- 18-22. G. D. Kerr
- 23-27. D. C. Kocher
- 28-32. R. W. Leggett
33. C. R. Richmond
34. J. C. Ryman
35. C. S. Sims
36. C. C. Travis
37. P. J. Walsh
- 38-42. B. P. Warren
43. L. R. Williams
44. H. A. Wright
45. Central Research Library
46. Document Reference Section
- 47-48. Laboratory Records
49. Laboratory Records, ORNL - RC
50. ORNL Patent Office
51. RSIC Library

## EXTERNAL DISTRIBUTION

52. Office of the Assistant Manager for Energy Research and Development, Department of Energy, Oak Ridge Operations Office, Oak Ridge, TN 37831
- 53-82. Technical Information Center, Office of Scientific and Technical Information, U.S. Department of Energy, P. O. Box 62, Oak Ridge, TN 37831
83. N. Adams, National Radiological Protection Board, Chilton, Didcot, Oxon, OX11 0RQ, England
84. W. D. Adams, U.S. Department of Energy, Oak Ridge Operations, Federal Building, Oak Ridge, TN 37831
85. S. J. Adelstein, Harvard Medical School, 25 Shattuck Street, Boston, MA 02115

86. R. E. Alexander, Office of Nuclear Regulatory Research, Occupational Radiation Protection Branch, Division of Facility Operations, U.S. Nuclear Regulatory Commission, MS 1130-SS, Washington, DC 20555
87. P. R. Almond, James Graham Brown Cancer Center, Radiation Oncology, 529 S. Jackson Street, Louisville, KY 40202
88. H. L. Atkins, Department of Radiology, Health Sciences Center, State University of New York, Stony Brook, NY 11794
89. W. J. Bair, Manager, Environment, Health and Safety Research Program, Battelle Pacific Northwest Laboratory, P. O. Box 999, Richland, WA 99352
90. Gunnar Bengtsson, Statens Stralskyddsinstitut, Box 60204, S-10401 Stockholm, Sweden
91. Luiz Bertelli, Instituto de Radioprotecao e Dosimetria/CNEN, Av. das Americas Km 11.5, Barra da Tijuca - Rio de Janeiro - RJ, CEP 22700 - Brazil
92. R. J. Berry, Department of Oncology, The Middlesex Hospital Medical School, London W1P 7PN, UK
93. J. A. Bianco, The Commonwealth of Massachusetts, University of Massachusetts Medical Center, Department of Nuclear Medicine, Worcester, MA 01605
94. W. R. Bibb, U.S. Department of Energy, Oak Ridge Operations, Federal Building, Oak Ridge, TN 37831
95. R. E. Bigler, Sloan-Kettering Institute for Cancer Research, 1275 York Avenue, New York, NY 10021
96. J. L. Blair, Director, Human Health and Assessment Division, ER-73, Office of Health and Environmental Research, U.S. Department of Energy (GTN), Washington, DC 20454
97. B. B. Boecker, Inhalation Toxicology Research Inst., Lovelace Biomedical and Environmental Research Institute, P. O. Box 5890, Albuquerque, NM 87185
98. V. P. Bond, Assoc. Director for Life Sciences and Safety, Brookhaven National Laboratory, Upton, NY 11973
99. A. B. Brill, Medical Department, Brookhaven National Laboratory, Upton, NY 11973
100. A. L. Brooks, Inhalation Toxicology Research Inst., Lovelace Biomedical and Environmental Research Institute, P. O. Box 5890, Albuquerque, NM 87185
101. T. F. Budinger, Donner Laboratory, Rm. 230, University of California, Berkeley, CA 94720
102. Georg Burger, Institut fuer Strahlenschutz, Gesellschaft fuer Strahlen- und Umweltforschung, Ingolstaedter Landstrasse 1, D-8042 Neuherberg/Munich, Federal Republic of Germany
103. W. W. Burr, Jr., Oak Ridge Associated Universities, Medical Division, P. O. Box 117, Oak Ridge, TN 37831

104. Xing-an Chen, Laboratory of Industrial Hygiene, National Center for Preventive Medicine, 2 Xinkang Street, Deshengmenwai, Beijing 100011, People's Republic of China
105. R. F. Christy, Department of Physics, California Institute of Technology, Pasadena, CA 91125
106. R. H. Clarke, National Radiological Protection Board, Chilton, Didcot, Oxon OX11 0RQ, UK
107. R. J. Cloutier, Radiopharmaceutical Internal Dose Center, Oak Ridge Associated Universities, MERT, P. O. Box 117, Oak Ridge, TN 37831
108. C. R. Cothorn, U.S. Environmental Protection Agency, Office of Drinking Water (WH-550), 401 M Street, S.W., Washington, DC 20460
109. R. G. Cuddihy, Inhalation Toxicology Research Inst., Lovelace Biomedical and Environmental Research Institute, P. O. Box 5890, Albuquerque, NM 87185
110. R. F. Dannals, Div. of Nuclear Medicine, Johns Hopkins Medical Institute, Baltimore, MD 21205
111. Li Deping, Institute of Radiation Protection, MNI, P.O. Box 120, Taiguan, Shanxi, People's Republic of China
112. L. T. Dillman, 184 W. Lincoln Ave., Delaware, OH 43015
113. Gunter Drexler, Gesellschaft fuer Strahlen- und Umweltforschung mbH, Institut fuer Strahlenschutz, Ingolstaedter Landstrasse 1, D-8042, Neuherberg, Federal Republic of Germany
114. H. J. Dunster, National Radiological Protection Board, Chilton, Didcot, Oxon OX11 0RQ, UK
115. P. W. Durbin, 101-74B, Lawrence Berkeley Laboratory, University of California, Berkeley, CA 94720
116. V. Elsasser, Institut fuer Strahlenhygiene des Bundesgesundheitsamtes, Ingoldstadter Landstrasse 1, D-8042 Neuherberg, Federal Republic of Germany
117. J. I. Fabrikant, Donner Laboratory, University of California, Berkeley, CA 94720
118. Thomas Fearon, Dept. of Radiology, Children's Hospital, National Medical Center, 111 Michigan Ave., N.W., Washington, DC 20010
119. D. J. Fehring, Office of Nuclear Materials Safety and Safeguards, MS 697-SS, U.S. Nuclear Regulatory Commission, Washington, DC 20555
120. L. E. Feinendegen, Institute of Medicine, Nuclear Research Center Julich GmbH, P. O. Box 1913, D-5170 Julich, Federal Republic of Germany
121. J. D. Foulke, Office of Nuclear Regulatory Research, U.S. Nuclear Regulatory Commission, MS 1130-SS, Washington, DC 20555
122. A. M. Friedman, University of Chicago, Dept. of Radiology, Nuclear Medicine Section, Box 429, Chicago, IL 60637

123. D. M. Goldenberg, New Jersey Medical School, 100 Bergen Street, Newark, NJ 070103
124. Marvin Goldman, Director, Laboratory for Energy-Related Health Research (LEHR), University of California, Davis, CA 94616
125. D. R. Hamilton, Nuclear Medicine Branch, OTA/NCDRH, U.S. Food and Drug Administration, Rockville, MD 20857
126. N. H. Harley, Department of Environmental Medicine, New York University Medical Center, 550 First Avenue, New York, NY 10016
127. J. D. Harrison, National Radiological Protection Board, Chilton, Didcot, Oxon OX11 0RQ, UK
128. K. Henrichs, Institut fuer Strahlenschutz der Gesellschaft fuer Strahlen- und Umweltforschung mbH, Ingolstaedter Landstr. 1, D-8042 Neuherberg, Federal Republic of Germany
129. K. Hubner, Department of Radiology, University of Tennessee Memorial Hospital, 1924 Alcoa Highway, Knoxville, TN 37920
130. V. Husak, Department of Nuclear Medicine, University Hospital, 775 02 Olomouc, Czechoslovakia
131. J. Inaba, 9-1, Anagawa-4-chome, National Inst. of Radiol. Sciences, Chiba-shi 260 Japan
132. C. E. Iranzo, Paseo de la Castellana 201, Madrid 28046, Spain
133. G. V. Iyengar, National Bureau of Standards, Department of Commerce, Gaithersburg, MD 20899
134. Wolfgang Jacobi, Institut fuer Strahlenschutz der Gesellschaft fuer Strahlen- und Umweltforschung mbH, Ingolstaedter Landstr. 1, D-8042 Neuherberg, Federal Republic of Germany
135. P. H. Jensen, Applied Health Physics Section, Dept. of Health Physics, Riso National Laboratory, Postbox 49, DK-4000 Roskilde, Denmark
136. L. Johansson, Dept. of Radiation Physics and Nuclear Medicine, University of Goteborg Sahlgren Hospital, S-413 45 Goteborg, Sweden
137. J. R. Johnson, Atomic Energy of Canada, Ltd., Chalk River, Canada
138. J. Kalef-Ezra, Department of Medical Physics, Medical School, University of Ioannina, Ioannina, Greece
139. A. Kaul, Institut fuer Strahlenhygiene des Bundesgesundheitsamtes, Ingolstaedter Landstrasse 1, D-8042 Neuherberg, Federal Republic of Germany
140. H. Kawamura, Division of Radioecology, National Institute of Radiological Sciences, Isezaki, Nakaminato, Ibaraki 311-12, Japan
141. J. G. Kereiakes, E555 Medical Sciences Building, University of Cincinnati, Cincinnati, OH 45267
142. G. G. Killough, 105 Netherland Rd., Oak Ridge, TN 37830

143. Rene Kirchmann, GEN/SCK Laboratories, Department of Radiobiology, Boeretang 200, B-2400, Mol, Belgium
144. L. Koblinger, Magyar Tudomanyos Adademia, Kozponti Fizikai Kutato Intezete, Budapest XII., Konkoly Thege ut 29-33, H-1525 Budapest P.O.B. 49, Hungary
145. J. Kruger, Nuclear Development Corporation, Private Bag X256, Pretoria 0001, South Africa
146. Emil Kunz, Institute of Hygiene & Epidemiology, Radiation Hygiene Department, Srobarova 48, 100 42 Parah 10-Vinohrady, Czechoslovakia
147. K. A. Lathrop, Hospital Box 433, University of Chicago Medical Center, 5841 S. Maryland Avenue, Chicago, IL 60637
148. J. S. Laughlin, Sloan-Kettering Institute for Cancer Research, 1275 York Avenue, New York, NY 10021
149. Gee-Fong Liang, Radiation Laboratory, Taiwan Power Company, P.O. Box 7, Shinmen, Taiwan 253, Republic of China
150. J. Liniecki, Department of Nuclear Medicine, Medical Academy of Lodz, Czechoslovakia 8/10, 92-216 Lodz, Poland
151. R. D. Lloyd, Building 351, University of Utah, College of Medicine, Salt Lake City, UT 84112
152. Robert Loevinger, Radiation Physics C210, National Bureau of Standards, Gaithersburg, MD 20899
153. J. Logic, University of Alabama Medical Center, Birmingham, AL 35233
154. C. M. Luccioni, IPSN/DPS/SEAPS/LBA, Commissariat a' e' Energie Atomique, BP 6, 92260 Fontenay aux Roses, France
155. O. Matsuoka, National Institute of Radiological Sciences, 9-1 Anagawa-4-chome, Chiba-shi, Japan 260
156. S. Mattsson, Dept. of Radiation Physics and Nuclear Medicine, University of Goteborg Sahlgren Hospital, S-413 45 Goteborg, Sweden
157. H. R. Maxon, E. L. Saenger Radioisotope Lab., University of Cincinnati, Box 577, College of Medicine, Cincinnati, OH 45267
158. C. W. Mays, Radiobiology Division, University of Utah, Salt Lake City, UT 84112
159. R. O. McClellan, Lovelace Inhalation Toxicology Research Institute, P. O. Box 5890, Albuquerque, NM 87185
160. C. B. Meinhold, Chief, Safety and Environmental Protection Division, Bldg. 535A, Brookhaven National Laboratory, Upton, NY 11973
161. W. A. Mills, 2915 Ascott Lane, Olney, MD 20832
162. I. Mitsuhashi, Nuclear Engineering Department, NAIG Nuclear Research Laboratory, Nippon Atomic Industry Group Co., Ltd., Kawasaki-ku, Kawasaki-city, Japan

163. J. P. Moroni, SCPRI, B.P. No 35, F-78110 LeVosinet, France
164. Y. I. Moskalev, Institute of Biophysics, Ministry of Public Health, Zhivopisnoya 116, Moscow D-182, USSR
165. C. B. Nelson, U.S. Environmental Protection Agency, 401 M Street, S.W., (ANR-461), Washington, DC 20460
166. D. R. Nelson, Health Physics Branch, EH-133.2, Office of Nuclear Safety, U.S. Department of Energy (GTN), Washington, DC 20545
167. Neal Nelson, U.S. Environmental Protection Agency, 401 M Street, S.W., (ANR-461), Washington, DC 20460
168. J. C. Nenot, Institut de Protection et de Surete Nucleaire, Departement de Protection, Services de Pathologie et de Protection Sanitaire, Service de Protection Sanitaire, Centre d'Etudes Nucleaires, B.P. No. 6, 92260 Fontenay-aux-Roses, France
169. Y. C. Ng, Environmental Science Division, Lawrence Livermore National Laboratory, P. O. Box 808, Livermore, CA 94550
170. D. Nosske, Institut fuer Strahlenhygiene, Ingoldstadter Landstrasse 1, D-8042 Neuherberg, Federal Republic of Germany
171. M. C. O'Riordan, National Radiological Protection Board, Chilton, Didcot, Oxon, England
172. J. M. Palms, Vice President for Academic Affairs, Emory University, Atlanta, GA 30322
173. N. Parmentier, Republique Francaise, Commissariat A L'Energie Atomique, Department de Protection Sanitaire, Fontenay Aux Roses, France
174. C. L. Partain, Director, Nuclear Medicine, Vanderbilt University School of Medicine, Nashville, TN 37232
175. C. Pomroy, Atomic Energy Control Board, Ottawa K1P5S9, Canada
176. J. W. Poston, Dept. of Nuclear Engineering, College of Engineering, Texas A&M University, College Station, TX 77843
177. A. K. Poznanski, Department of Radiology, The Children's Memorial Hospital, 2300 Children's Plaza, Chicago, IL 60614
178. N. D. Priest, National Radiological Protection Board, Chilton, Didcot, Oxon OX11 0RQ, UK
179. P. V. Ramzaev, Institute of Radiation Hygiene, 8 Mira ul, Leningrad 197101, U.S.S.R.
180. Dr. Thomas Reavey, Office of Radiation Programs (ANR-461), U.S. Environmental Protection Agency, 401 M Street SW, Washington, DC 20460
181. H. D. Roedler, Institut fuer Strahlenhygiene, Ingolstaedter Landstrasse 1, D-8042 Neuherberg, Federal Republic of Germany
182. J. S. Robertson, Human Health and Assessments Division, Office of Energy Research, ER-73, U.S. Department of Energy (GTN), Washington, DC 20545

183. E. L. Saenger, Eugene L. Saenger Radioisotope Laboratory, University of Cincinnati Hospital, Cincinnati General Division, 234 Goodman Street, Cincinnati, OH 45267
184. R. A. Schlenker, Building 203, Center for Human Radiobiology, Argonne National Laboratory, 9700 Cass Avenue, Argonne, IL 60439
185. Itsuzo Shigematsu, Chairman, Radiation Effects Research Foundation, 5-2 Hijiyama Koen, Minami-ku, Hiroshima-shi, 730, Japan
186. W. K. Sinclair, President, National Council on Radiation Protection and Measurement, 7910 Woodmont Avenue, Suite 1016, Bethesda, MD 20814
187. G. Silini, Secretary of UNSCEAR, Vienna International Center, P. O. Box 500, A-1400 Vienna, Austria
188. K. W. Skrable, University of Lowell, Lowell, MA 01854
189. J-O. Snihs, Statens Stralskyddsinstitut, Box 60204, S-10301 Stockholm, Sweden
190. M. G. Stabin, Radiopharmaceutical Internal Dose Center, Oak Ridge Associated Universities, MERT, P. O. Box 117, Oak Ridge, TN 37831
191. J. N. Stannard, 17441 Plaza Animado, Apt. 132, San Diego, CA 92128
192. H. W. Strauss, Director, Nuclear Medicine Division, Massachusetts General Hospital, Fruit Street, Boston, MA 02114
193. R. E. Sullivan, U.S. Environmental Protection Agency, 401 M Street, S.W., (ANR-461), Washington, DC 20460
194. Eizo Tajima, Vice Chairman, Atomic Energy Safety Commission, 2-2-1 Kasumigaseki, Chiyoda-ku, Tokyo 100, Japan
195. G. Tanaka, Division of Radiocology, National Institute of Radiological Sciences, Isezaki, Nakaminato, Ibaraki 311-12, Japan
196. A. C. Taner, Ankara Nuclear Research and Training Center, Fen Fakultesi Arkasi, Besevler-Ankara, Turkey
197. D. M. Taylor, Institute for Genetics & Toxicology, Kernforschungszentrum Karlsruhe, Postfach 3640, D-7500 Karlsruhe 1, Federal Republic of Germany
198. G. N. Taylor, Division of Radiobiology, Building 522, University of Utah, Salt Lake City, UT 84112
199. R. H. Thomas, Director's Office, Building 50A-4112, Lawrence Berkeley Laboratory, University of California, Berkeley, CA 94720
200. S. R. Thomas, Dept. of Radiology Physics, Medical Sciences Building, E-465, Cincinnati, OH 45267
201. R. C. Thompson, Battelle Pacific Northwest Laboratories, 331 Bldg./300 Area, Richland, WA 99352

202. M. C. Thorne, Associated Nuclear Services, 123, High Street, Epsom, Surrey KT19 8EB, England
203. J. E. Till, Route 2, Box 122, Neeses, SC 29107
204. S. Treves, Head, Nuclear Medicine, Children's Hospital Medical Center, 300 Long Wood Avenue, Boston, MA 02115
205. M. Uchiyama, National Institute of Radiological Sciences, Division of Physics, 9-1, Anagawa-4-chome, Chiba-shi 260, Japan
206. D. Van As, Nuclear Development Corporation, Private Bag X256, Pretoria 0001, South Africa
207. N. Veall, Radioisotopes Division, Clinical Research Centre, Watford Road, Harrow, Middlesex HA1 3UJ, England
208. B. W. Wachholz, Low Level Radiation Effects Branch, National Cancer Institute, Landow Building 8C-09, 9000 Rockville Pike, Bethesda, MD 20205
209. H. N. Wagner, Jr., Division of Nuclear Medicine, Johns Hopkins Medical Institute, Baltimore, MD 21205
210. J. T. Walker, U.S. Environmental Protection Agency, 401 M Street, S.W., (ANR-461), Washington, DC 20460
211. E. E. Watson, Radiopharmaceutical Internal Dose Center, Oak Ridge Associated Universities, MERT, P. O. Box 117, Oak Ridge, TN 37831
212. D. A. Weber, University of Rochester, Medical Center, 601 Elmwood Avenue, Rochester, NY 14642
213. B. C. Winkler, Private Bag X256, Pretoria, 0001, South Africa
214. Walter Wolf, School of Pharmacy, University of Southern California, Los Angeles, CA 90033
215. R. W. Wood, Physical and Technology Research Div., ER-74, Office of Health and Environmental Research, U.S. Department of Energy (GTN), Washington, DC 20545
216. M. E. Wrenn, Director, Radiobiology Division, Department of Pharmacology, School of Medicine, University of Utah Medical Center, Salt Lake City, UT 84112
217. H. O. Wycoff, Chairman, International Commission on Radiation Units and Measurements, 7910 Woodmont Avenue, Suite 1016, Bethesda, MD 20814
218. S. Wynchank, Research Institute for Medical Biophysics (RIMB), P. O. Box 70, Tygerberg 7505, Republic of South Africa
219. Hiroshi Yamaguchi, National Institute of Radiological Sciences, Division of Physics, 9-1, Anagawa-4-chome, Chiba-shi 260, JAPAN
220. Shlomo Yaniv, Health Effects Branch - MS 1130-SS, Division of Health, Siting and Waste Management, RES, U.S. Nuclear Regulatory Commission, Washington, DC 20555
221. R. W. Young, Armed Forces Radiobiology Research Institute, Naval Medical Center, Bethesda, MD 20814-5145

222. P. B. Zanzonico, Sloan-Kettering Institute for Cancer Research,  
1275 York Avenue, New York, NY 10021

★U.S. GOVERNMENT PRINTING OFFICE: 1987-748-158/60088